

Characterization of a Sea-State Simulator for Ergonomic Studies

David Brenton Bateman

Thesis submitted to the faculty of the Virginia Polytechnic Institute and State University
in partial fulfillment of the requirements for the degree of

Master of Science
In
Industrial and Systems Engineering

Robert H. Sturges, Chair
Thurmon E. Lockhart
Jaime A. Camelio

March 30, 2011
Blacksburg, Virginia

Keywords: Sea-State, Simulator, Control Systems

Copyright 2011

Characterization of a Sea-State Simulator for Ergonomic Studies

David Brenton Bateman

ABSTRACT

With the use of tow-tank experiments, data may be generated for ships of various classes using comprehensive instrumentation. This data gives the ability to determine the response of ships to various sea-state conditions far in advanced of their construction and launch. However, this data does not indicate the effects of those sea-states to the individuals aboard that ship.

In order to define these effects a sea-state simulator must be designed and built. Once construction is completed a series of test must be conducted to determine the response of the simulator. This response allows the comparison to actual tow-tank data to determine if the simulator is capable of performing the desired research.

Dedication

*To my mother and father
my brothers and sister
and my fiancée.*

Acknowledgements

I would like to thank my advisor and committee chairman Dr. Robert Sturges for the opportunity to work on the Office of Naval Research project N00178-09-D-3017-0008, which has led to this thesis. His guidance and advice throughout my studies has been invaluable to my success here at Virginia Tech. His encouragement, thoughtfulness, and willingness to help are deeply appreciated.

I would also like to thank my committee members: Dr. Thurmon Lockhart and Dr. Jaime Camelio for their support and belief in me. It has been an honor to have worked and learned from them.

A special thanks to Igor Zamlinsky who's in-depth knowledge on LabVIEW helped create the current system controller discussed in Section 4.4.

Thanks to Mrs. Angie Parvin for her help in administrative matters.

I would like to thank all the people and friends I have met at Virginia Tech and their support throughout my endeavors.

Most importantly, I would like to thank my family and fiancée without whose support and patience I would have never of reached this point: my father, Mr. Lionel Bateman, and my mother, Mrs. Sandra Bateman. I am forever grateful for their love, kindness, and devotion. To my fiancée, Ms. Jennifer Coggins, your love, strength, and ability to listen will always be cherished.

Finally, thanks to my heavenly father and creator God for giving me the ability, knowledge, and perseverance to be where I am now. Without your love and forgiveness nothing would be possible.

Table of Contents

Chapter 1: Introduction	1
1.1 Background and Motivation	1
1.2 Research Objectives	2
Chapter 2: Literature Review	4
2.1 Scale Model of Ship-X.....	4
2.1.1 Model Testing of Ship-X.....	4
2.2 FREDYN Model Simulation.....	5
2.2.1 Ship-X Simulation	5
2.2.2 Ship-X Simulation Method.....	5
2.2.3 Ship-X Model Inputs	6
2.3 Design of Control Systems	6
2.3.1 Laplace Transform.....	7
2.3.2 Stability of a System.....	8
2.3.3 Transfer Functions	9
2.3.4 Diagrammatic Representation	9
2.4 Proportional, Integral, and Derivative Control	10
2.4.1 Transfer Function of PID Control	11
2.4.2 Step Response of PID Control.....	12
Chapter 3: Initial System Design	15
3.1 Lab Facilities and Platform Layout.....	15
3.2 Hydraulic System.....	15
3.3 Electrical Signal System	17
3.4 LabVIEW Virtual Instrument Design.....	23
3.4.1 Platform Over-Tilt	23
3.4.2 Operator Error with the VI	25
3.4.3 Data Collection	25
3.4.4 Data Representation.....	25
3.4.5 Characterization of the PD Controller	26
3.4.6 PD Controller Response Test	30
3.4.7 PD Bode and Phase Plots.....	34
3.4.8 PD Bode Plot Comparison.....	40

3.4.9 Initial PD Controller Conclusions	42
Chapter 4: Current System Design	43
4.1 Hardware Modifications	43
4.2 Electrical Signal System Modifications.....	43
4.3 Characterizing the Response of the System.....	47
4.4 LabVIEW Virtual Instrument Design.....	48
4.4.1 Motion File Creation	48
4.4.2 Platform Controller.....	49
4.4.3 Determination of K_P and K_D Values	53
4.5 Response of the System	54
4.5.1 Square Wave Response Test.....	54
4.5.2 Square Wave Response Test Result	55
4.5.3 Sine Wave Response Test.....	56
4.5.4 PD Bode and Phase Plots.....	57
4.6 Current PD Controller Conclusion.....	59
Chapter 5: Conclusions	61
Bibliography	62
Appendices.....	64
Appendix A: Initial Controller LabVIEW Back Panel.....	64
Appendix B: Initial Controller Front Panel	68
Appendix C: Initial Controller Sine Wave Response Results	70
Appendix D: Bode Plot Methodology and Results.....	73
Appendix E: Initial Controller's Matrix Transformation.....	82
Appendix F: Current Controller Back Panel.....	85
Appendix G: Back Panel Control States.....	90
Appendix H: Current Controller Front Panel.....	94
Appendix I: MATLAB Gain Value Coding	95
Appendix J: Current Controller Sine Wave Response.....	96

List of Figures

Figure 2.1: Closed-Loop Feedback Block Diagram	10
Figure 2.2: Step response of a process with self-regulation	12
Figure 2.3: Step response of an integrating process	13
Figure 3.1: Lab Facility and Platform Layout	15
Figure 3.2 Hydraulic Components	16
Figure 3.3: Electrical Components	17
Figure 3.4: Potentiometers	18
Figure 3.5: Potentiometers Signal Feed	19
Figure 3.6: Signal Wire Connections	19
Figure 3.7: Positioning Signal Wire Diagram	20
Figure 3.8: Relay and Breaker Board Diagram	21
Figure 3.9: Switches Wiring Diagram	22
Figure 3.10: Emergency Stop Wiring Diagram	22
Figure 3.11: Mass-Spring-Damper	26
Figure 3.12: Platform Feedback Diagram	28
Figure 3.13: Modified Platform Feedback Diagram	28
Figure 3.14: PD Controller Schematic Diagram	29
Figure 3.15: Damping Coefficients	30
Figure 3.16: Square Wave Test Input	31
Figure 3.17: Square Wave Response Test with All Derivative Values	32
Figure 3.18: Close up of Square Wave Response Test with All Derivative Values	32
Figure 3.19: Sine Wave Response Input for Heave	33
Figure 3.20: Sine Wave Response Heave Test with Max-Min Derivative	34
Figure 3.21: Roll Amplitude versus Frequency Test	36
Figure 3.22: Pitch Amplitude versus Frequency Test	37
Figure 3.23: Pitch Amplitude versus Frequency Test	37
Figure 3.24: Initial Controller's Roll Phase Plot	38
Figure 3.25: Initial Controller's Heave Phase Plot	39
Figure 3.26: Initial Controller's Pitch Phase Plot	40
Figure 3.27: Roll Comparison	41
Figure 3.28: Pitch Comparison	41
Figure 3.29: Heave Comparison	42
Figure 4.1: Modified Electrical Component Layout	44
Figure 4.2: DAQ Card Signal and Feedback Schematic	45
Figure 4.3: Modified Signal Wire Connections	45
Figure 4.4: Modified Positioning and Meter Voltage Wire Diagram	46
Figure 4.5: Emergency Stop Modified Wiring Diagram	47
Figure 4.6: 3-D Imaging Code and Layout Diagram	50
Figure 4.7: Lift Position Indicator Diagram	51
Figure 4.8: MATLAB Simulink Diagram	54
Figure 4.9: Square Wave Response Input	55
Figure 4.10: Square Wave Response Test	56
Figure 4.11: Roll Amplitude versus Frequency Current Controller Test	57
Figure 4.12: Pitch Amplitude versus Frequency Current Controller Test	58
Figure 4.13: Pitch Amplitude versus Frequency New Controller Test	58

Figure 4.14: Current Controller's DOF Phase Change Comparison	59
Figure A.1: Back Panel Display.....	66
Figure A.2: Initial Controller Platform Function Block Diagram	67
Figure B.1: Initial Controller Front Panel.....	69
Figure C.1: Roll Sine Wave Response Results.....	70
Figure C.2: Pitch Sine Wave Response Results.....	71
Figure C.3: Heave Sine Wave Response Results.....	72
Figure D.1: Wave Bode Plot Calculation Diagram	73
Figure F.1: Back Panel Input Section	85
Figure F.2: Back Panel Potentiometer Conversion Section.....	86
Figure F.3: Back Panel Control State Section	86
Figure F.4: Back Panel PD Controller	87
Figure F.5: Back Panel Output.....	88
Figure F.6: Current Controller Function Block Diagram	89
Figure G.1: Stop Control State.....	90
Figure G.2: Lower Control State	90
Figure G.3: Ready Control State.....	91
Figure G.4: Run Control State	91
Figure G.5: Loop Control State	92
Figure G.6: Pause Control State.....	92
Figure H.1: Current Controller's Front Panel	94
Figure J.1: Current Controller's Sine Wave Roll Test	96
Figure J.2: Current Controller's Sine Wave Pitch Test.....	97
Figure J.3: Current Controller's Sine Wave Heave Test.....	97

List of Tables

Table 1.1: Annual Sea-State Occurrences in the North Atlantic	2
Table 2.1: Proportional, Integral, and Derivative Action Modes	12
Table D.1: Original Internal PID Controller Roll Data	74
Table D.2: Original Internal PID Controller Pitch Data	75
Table D.3: Original Internal PID Controller Heave Data	75
Table D.4: External PD Controller Roll Data at Derivative 0	76
Table D.5: External PD Controller Roll Data at Derivative 50	76
Table D.6: External PD Controller Pitch Data at Derivative 0	77
Table D.7: External PD Controller Pitch Data at Derivative 50	78
Table D.8: External PD Controller Heave Data at Derivative 0	78
Table D.9: External PD Controller Heave Data at Derivative 50	79
Table D.10: Current PD Controller Roll Data	79
Table D.11: Current PD Controller Pitch Data	80
Table D.12: Current PD Controller Heave Data	80

Chapter 1: Introduction

1.1 Background and Motivation

The purpose of the ONR project, award number N00178-09-D-3017-0008, was to analyze and optimize the sequence in which remote multi-mission vehicle (RMMV) launch processes took place by leveling the effort required for each task in order to meet the manning requirements for the mission. In addition, the research was to expand the current knowledge of the effects of motion-induced interruptions (MIIs) and motion-induced fatigue (MIF) on working in a moving environment. Biomechanical as well as time study data was to be collected on the sea-state simulator and analyzed to determine the influence of both sea-state and sea-state related perturbation on work performance.

In order to properly test MIIs and MIFs a three degree of freedom (DOF) platform was designed and constructed. The motion simulator discussed in the document spans nearly 96 square feet of useable area. A range of sea-state conditions was created by mounting a substantially rigid platform on three hydraulic lifts with universal bearings at their attachment points. In this way, the principal motions of roll, pitch, and heave could be generated according to a range of predetermined and/or random ship motions. The other three DOF sway, surge, and yaw represent second-order movements. Therefore, they were not considered for the purpose of this research. The control system, powered by LabVIEW, processes lifts motion derived from the desired platform positions, velocities, and accelerations in three degrees of freedom. With space and equipment restrictions the simulator was capable of performing sea-state conditions 0, 1, 2, and 3. These conditions are defined by Edward V. Lewis "Principles of Naval Architecture" Volume III, on the next page, as:

Table 1.1: Annual Sea-State Occurrences in the North Atlantic

Sea-State Number	Significant Wave Height (ft)		Percentage Probability	Modal Wave Period (sec)	
	Range	Mean		Range	Most Probable
0	0	0	0.70	-	-
1	0 – 0.3	0.15	0.70	-	-
2	0.3 – 1.6	1.0	6.80	3.3-12.8	7.5
3	1.6 – 4.1	2.9	23.70	5.0-14.8	7.5

To determine the maximum capabilities of the platform simulator the system had to be properly characterized, thus giving us the ability to determine the response of the system.

1.2 Research Objectives

The main objectives for this research was to design and construct a LabVIEW control system and properly characterize the response of the system. Modifications were to be made to the controller during the research to properly tune the system and for ease of use. The first step of achieving this objective was to design a control system capable of maximizing the systems potential. In order to properly define the response of the system a sine wave input file of varying frequencies had to be used. The feedback files from these tests were to be analyzed through the use of bode and phase plots. These plots then gave the ability to determine the response of the system based on frequency versus amplitude and phase versus amplitude. Through this methodology we determined that we could define the response of the system.

The final objective of this research was to provide documentation of the platform’s hydraulic, electrical, and control system for future use. Currently, the scheduled ONR project funding will end in the spring of 2010. Therefore, this documentation was essential for future operators when additional funding became available.

It is important to note that this thesis holds dual purposes. The first is to document the work that I, David Bateman, have completed individually. This work includes characterization of the system, determining the response of the system, determination of the proportional and derivative gains, the previous controller design, and testing. The

sections discussing the hydraulic system, electrical system, and the new LabVIEW controller have been written by me, however, they have been worked on by various members of the ONR research team, including myself at times. Therefore, I do not claim sole responsibility for all the work done on these components.

Chapter 2: Literature Review

In this chapter, a summary of previous testing completed by the Naval Surface Warfare Center, Carderock Division (NSWCCD) using a scale model of Ship-X and simulation software is discussed. Due to the nature of this data, some “secure” information may not be presented. This summary is followed by two sections on the design of control systems and PID control. The first section has four subsections which will discuss: the Laplace transform, stability of a system, transform functions, and diagrammatic representation. The second section has two subsections which will discuss the PID transfer function and step response.

2.1 Scale Model of Ship-X

A 1/30th scale model of Ship-X hull form was designed for tow tank testing and data collection. The model was a free running, radio controlled model with four reversing water jets and passive anti-roll fins. The model was designed, constructed, and tested on-site at the NSWCCD.

2.1.1 Model Testing of Ship-X

The model test provided data for design assessment and FREDYN validation. The test consisted of four parts: roll decrement, maneuvering, irregular sea-keeping and regular wave dynamics stability. Roll damping was measured in calm water by performing roll decrements at five different speeds. The scale model followed a carriage ensuring a straight track and proper speed. The model was excited in roll once at a desired speed and on a straight course beneath the moving carriage, for each measurement. Multiple runs were made to ensure the proper amount of data was collected.

Maneuvering tests consisted of turning circles and zigzags. The purpose of this testing was to quantify any difference due to loading conditions. The sea-keeping tests were completed at five different headings and four different ship speeds for Sea States 4 and 5. However, unlike the roll decrement tests the model was controlled manually.

Sea keeping data was collected for the equivalent of 30 minutes full-scale, with a 95% confidence level of a stable statistical result. A series of shorter passes were concatenated to accumulate the desired time of full-scale data. Any data that was corrupted was removed before analysis at NSWC.

2.2 FREDYN Model Simulation

The FREDYN simulation program was developed by the Cooperative Research Navies (CRNAV) Dynamic Stability Working Group. The program simulates the dynamic behavior of a steered ship subjected to waves and wind, including the ability to perform arbitrary maneuvers. The primary purpose of the software is to aid in the initial design stage when model test are unavailable. FREDYN computes all six degrees of freedom in the time domain.

2.2.1 Ship-X Simulation

The FREDYN simulation program was used by the NSWCCD, to provide an initial estimate of the dynamic stability for Ship-X. The scope of the research was focused on developing capsizing polar plots for two loading conditions in a given sea-state. The loading conditions selected were Minimum Operating Condition (MinOp) and Full Load Departure (FLD). Since hydrodynamic excitation forces calculated by the FREDYN were based on strip theory, the analysis had to be limited to a given speed. Even so, the event of Ship-X operating in that given sea-state at a greater speed was highly unlikely.

Prior to the simulation, NSWCCD compared the FREDYN model to known hydrostatic values in order to validate the geometry FREDYN modeled. Initial testing involved calm waters and simple wave simulations, which showed no unusual behavior. Dynamic stability runs were then executed to generate polar plots of capsizing, broaching, and surf-riding performance.

2.2.2 Ship-X Simulation Method

In order for NSWCCD to produce polar plots of dynamic stability event likelihood for a given set of speeds and headings, almost 2,000 simulations had to be performed. The simulations were 30 minutes in length, which included a 60 second ramp-up of the wave

amplitude. A total of 25 simulations were completed for each speed-heading combination, where each simulation had a different seed number for the seaway random phase generator.

In order to manage the execution and compilation of these numerous runs, a program named FRESCATE was used. The program calls the FREDYN program, calculates the statistics of a run, identifies dynamic stability events for each run, and compiles the results for all the speeds and headings.

2.2.3 Ship-X Model Inputs

There were three input files required to define the ship and its operating condition in FREDYN. They included the geometry input, the ship specific input, and the simulation specific input. The simulation specific input file was generated by a program called FRESCATE, which is designed to automatically run thousands of simulations and save the useful motion information for dynamic stability assessment. The information needed to develop and check these inputs to the FREDYN model were provided by an external source or developed from past practices.

2.3 Design of Control Systems

A common definition for a control system is, an arrangement of physical components connected or related in such a manner as to command, direct or regulate itself or another system (DiStefano, Joseph, et al. 1990 [1]). A control system is able to identify or define the inputs and outputs. If these are given, it is then possible to identify or define the nature of the system's components. The main objective of a control system is to obtain a desired response for a given system. This objective can be achieved with the implementation of either an open-loop system or closed loop system.

An open-loop control system utilizes a device to control the process without using feedback. This system's ability to perform accurately is determined by their calibration. Additionally, these systems do not normally suffer from instability as closed-systems do.

A closed-loop control system, which is the system of interest in this research, uses a measurement of the output and compares it with the desired output. Simply stated the system is dependent on the output. These systems are commonly called feedback control systems. Feedback is defined as the property of a closed loop system which permits the output to be compared with the input to the system so that the appropriate control action may be formed as some function of the output and input (DiStefano, Joseph, et al. 1990 [1]). A system that is considered to be closed-loop has five important features that feedback imparts to it:

- 1.) Increased accuracy
- 2.) Reduced sensitivity of the ratio of output to input to variations in the system characteristics
- 3.) Reduced effects of nonlinearities and distortion
- 4.) Increased bandwidth
- 5.) Tendency toward oscillation or instability.

2.3.1 Laplace Transform

The Laplace transform was created in order to provide a method for representing and analyzing linear systems using algebraic methods. When defining this term, it is described as a transformation technique relating time functions to frequency dependent functions of a complex variable. When written algebraically the definition takes the form of Equation 2.1.

$$F(s) = \int_0^{\infty} f(t)e^{-st} dt \quad 2.1$$

where, $f(t)e^{-st}$ is the function in terms of time t and $F(s)$ is the function in terms of the Laplace s .

Using the Laplace transform converts a problem from the real variable time domain into the complex variable “ s ” domain. Therefore, when applying the Laplace transform to analyze a linear system there are five basic steps to follow, which are listed below:

- 1.) Conversion of the system transfer function, or differential equation, to the s-domain by replacing “D” with “s”.
- 2.) Converting the input function(s) to the s-domain using transform tables.
- 3.) Algebraically combining the input and transfer function to find an output function.
- 4.) Use of partial fractions to reduce the output function to simpler components.
- 5.) Converting the output equation back to the time-domain using the tables.

2.3.2 Stability of a System

The stability of a system is determined by the systems response to inputs or disturbances. A stable system will remain at rest unless excited by an external source and will return to rest after all excitations are no longer present. A common definition is that a system is considered stable if its impulse response approaches zero as time approaches infinity. Alternatively, if the definition is based upon the response of the system to inputs whose magnitude are less than some finite value for all time the definition can be rephrased. The new definition would state that a system was stable if and only if every bounded input produced a bounded output.

Consideration must be made on the degree of stability of the system, which is the concept of relative stability. Normally, relative stability is expressed in terms of some allowable variation of a particular system parameter for which the system will remain stable (DiStefano, Joseph, et al. 1990 [1]). In order for a system to be considered stable the real parts of the roots of the characteristic equation must have negative real parts, which will ensure that the impulse response will decay exponentially with time. If the system does not meet this condition, but has some roots with real parts equal to zero and none with positive real parts the system is considered to be marginally stable. Nevertheless, certain inputs will produce unbounded outputs, which mean a marginally stable system is actually unstable. Various methods are available in determining the stability of a system. They include the Routh stability criterion, the Hurwitz stability criterion, and the continued fraction stability criterion.

2.3.3 Transfer Functions

The transfer function of a linear system is defined as the ratio of the Laplace transform of the output variable to the Laplace transform of the input variable, with all initial conditions assumed to be zero (Dorf and Bishop, 2005 [2]). The transfer function of a system delineates the relationship characterizing the dynamics of the system under consideration. Only systems that are linear or stationary may be defined by transfer functions. If a system is determined to be non-stationary, which may be defined as a time-varying system, it has one or more time-varying parameters. Therefore, the Laplace transformation cannot be used.

In addition, a transfer function is an input-output representation of the behavior of the system. As a result, the transfer function description doesn't include any information concerning the internal structure of the system or its behavior.

2.3.4 Diagrammatic Representation

Control systems are primarily concerned with the control of specific variables. These controlled variables must relate to the controlling variables. The relationship between these two is typically represented by the transfer function of the subsystem. This relationship of the system variables can be illustrated by the block diagram. Block diagrams consist of unidirectional, operational blocks that represent the transfer function of the variables of interest. The various components of a control system are connected in a way that characterizes their functional relationship within the given system. The basic structure of a simple closed-loop feedback control system is illustrated in the block diagram in Figure 2.1.

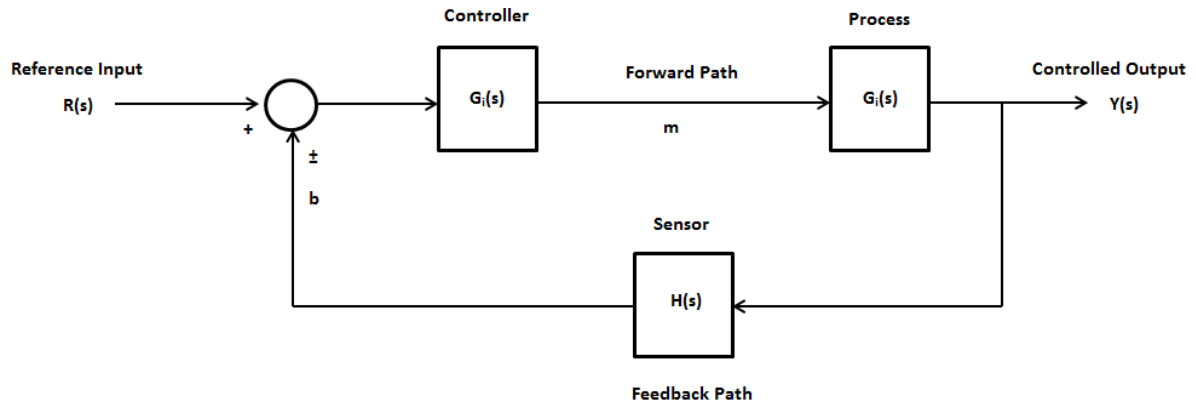


Figure 2.1: Closed-Loop Feedback Block Diagram

The reference input $R(s)$ normally represents the ideal output behavior from the process block, also known as the plant. The reference point is defined as the external signal applied to a feedback control system in order to command a specified action of the process. Once the external signal is applied it feeds into the controller, also known as the control element. At this juncture the appropriate control signal is generated, known as m , and applied to the process. When the signal reaches the process it is then controlled, the signal can either be a particular quantity or condition. When the signal leaves the process block it can then take two paths. First, it can become a controlled output, which is simply the quantity or condition of the process which is controlled. Secondly, it can follow the feedback path to the sensor block $H(s)$. Here the components will be required to establish the functional relationship between the feedback signal “ b ” and the controlled output $Y(s)$. The signal will then be algebraically summed with the reference input to obtain the actuating signal. Depending on the summing point the feedback will either be negative or positive.

2.4 Proportional, Integral, and Derivative Control

A proportional, integral, and derivative controller, is most commonly referred to as a PID controller. First, the P element is proportional to the error at the instant t , also known as the present error. Secondly, the I element is proportional to the integral of the error up to the instant t , which can be interpreted as the accumulation of the past error. Finally, the D element is proportional to the derivative of the error at the instant t , which is normally interpreted as the prediction of the future error. Simply stated, the PID controller takes the present, the past, and the future of the error into consideration.

There are two common types of PID controllers, which are often combined with logic, sequential functions, selectors, and simple function blocks. First, there is the stand-alone system which may control anywhere from one to three loops. Secondly, there are the controllers that are embedded in a special-purpose control system. With the implementation of microprocessors the opportunity to provide additional features such as automatic tuning, gain scheduling and continuous adaptation has been gained for these controllers.

2.4.1 Transfer Function of PID Control

The transfer function of a PID controller is given in Equation 2.2.

$$C(s) = K_p \left\{ 1 + \frac{1}{T_I s} + T_D D(s) \right\} \quad 2.2$$

This is provided that all three elements are utilized in the controller. In Equation 2.2 K_p , T_I , and T_D are positive parameters, which are referred to as proportional gain, integral time, and derivative time. $D(s)$ in Equation 2.2 is the transfer function given in Equation 2.3 and is called the approximate derivative.

$$D(s) = \frac{s}{1 + \left(\frac{T_D}{\gamma}\right)s} \quad 2.3$$

A pure derivative “s” is replaced with the approximate derivate $D(s)$ because a pure derivative is impossible to realize physically. In Equation (2.3), γ is a positive parameter, which is referred to as the derivative gain. As γ increases the response of the approximate derivative approaches that of the pure derivative. However, if a large value of γ is chosen the amplification of detection noise will increase and cause a malfunction of the controller. In essence this means that the pure derivative is not the ideal element to use in practical situations. It is common practice to use a fixed value of γ ; however, it is possible to use γ as a design parameter for the purpose of compensating for a zero of the transfer function of the process (Mituhiko [3]). Zeroes are the roots of the numerator polynomial of the transfer function.

In the application of PID control there is a freedom of using the three functional elements in any combination. The combination of element(s) used is called the action mode of the

controller. Theoretically, there are seven action modes. In practice though, the most common five are listed in Table 2.1 on the next page, with the revised transfer function depending on the structure of the controller.

Table 2.1: Proportional, Integral, and Derivative Action Modes

Action Mode	Element(s) Used	Transfer Function C(s)
Proportional (P)	P element Only	$C(s) = K_p$
Integral (I)	I element Only	$C(s) = \frac{K_p}{s}$
Proportional-Integral (PI)	P and I elements	$C(s) = K_p \left(1 + \frac{1}{T_I s}\right)$
Proportional-Derivative (PD)	P and D elements	$C(s) = K_p (1 + T_D D(s))$
Proportional-Integral-Derivative (PID)	All Elements	$C(s) = K_p \left\{1 + \frac{1}{T_I s} + T_D D(s)\right\}$

2.4.2 Step Response of PID Control

The unit step function $f_{step}(t)$ is defined by

$$f_{step}(t) = \begin{cases} 0 & t < 0 \\ 1 & t \geq 0 \end{cases}$$

The response $y_{u, step}(t)$ of the process variable to the unit-step manipulated variable $u(t) = f_{step}(t)$ directly added to the process at rest is called the step response of the process (Araki M.). The process is considered to be self regulatory if the step response converges to a finite value K when $t \rightarrow \infty$, while K is described as stationary gain. Figure 2.2 illustrates the step response of a process with self-regulation.

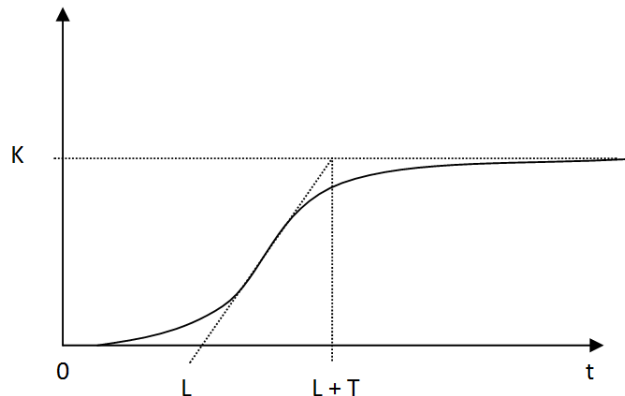


Figure 2.2: Step response of a process with self-regulation

Now if the step response of the process deviates when $t \rightarrow \infty$, the process is considered to be without self-regulation. If the step response of the process approaches a straight line

with slope R and the process is without self-regulation the process is then considered to be integrating. Figure 2.3 illustrates the step response of an integrating process.

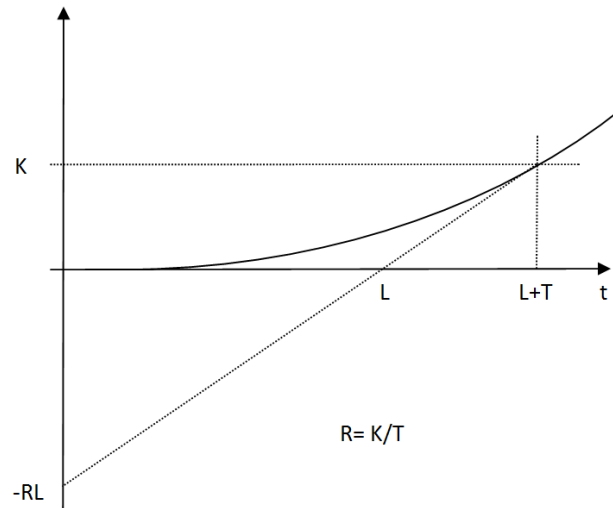


Figure 2.3: Step response of an integrating process

Observations have shown that step responses of many processes to which PID controllers are applied have monotonically increasing characteristics as shown in Figure 2.2 and 2.3 (Mituhiko [3]). Therefore, most traditional design methods for PID controllers have been developed implicitly assuming this property. However, it must be noted that some processes exhibit oscillatory responses to step inputs.

Another design method, with a more basic assumption, is linearity. If the process is at rest at the initial instant this means that the response of the process variable to inputs $u_1(t)$ and $u_2(t)$ are, respectively $y_1(t)$ and $y_2(t)$, then its response to the summed-up input $u_1(t) + u_2(t)$ becomes $y_1(t) + y_2(t)$ (Mituhiko [3]). It is generally accepted in systems theory that linearity approximately holds true in small ranges of variables, while the approximation error increases as the range increases. This expectation however can upset a process. At times a process response to a negative step is largely different from the inverse of the response to the positive step. Even with this reality, the linearity assumption is widely employed. The reasons being, that first it is difficult to establish a practically tractable general method without this assumption, secondly because research shows that the design results work approximately well for many processes, and thirdly because the trial-and-error adjustments are always needed, and the nonlinear property can be considered in that procedure (Mituhiko [3]).

With these assumptions, a new model can be constructed for the transfer function of a process. The simplest model for a process with self-regulation is shown in Equation 2.4.

$$P(s) = \frac{K}{1 + Ts} e^{-Ls} \quad 2.4$$

This model is known as the “first-order-lag + pure-delay” model, since $\frac{K}{1+Ts}$ is the transfer function of the first-order-lag element whose stationary gain is K and time constant is T, and e^{-Ls} is that of a pure delay whose delay time is L (Mituhiko [3]). The simplest model for a process with integration, which is shown in Equation 2.5, is known as the “integrator + pure-delay” model. Equation 2.6 gives the formula for determining “R” in Equation 2.5.

$$P(s) = \frac{R}{s} e^{-Ls} = \frac{K}{Ts} e^{-Ls} \quad 2.5$$

$$R = \frac{K}{T} \quad 2.6$$

Since the parameters of the second expression are redundant by one there is no mathematical way to determine them uniquely (Mituhiko [3]). Nevertheless, this expression can still be used with the understanding that the parameter T is the time constant of the process. T is considered the time constant first in order to make the denominator Ts dimensionless and secondly in order to make the equation giving the steepest slope of the reaction curve the same as that for the first-order-lag + pure delay model (Mituhiko [3]).

Chapter 3: Initial System Design

In this chapter, a discussion of the initial system design will be given. Included in this discussion will be the facilities, hydraulics, electrical, and control system. In addition, the methodology for testing and the results will be given with supporting appendices.

3.1 Lab Facilities and Platform Layout

The platform simulator is located in Durham 197. The lab contains all the equipment needed to operate the platform. The platform is surrounded by three hydraulic lifts, which actuate the platform with three degrees of freedom (DOF). On the north side of the lab the hydraulic power unit and valves that provide flow of hydraulic fluid can be found. The “soft” start and emergency shut off buttons switch electrical power to the hydraulic power unit. On the closest side to the door, are located the LabVIEW computer and the emergency stop button. The LabVIEW computer controls the proportional hydraulic valves, while the emergency stop button is used to shut off power to these valves in case of an emergency. An approximate layout of the equipment is illustrated in Figure 3.1.

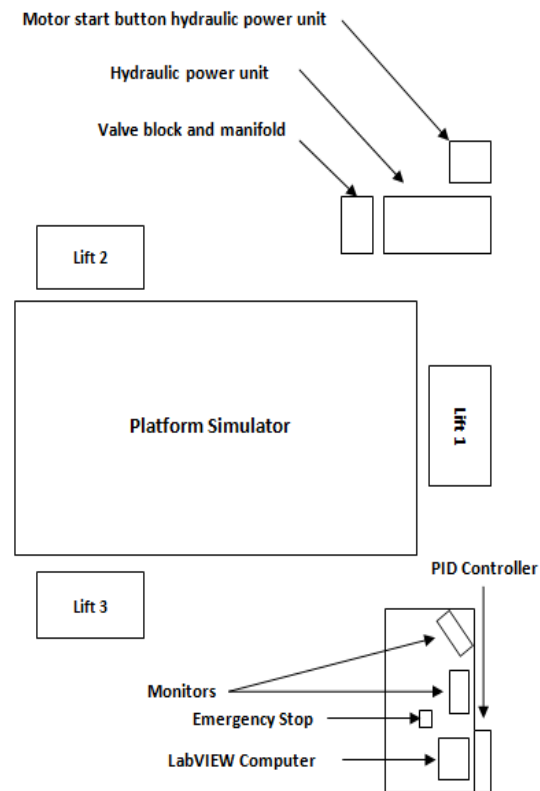


Figure 3.1: Lab Facility and Platform Layout

3.2 Hydraulic System

Power to operate the platform comes from pressurized hydraulic fluid. Proportional valves allow hydraulic fluid to be pumped into the lift cylinders to raise the platform. The same valves allow hydraulic fluid to flow back out of the cylinders into a tank as gravity

forces the platform down. The proportional valves operate with an input signal ranging from -10 V DC to +10 VDC. At -10 V the valves are fully open in the drain direction and the lifts lower. At +10 V the valves are fully open in the raise direction and the lifts elevate.

The system is designed to operate at up to 1500 psi. The weakest link in the system is the largest hydraulic feed or pressurized hose, which is rated at 1800 psi. The system is set to operate at 900 psi, as this pressure is adequate to operate the platform and provides a large safety margin. The operating pressure is set on the hydraulic pump, which is a variable displacement constant pressure pump. The flow of the pump varies to maintain the set pressure.

The hydraulic pump is driven by a 40 HP 440 V 3 phase AC motor. The motor soft start control, located on a pedestal next to the power unit, starts the motor without drawing excessive current and provides for emergency shut off of the motor. For all emergency situations not directly related to the pressurized hydraulic fluid, hydraulic pump, or drive motor, the emergency stop button on the computer desk should be used. This emergency stop button shuts off power to the proportional valves. If the emergency stop for the motor is hit, power is cut off from the motor and the pump will stop. Once this emergency stop is pressed it must be pulled to the out position before platform operation may continue.

Figure 3.2, illustrates how the hydraulic components are connected. Pressurized hydraulic fluid flows in a common manifold to each proportional valve. A gauge on the manifold registers the pressure of the fluid. The proportional valves control the flow to and from the lifts

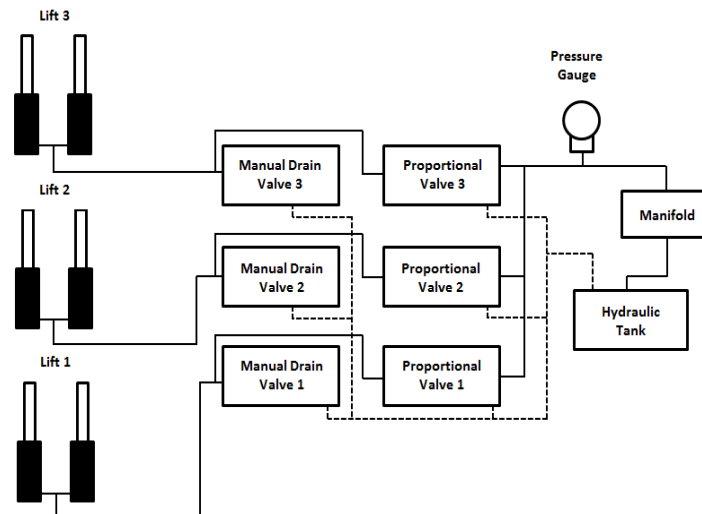


Figure 3.2 Hydraulic Components

individually. Flow from the lifts passes through the respective proportional valve and into the low pressure side of the common manifold, and from there back to the hydraulic tank. Manual drain valves were included to have a means of lowering the platform in an emergency. When opened hydraulic fluid flows from an individual lift, through the corresponding manual drain valve, into the common low pressure manifold and then to the tank.

3.3 Electrical Signal System

The electrical system which transfers signals related to platform control can be divided into four different sections.

- 1) The PD controller which uses output from the VI to control the platform position.
- 2) The feedback section which provides feedback of lift position to the PD controller and VI.
- 3) The valve signal section which sends a signal to the proportional valves.
- 4) The valve power and over-tilt safety system which provides power to the valves and shuts off power to the valves in emergency situations.

The hub of these electrical systems is mounted to a board on the wall over the operator desk, which layout of the components is shown in Figure 3.3. The project power supply provides +15 V DC and -15 V DC to the PD controller as well as +5 V DC to the string potentiometers. The 24 V DC power supply is mounted to the board, which power the proportional

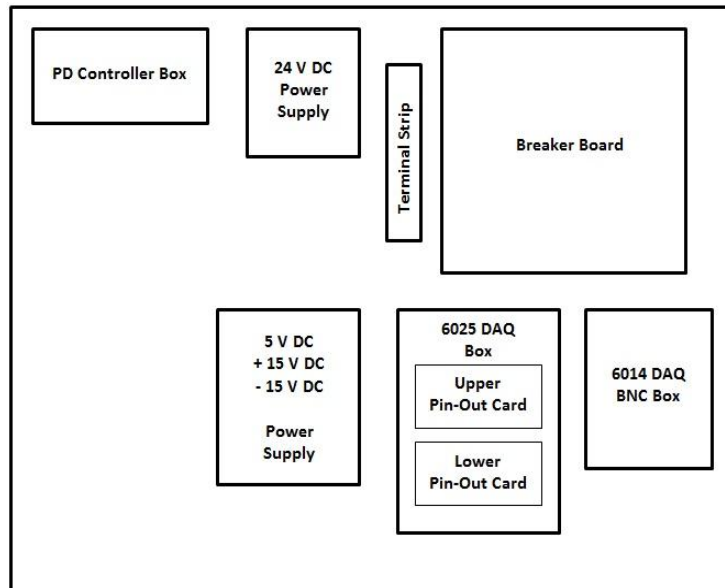


Figure 3.3: Electrical Components

vales. The terminal strip allows for connections with the breaker board. The breaker

board uses relays to shut power on or off to the proportional valves. The two DAQ cards provide connections with LabVIEW. While the PD controller takes inputs from the LabView VI, the string potentiometers send output signals to the proportional valves to control the platform position.

The displacements of the three hydraulic lifts are measured with string potentiometers mounted on the lifts. These potentiometers are each wired for power and signal, as shown in Figure 3.4. All three of the feedback signals from the string potentiometers feed into the PD controller. The signals from the string potentiometers also feed into the 6014 DAQ card. The connections are shown in Figure 3.5. The potentiometers are fed 5 V DC and return a fraction of that voltage proportional to the displacement of the lift. Power for the string potentiometers comes from the 5 V DC output on the power supply via a terminal strip within the PD controller box. The return signal from the three potentiometers is fed into the PD controller as well as three analog input channels on one of the two DAQ cards. The specific connection of these signal wires is shown in Figure 3.6.

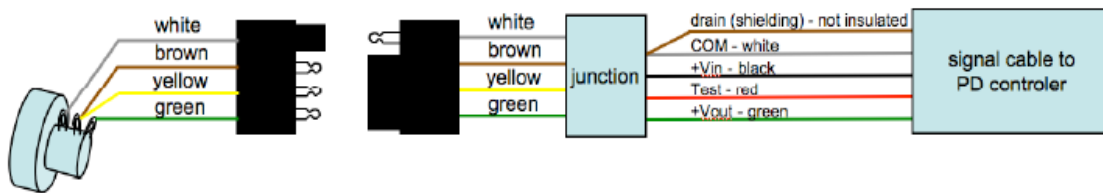


Figure 3.4: Potentiometers

Figure 3.4 illustrates the standard four prong towing connectors that were used as a disconnect near the string potentiometers on the lifts. A shielded data cable was used to run the signal and power wires from the string potentiometers to the PD controller box.

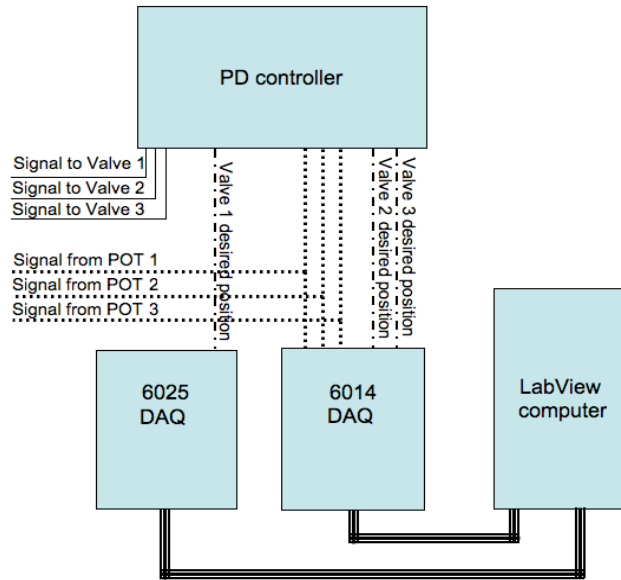


Figure 3.5: Potentiometers Signal Feed

Figure 3.5 illustrates the signals from the string potentiometers that feed into the PD controller as well as the 6014 DAQ card. The DAQ cards sends the desired position signals to the PD controller which then sends control signals to the proportional valves.

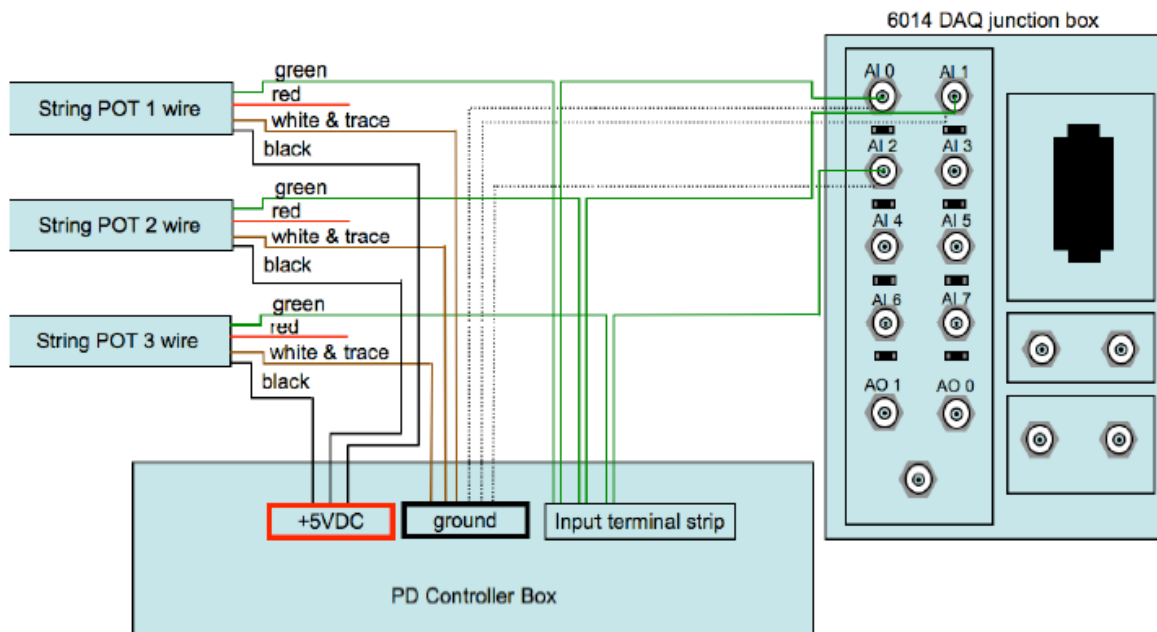


Figure 3.6: Signal Wire Connections

Figure 3.6 illustrates how signal wires from the string potentiometers connect to the PD controller as well as three analog input channels on the 6014 DAQ card. Power for the

string potentiometers is provided by a 5 V DC power supply via terminal strips within the PD controller box.

The signal for the valves is generated by the PD controller using an input signal from LabVIEW. It varies from -10 V DC to +10 V DC. Electronics within the proportional valve amplify the signal to actuate a solenoid which positions the valve spool. Positioning signals for valves 1 and 2 are from the 6014 DAQ card, while the signals for valve 3 come from the 6025 DAQ card. The connections for these outputs are shown in detail in Figure 3.7.

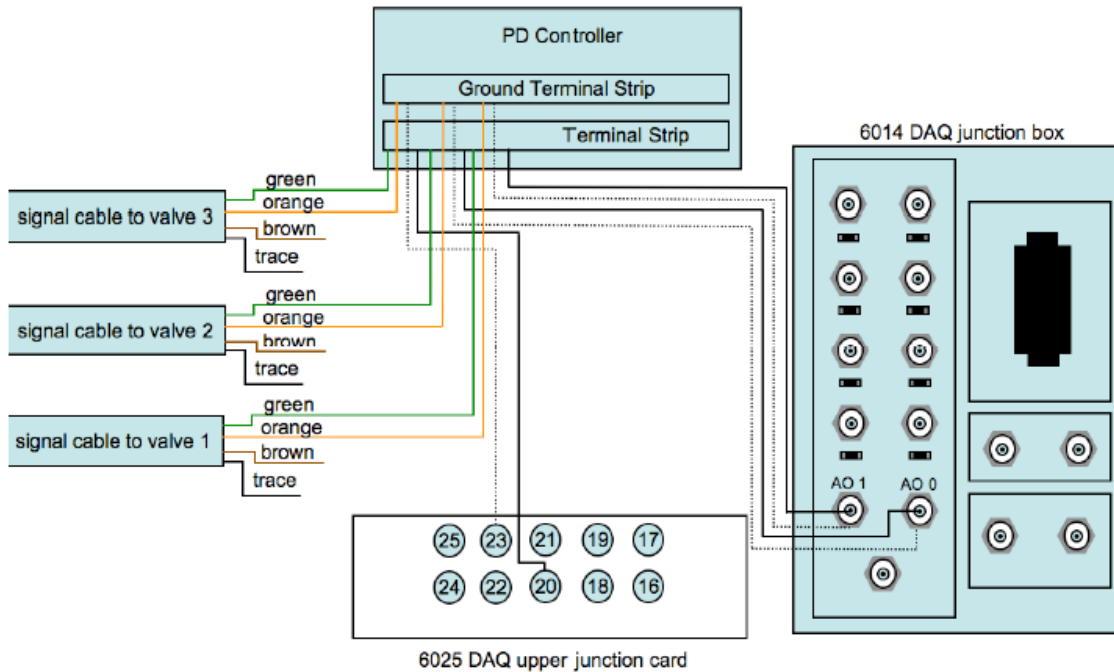


Figure 3.7: Positioning Signal Wire Diagram

Figure 3.7 illustrates how the two analog outputs on the 6014 DAQ upper junction card are used for the desired positioning signals to valves 1 and 2. The desired positioning signal for valve 3 comes from the 6025 DAQ.

As previously mentioned the valves are powered by a 24 V DC power supply. Without this power the valve's internal amplifier will not activate the valve solenoid and the spools center, thus blocking all flow. Because of this, cutting off power to the valves is a very effective way of stopping the platform in an emergency. Power to the valves is

switched on by a set of three relays. A schematic for the relays and breaker board is shown in Figure 3.8. The solenoids are connected to over-tilt switches mounted under the platform, which are wired in series and are normally closed. This wiring diagram is shown in Figure 3.9.

If the platform tilts more than 10 degrees in roll or pitch, one of the over-tilt switches will open. With one or more switches open the relays will shut off power to the valves and the platform will be hydraulically locked in position. Additionally, power from the 24 V DC power supply must first pass through an emergency stop button on the desk near the LabVIEW computer before it is fed to the over-tilt switches, relays, or valves. The wiring diagram for this is shown in Figure 3.10. Hitting this emergency stop button also freezes the platform. In the event that the platform is frozen or locked in position, once the emergency stop is depressed and LabVIEW is stopped, the platform can be manually lowered using the small metering valves on the valve block.

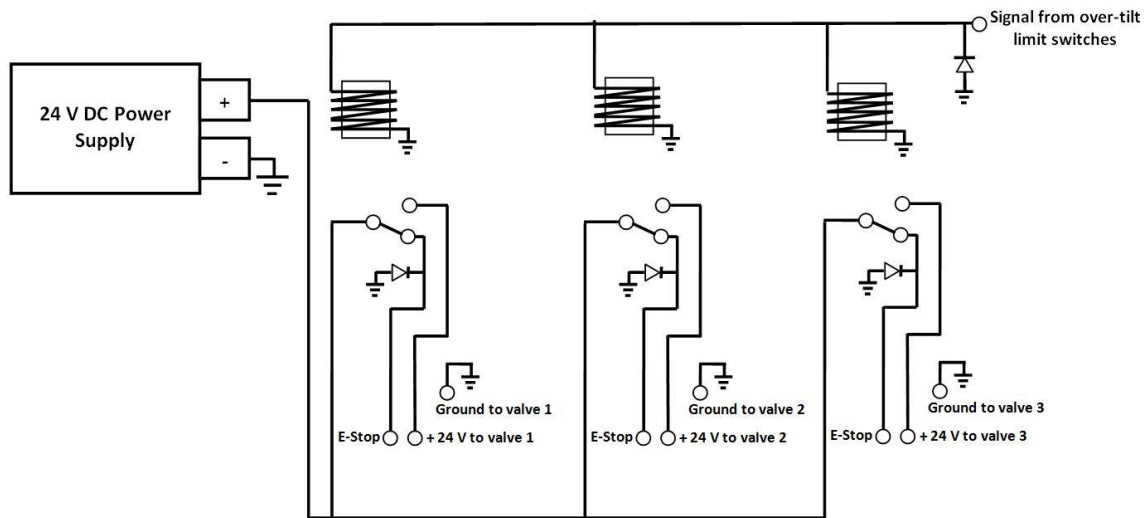


Figure 3.8: Relay and Breaker Board Diagram

Figure 3.8 illustrates how the three relays are mounted to the circuit board and how they disconnect the power to the proportional valves in the event of platform over-tilt.

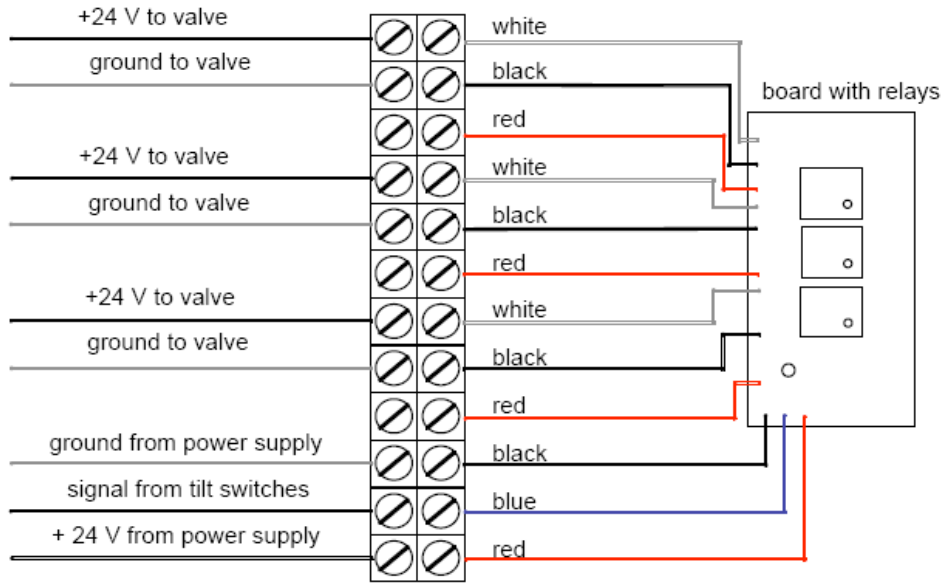


Figure 3.9: Switches Wiring Diagram

Figure 3.9 illustrates the set of relays that cut off power to the valves if any tilt switch is triggered. These signals and power connections are made on a connector strip.

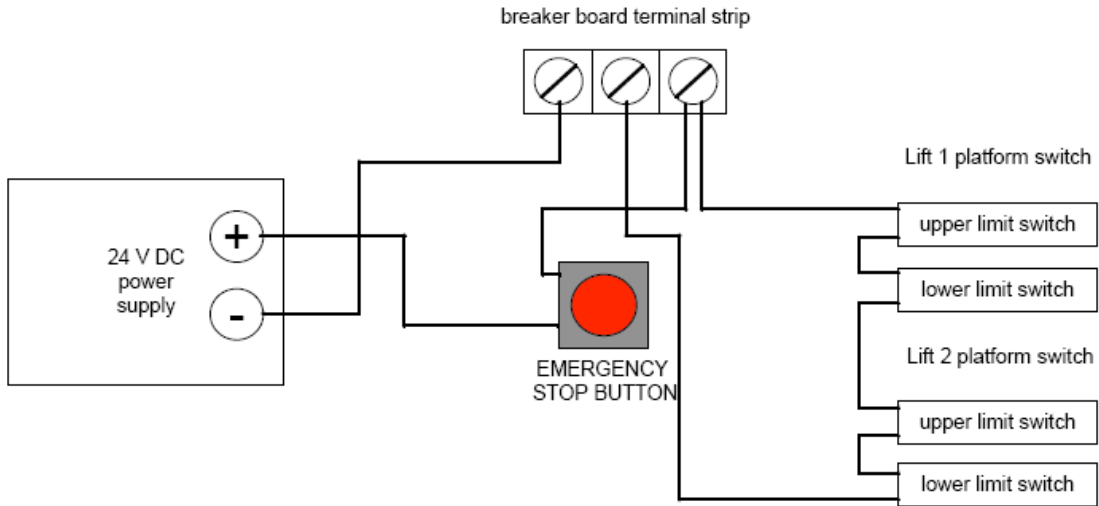


Figure 3.10: Emergency Stop Wiring Diagram

Figure 3.10 illustrates how the power is wired to the relays and how the emergency stop button, located on the desk with the LabVIEW computer, can shut off the proportional valves.

3.4 LabVIEW Virtual Instrument Design

The initial LabVIEW Virtual Instrument (VI) was designed to help control the movement of the platform by providing signals to an external PD controller, which corresponded to the desired lift position. Because the VI was complicated and was running on an intricate machine and operating system, safety precautions external to the computer had to be put in place.

More detail on the construction of the VI can be found in Section (3.4.4) Data Representation. However, a few basics should be noted about the four different operating methods the VI used for platform control.

- 1.) In manual control the platform could move up and down, while level, by a slide control located on the front panel of the VI.
- 2.) In time-series control the VI read-in heave, pitch, and roll data from a comma separated value (csv) file to operate the platform.
- 3.) In wave control the VI generated oscillations of set frequencies and magnitudes to control the heave, pitch, and roll of the platform.
- 4.) The platform could be momentarily perturbed by a set amount using the perturb button on the front panel.

It was very important for the operator to understand that these control methods all added to the output. That is, manual slide control, time series control, wave control, and perturbation control were all separate signals which summed to form the output signal. The operator had bear in mind what could happen when those signals were summed, such as an unexpected jump in height or over-tilt.

3.4.1 Platform Over-Tilt

In any VI, the platform was designed to tilt to a maximum of 10 degrees in both pitch and roll. Beyond this angle, the three bearings which join the platform to the hydraulic lifts would bind causing possible damage or breakage to the joints. Therefore, measures were put in place to prevent this from occurring.

First, the roll and pitch values used in the motion csv input file were limited to 10 degrees or less. Second, limit switches were located on the underside of the platform at the number one and number two bearings. If the platform tilted by more than ± 10 degrees in pitch or roll, one of the limit switches would be activated. These limit switches were wired in series, as previously mentioned, which allowed current to continually flow through all the limit switches and activate the relays. The relays provided power to the hydraulic proportional valves. If a limit switch is tripped, the relays stopped providing power to the proportional valves. The valves would then center and fluid would not flow in or out of the hydraulic lifts. With the lifts locked, over-tilt was prevented.

With the platform locked in position, it was then necessary to manually lower the platform. This could be done with the three small metering valves on the valve block located near the hydraulic pump. When manually lowering the platform there was no over-tilt prevention, therefore, care had to be taken by the operator. If LabVIEW and the PD controller were left running and power was still supplied to the proportional valve relays and tilt switch circuits, the proportional valves would activate again as soon as the platform came back within the tilt range. Therefore, the LabVIEW VI had to be stopped manually and more importantly, power had to be cut off to the proportional valve relay circuit before manually lowering the platform.

Power could be cut off from the proportional valves, proportional valve relays, and tilt switch circuit by depressing the emergency stop button located near the LabVIEW computer. When this emergency stop button was depressed the proportional valves centered and the platform was locked in position, however, LabVIEW continued to run. This meant that once the platform was unlocked from the over-tilt position the entire test sequence had to be restarted.

The emergency stop button located beside the hydraulic pump power supply would only cut power off to the hydraulic pump. Even with the hydraulic pump off, the platform could tilt and fall. Safety procedures called for both emergency stop buttons to be depressed before any attempts to manually lower the platform.

3.4.2 Operator Error with the VI

When operating the platform with the LabVIEW VI and PD controller it had to be remembered that the VI only operated the valves with a given position input. If one input differed from the next by several feet the PD controller would attempt to reposition the platform almost instantaneously in accordance with the PD parameters. For this reason the operator had to plan ahead and predict how the platform would respond to changes in operation. In the initial VI, visual representation of each string pot was shown on the front panel.

3.4.3 Data Collection

Data was collected through the use of string potentiometers and a feedback file on the VI. As the platform performed the motion csv file the string potentiometers would send data back to the LabVIEW and store it in a feedback csv file on the desktop. The data collected was separated into columns by each lift, which allowed the data to be separated into roll, pitch, and heave.

3.4.4 Data Representation

A VI created in LabVIEW operated the platform in conjunction with an external analog PD controller. The VI sent a position signal for each lift to the PD controller. The controller then used the position feedback from the string potentiometers mounted on the lifts to generate a voltage signal which controlled the proportional valves. The proportional valves regulated hydraulic flow to and from the lifts in proportion to the signal from the PD controller. The string potentiometer feedback signals ranged from 0 V DC to 5 V DC. The desired position signals from the DAQ to the PD controller ranged from -10 V DC to 10 V DC. The signals from the PD controller to the proportional valves ranged from -10 V DC to 10 V DC. To center the platform about the center of gravity of the ship a math script was used to build a transformation matrix. Please review Appendix E for this matrix.

In LabVIEW, programming VI's are created with front-panels and back-panels. For a detailed description of the front panel and back panel refer to Appendices A and B. The

graphical code of the VI for controlling the platform consisted mainly of a loop. While the VI was running the loop iterated at a set frequency of 1 kHz. The signals for manual slide control, time series control, wave control and perturbation were all generated within the loop. The summed final output signal was updated and sent to the PD controller with each iteration of the loop.

3.4.5 Characterization of the PD Controller

In order to characterize the response of the system, the theory of an ideal second order system had to be analyzed. The ideal mass-spring-damper system with a mass m , spring constant k , and viscous damper of damping coefficient b , shown in Figure 3.11 on the following page, can help derive the second order system.

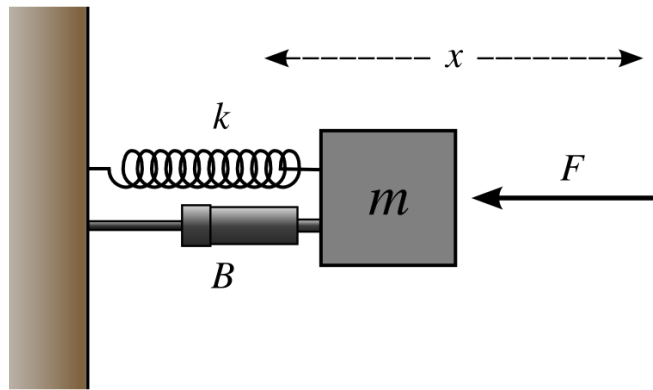


Figure 3.11: Mass-Spring-Damper

The system can be described by:

$$F_s = -kx \quad (3.1)$$

$$F_d = -cv = -c\dot{x} \quad (3.2)$$

$$F_d = -c \frac{dx}{dt} \quad (3.3)$$

Treating the mass as a free body and then applying Newton's 2nd law, we derive;

$$\sum F = ma = m\ddot{x} = m \frac{d^2x}{dt^2} \quad (3.4)$$

where;

a is the acceleration of the mass

x is the displacement of the mass relative to a fixed point

These equations can then be combined to form the equation of motion, a second-order differential equation for displacement x as a function of time t .

$$m\ddot{x} + c\dot{x} + kx = 0 \quad (3.5)$$

$$\ddot{x} + \frac{c}{m}\dot{x} + \frac{k}{m}x = 0 \quad (3.6)$$

In order for simplification of this equation w_n and ζ must be defined as;

$$w_n = \sqrt{\frac{k}{m}} \quad (3.7)$$

$$\zeta = \frac{c}{2\sqrt{km}} \quad (3.8)$$

The first parameter, w_n , is known as the undamped natural frequency of the system. The second parameter, ζ , is known as the damping ratio. The natural frequency represents an angular frequency expressed in rad/s, while the damping ratio is a dimensionless quantity. Once the proper substitutions are made the differential equation then becomes;

$$\ddot{x} + 2\zeta w_n \dot{x} + w_n^2 x = 0 \quad (3.9)$$

With this the ideal second order transfer function can be defined as;

$$G(s) = K \frac{w_n^2}{s^2 + 2\zeta w_n s + w_n^2} \quad (3.10)$$

where;

K is the system's gain

w_n is the system's natural frequency

ζ is the system's damping ratio

3.4.5.1 Block Diagram the System

In order to properly characterize the initial platform controller the closed-loop feedback diagram of the system had to be determined and analyzed. The system is represented in Figure 3.12

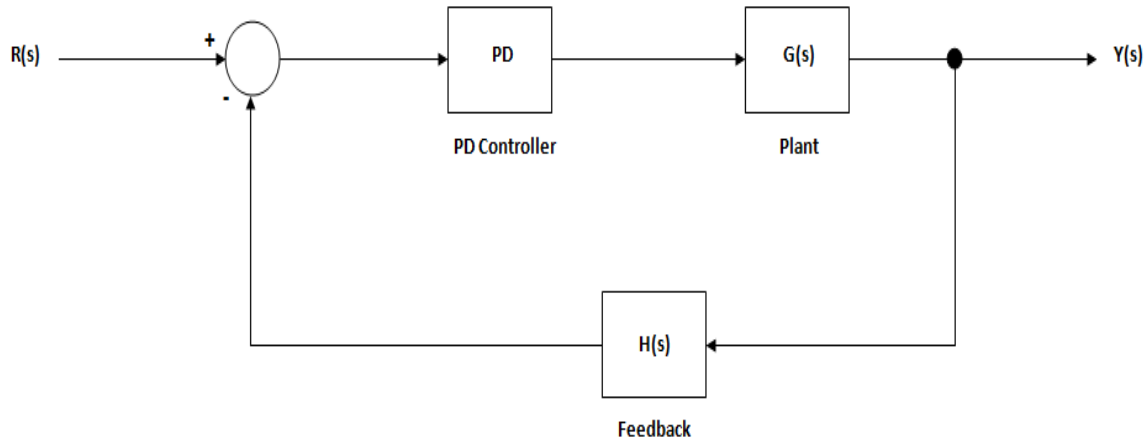


Figure 3.12: Platform Feedback Diagram

The feedback, $H(s)$, in the closed loop system is considered to be in unity. Therefore, $H(s) = 1$ and the closed loop system takes the configuration shown in Figure 3.13.

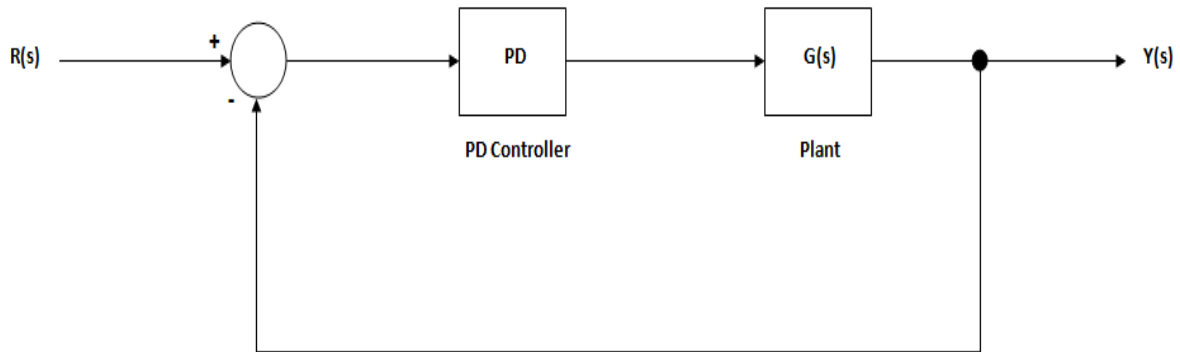


Figure 3.13: Modified Platform Feedback Diagram

With the modified closed loop feedback diagram the transfer function can be determined. First, the PD controller is determined to be:

$$G_c(s) = K_P + K_D(s) \quad (3.11)$$

Next, for the plant we use Equation 3.10. With this we are able to define our transfer function of the system as:

$$T(s) = \frac{G_c(s)G(s)}{1 + G_c(s)G(s)} \quad (3.12)$$

$$T(s) = \frac{(K_P + K_D s) \left(\frac{w_n^2}{s^2 + 2\zeta w_n s + w_n^2} \right)}{1 + (K_P + K_D s) \left(\frac{w_n^2}{s^2 + 2\zeta w_n s + w_n^2} \right)} \quad (3.13)$$

$$T(s) = \frac{(K_P + K_D s) w_n^2}{(s^2 + 2\zeta w_n s + w_n^2) + (K_P + K_D s) w_n^2} \quad (3.14)$$

3.4.5.2 Determination of K_P and K_D Values

The actual gain values for the initial platform controller were never determined. Instead, the controller could be manually tuned according to resistance values. The proportional gain value could have a resistance value from 0 k Ω to 50 k Ω on lift 1 and 0 to 100 k Ω on lift 2 and 3. The reason behind lift 1 having a lower adjustable rate than the other lifts was that initial testing showed that lift 1 had a higher response than lift 2 and 3. Therefore, the proportional gain only needed to be half the value for lift 1 than that of lift 2 and 3. The derivative gain resistance, which controlled overshoot, could be adjusted on each lift from 0 to 50 k Ω . Figure 3.14, illustrates how the PD controller was constructed.

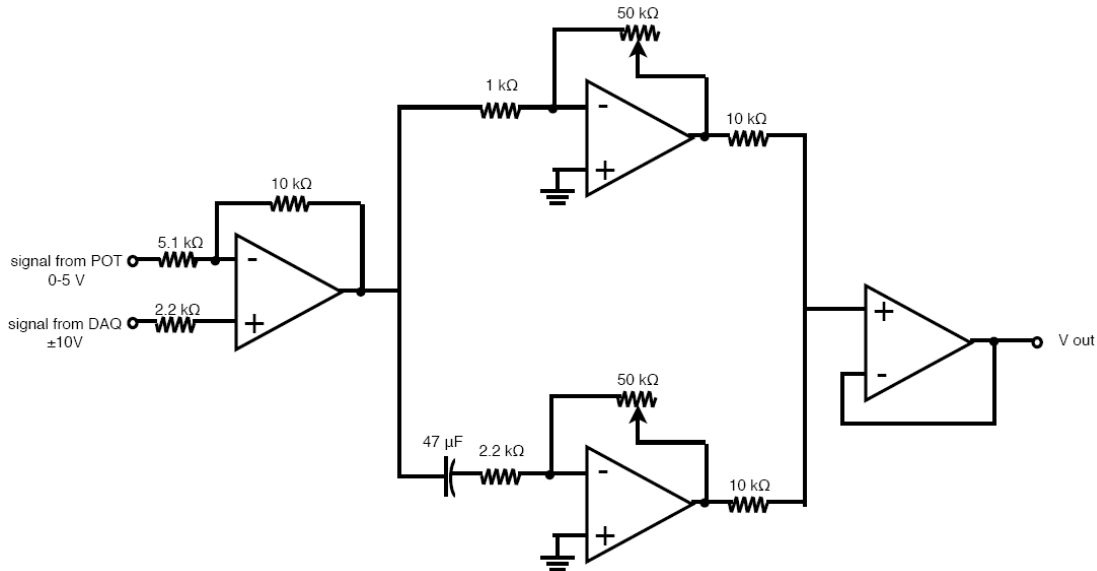


Figure 3.14: PD Controller Schematic Diagram

3.4.6 PD Controller Response Test

A number of tests were run on the platform to determine the response using an external PD controller. Previous tests using an internal PID controller, that LabVIEW implemented, showed poor response. The belief was that the current setup, at that time, had a memory leak from the

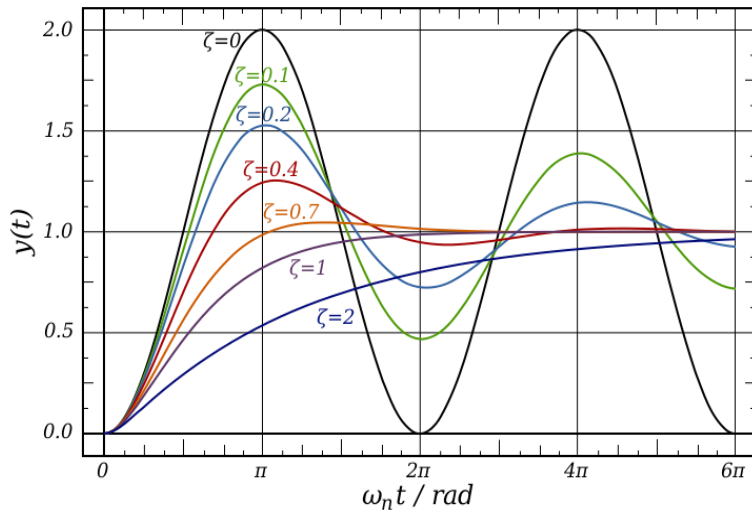


Figure 3.15: Damping Coefficients

desktop. So, to relieve some of the load an external PD controller was implemented. Once the new controller was completed a square wave test and sine wave test were completed. Even though the K_P and K_D values were unknown, the goal was to obtain a critically damped system. This meant that the system damping ratio, ζ , would be equal to one and that the system would have no oscillation. Figure 3.15, illustrates the various damping coefficients with 1 being considered critically damped, 2 over damped, and anything below 1 under damped.

3.4.6.1 Square Wave Response Test

Initial testing consisted of a 2 minute square wave input file with a maximum height of 25 inches. The data input informed the platform to rise to a height of 20 inches and stay there for approximately 20 seconds before raising a additional 5 inches. Once the data input reached this height a constant 25 inch height was feed into the platform for approximately 30 seconds. The platform repeated this process twice before it lowered back down into the resting position. During this two minute run the data output from the platform was feed back into the desktop and stored. The graphical input file is illustrated in Figure 3.16.

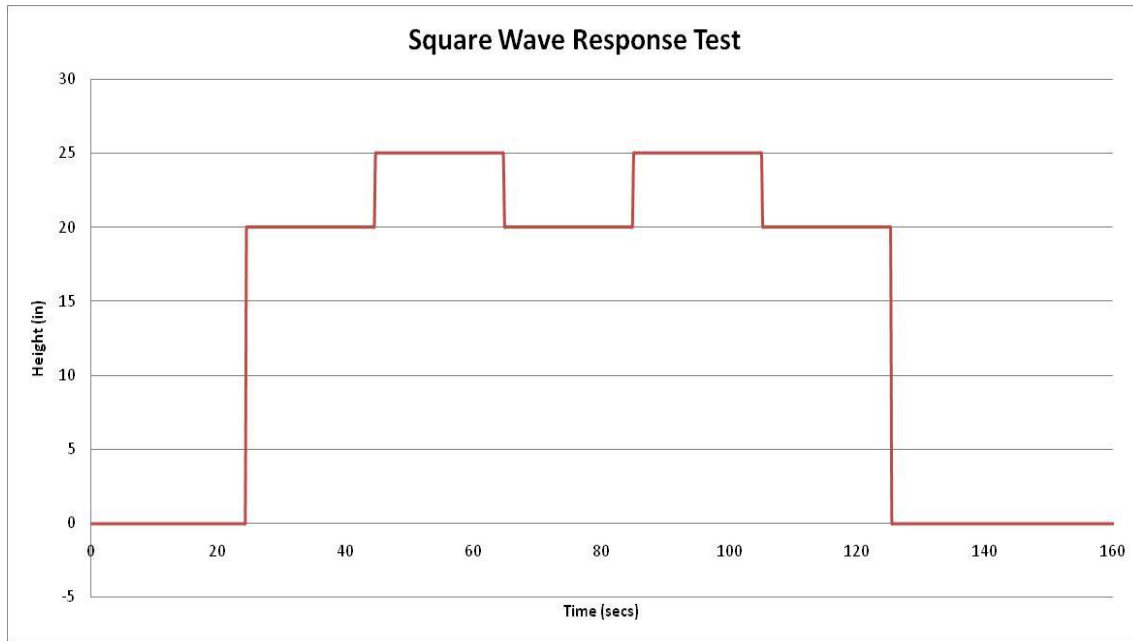


Figure 3.16: Square Wave Test Input

3.4.6.2 PD Controller Square Wave Response Result

The square wave response test was run for four different derivative values, which were 0 k Ω , 10 k Ω , 30 k Ω , and 50 k Ω . The proportional gain value, which made a change to the output that was proportional to the current error value, was kept at a value of 100 k Ω for all three lifts. Figures 3.17 and 3.18, on the next page, show the results from the square wave test.

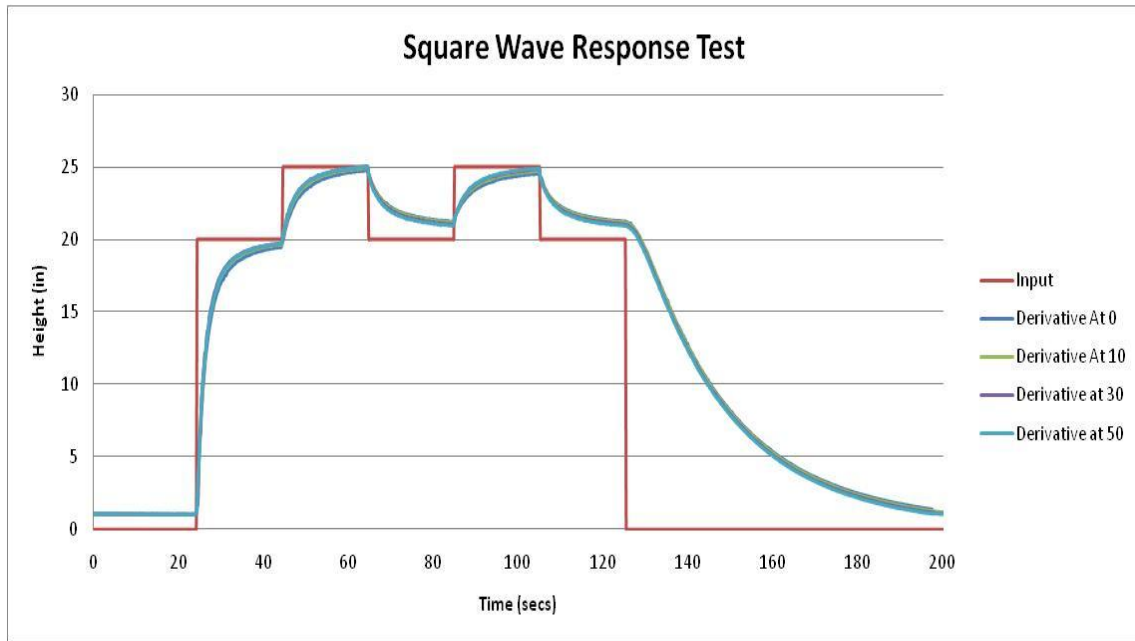


Figure 3.17: Square Wave Response Test with All Derivative Values

Figure 3.17, shows the overall results for the four different derivative values. A better view of these results can be found in Figure 3.18.

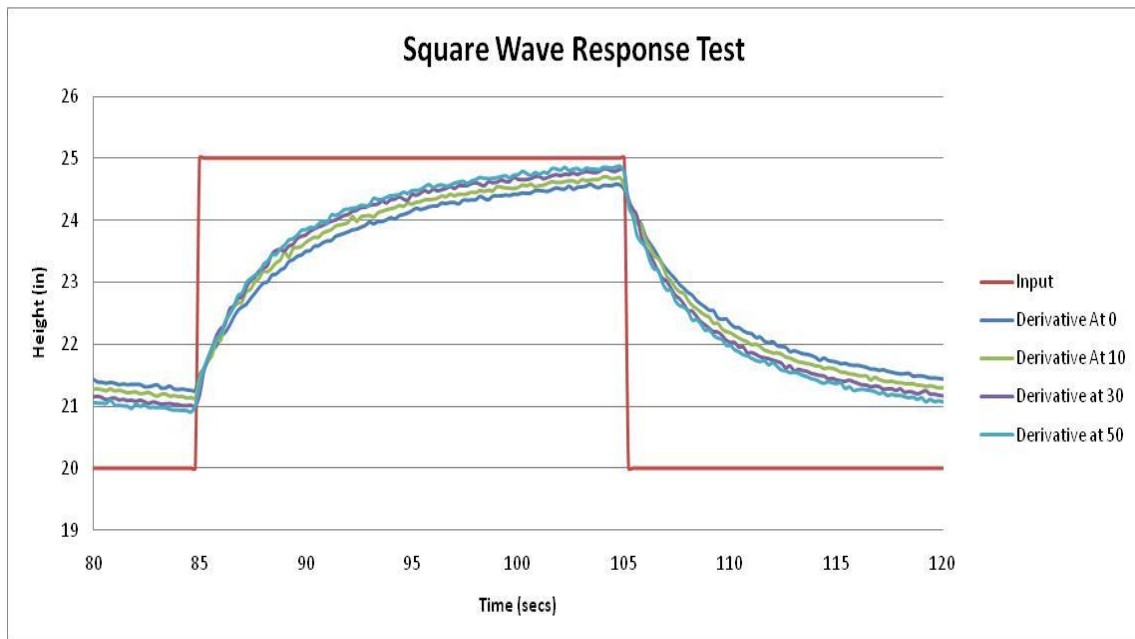


Figure 3.18: Close up of Square Wave Response Test with All Derivative Values

When comparing Figure 3.18 to the damping coefficient graph, Figure 3.15, the determination was made that the system was operating in the critically damped area of 1.

3.4.6.3 Sine Wave Response Test

Once the square wave test was completed a sine wave response test was run to characterize the response of the system. The test involved the use of various frequencies, which ranged from 0.01 Hz to 2.56 Hz. Initial testing showed that the platform became highly unstable at 2.56 Hz. Therefore, the actual testing and data collection of roll, pitch, and heave did not exceed 1.28 Hz for safety concerns. Figure 3.19, shows the graphical representation of the input data.

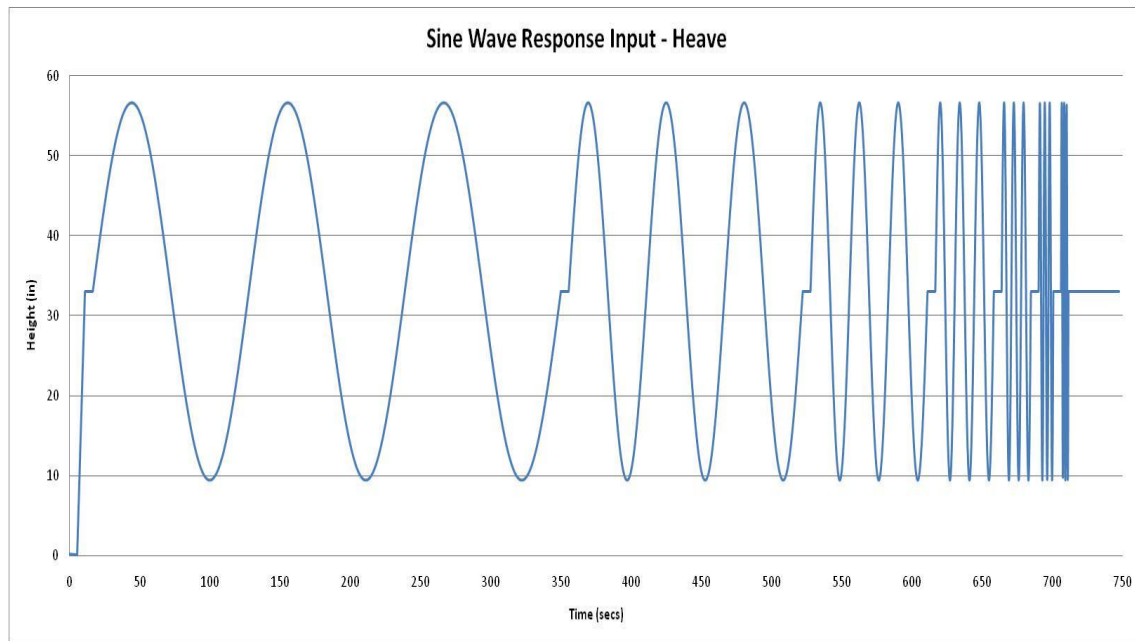


Figure 3.19: Sine Wave Response Input for Heave

In Figure 3.19, each frequency was given three waves with a short time for the platform to level off before the next set of frequencies was performed. The approximate time for completing a sine wave test was twelve minutes.

3.4.6.4 PD Controller Sine Wave Response Results

The tests were broken down into heave, roll and pitch. The sine wave frequency varied between 0.01 Hz to 1.28 Hz for roll and pitch and 0.01 Hz to 0.32 Hz for heave. As mentioned previously, the reason behind the testing never reaching the highest frequency, of 2.56 Hz, was due to safety concerns. Initial testing showed that heave was the most susceptible to instability at higher frequencies, since all three lifts were moving

simultaneously. When testing the sine wave response the derivative values were varied from 0 k Ω to 50 k Ω . Graphical results from the heave sine wave testing can be found in Figure 3.20. Please view Appendix C for a full page view of the roll, pitch, and heave sine wave graphical results.

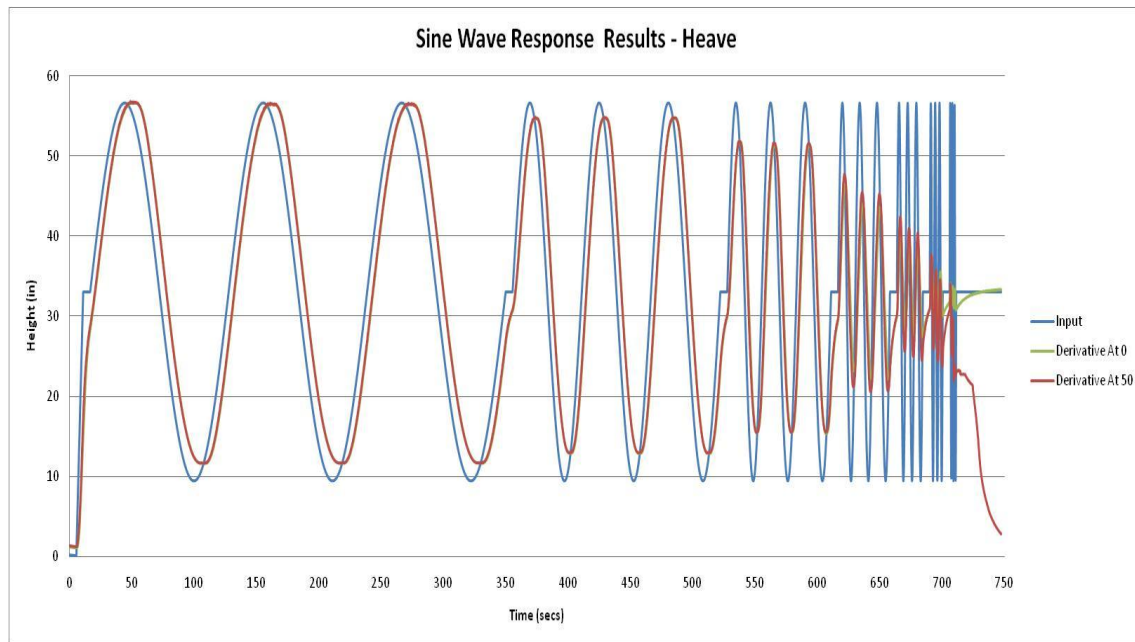


Figure 3.20: Sine Wave Response Heave Test with Max-Min Derivative

Figure 3.20, shows the results from the sine wave response test for heave varying from frequencies 0.01 Hz to 0.64 Hz. However, any data collected past 0.32 Hz, when the derivative was set to 50 k Ω , is considered null. The reason being, that the emergency stop was pressed when the platform began to show signs of instability. It can be seen from this figure that the platform is capable, under this controller, to maintain proper height at the lowest frequencies with only minimal lag. However, when the platform begins to encounter frequencies 0.04 Hz and above it is unable to keep the proper height. This means that instead of traveling the full 45 inch distance it begins to approximately drop 10 inches in total distance traveled per frequency.

3.4.7 PD Bode and Phase Plots

With the sine wave data collected and processed the next step was to create bode and phase plots of the response. In order to convert the data a series of steps had to be completed, which are listed as:

- 1.) Determine where each frequency began and ended.
- 2.) Determine the distance from peak to peak (period start to period end).
- 3.) Calculate the actual frequency from peak to peak.
- 4.) Calculate the displacement offset.
- 5.) Calculate the phase shift
- 6.) Determine the maximum and minimum displacement.
- 7.) Determine the reference amplitude.
- 8.) Calculate the amplitude (dB) value.

This process was completed for roll, pitch, and heave. The tables with equations and calculations can be found in Appendix D. The bode plot of each DOF at their maximum and minimum derivative values can be found in Figure 3.21, 3.22, and 3.23 on the following pages. Figures 3.24, 3.25, and 3.26 show the phase plots for each DOF.

A bode plots measures in the frequency domain much like an oscilloscope measures in the time domain. A bode plot has two parts, the gain curve and the phase curve. The gain curve displays the ratio of the output to the input in decibels or dB. Typically bode plots for motion systems have a gain of 0 dB at low frequencies and decline at higher frequencies. This is expected as output at low frequencies will precisely follow the input. However, once higher frequencies are encountered the motion system cannot keep up.

Responsiveness and stability can be read from a bode plot. Most of this information is in the gain plot. Responsiveness is usually measured by bandwidth. Higher bandwidth corresponds to faster settling times. Stability is measured in peaking; the characteristic where the gain plot first climbs a few dB before starting to fall. Peaking in the bode plot corresponds to overshoot in the scope plot. More than 1 or 2 dB is usually considered excessive. In the use of the phase plot, or phase curve, the change in degrees corresponds to a system's stability. Once a system begins to reach -180 degrees signs of instability may appear. It is once this threshold is passed that the system becomes unstable.

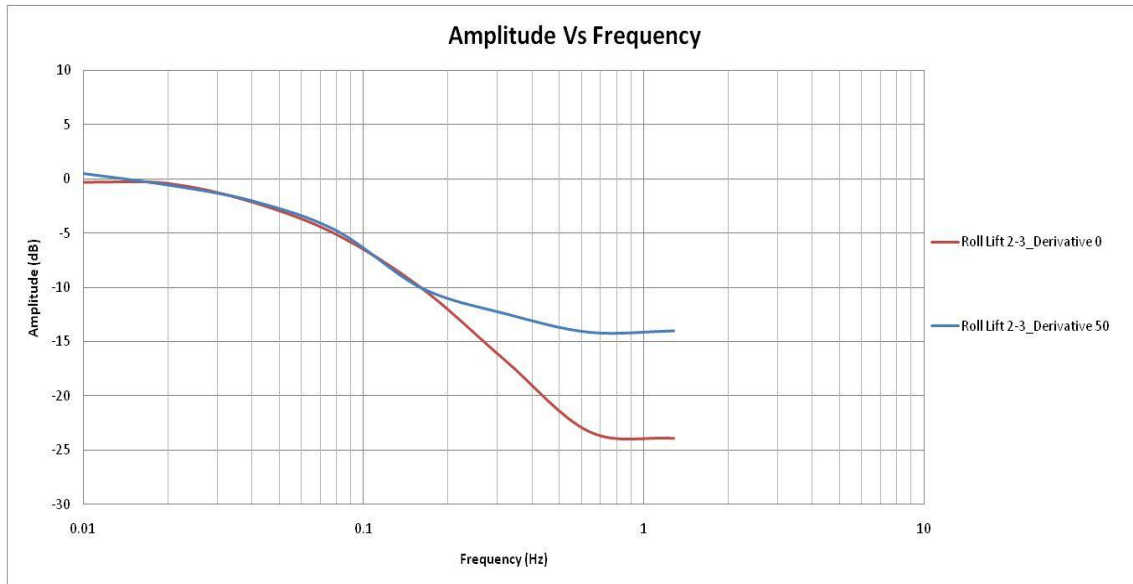


Figure 3.21: Roll Amplitude versus Frequency Test

Figure 3.21, illustrates the bode plot for the roll at the varying derivative values of 0 k Ω and 50 k Ω . The results show that at approximately 0.01 Hz the output of the system begins to differ from the systems input. After this point there is a gradual drop until approximately 0.64 Hz. At this point the system has reached a threshold at which any frequency above this will greatly differ the systems output from the input. Therefore, we are able to concluded that the maximum frequency the platform could possible perform in roll would be between the 0.64 Hz and 1 Hz range.

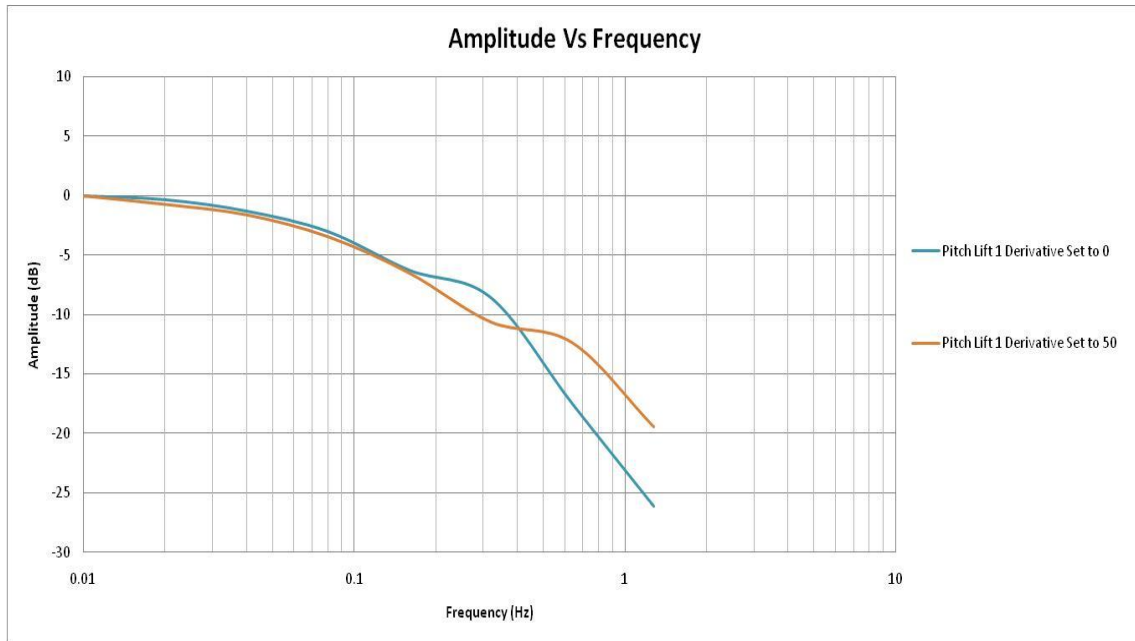


Figure 3.22: Pitch Amplitude versus Frequency Test

Figure 3.22, illustrates the bode plot data from the pitch test. As with the roll bode plot the steep drop in amplitude confirmed that at the frequencies 0.64 Hz to 1 Hz were the maximum frequencies and the platform began to encounter significant lag from the input to the output of the system. Please skip to the next page for the phase graphs.

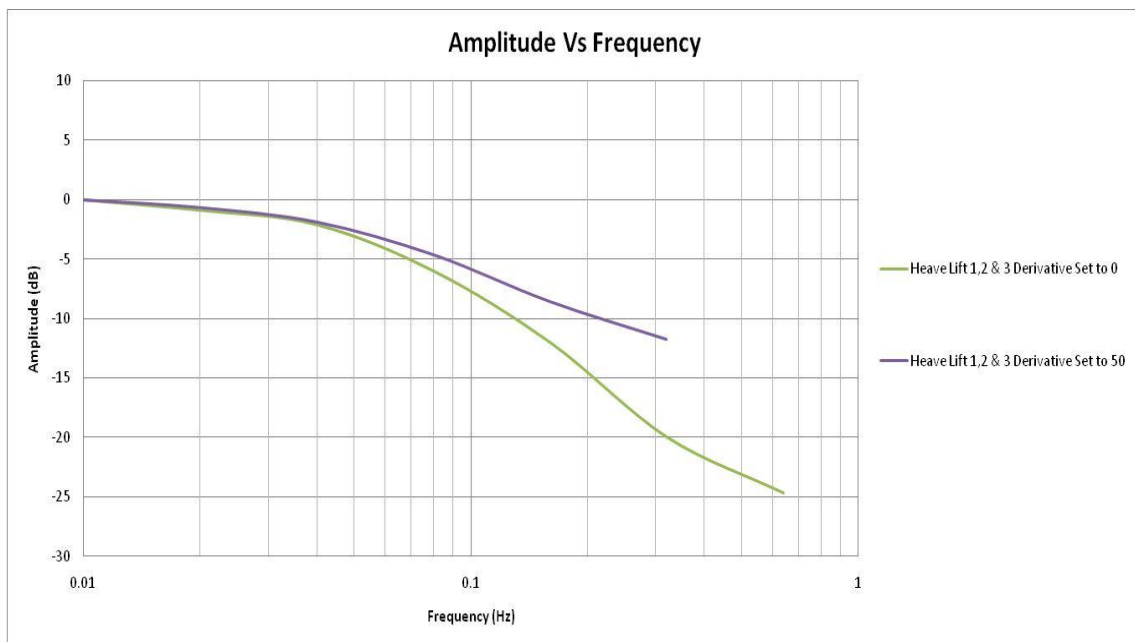


Figure 3.23: Pitch Amplitude versus Frequency Test

Figure 3.23, illustrates the bode plot for heave. As mentioned before, the tests for heave were unable to reach the same frequencies as that of roll and pitch. The results from the bode plot confirm that at approximately 0.32 Hz the platform begins to illustrate that the input differs from the output of the system.

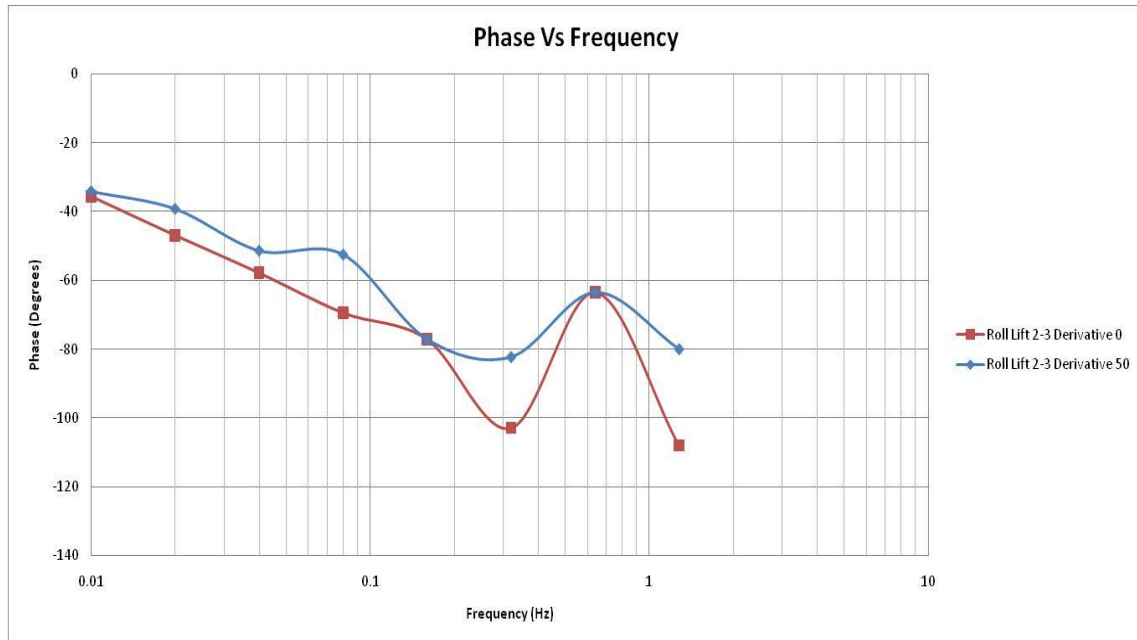


Figure 3.24: Initial Controller's Roll Phase Plot

Figure, 3.24 identifies the shifts in phase during the sine wave roll experiment. A general increase from 0.01 Hz to approximately 0.32 Hz is easily recognizable. This plot shows that during testing the amplitude of the platform begins to lag behind the input. At approximately 0.32 Hz the output is running behind 40 to 60 degrees, depending on the resistance. The figure gives us additional information about any instability within the system. The increase of phase at approximately 0.64 Hz hints of possible future instability. This quick ramp up in phase if extend would likely reach 180 degrees, which indicates that the system in creating a response from the system that is larger than the actual input. This means that the response will possibly spiral out of control until the system aborts or breaks.

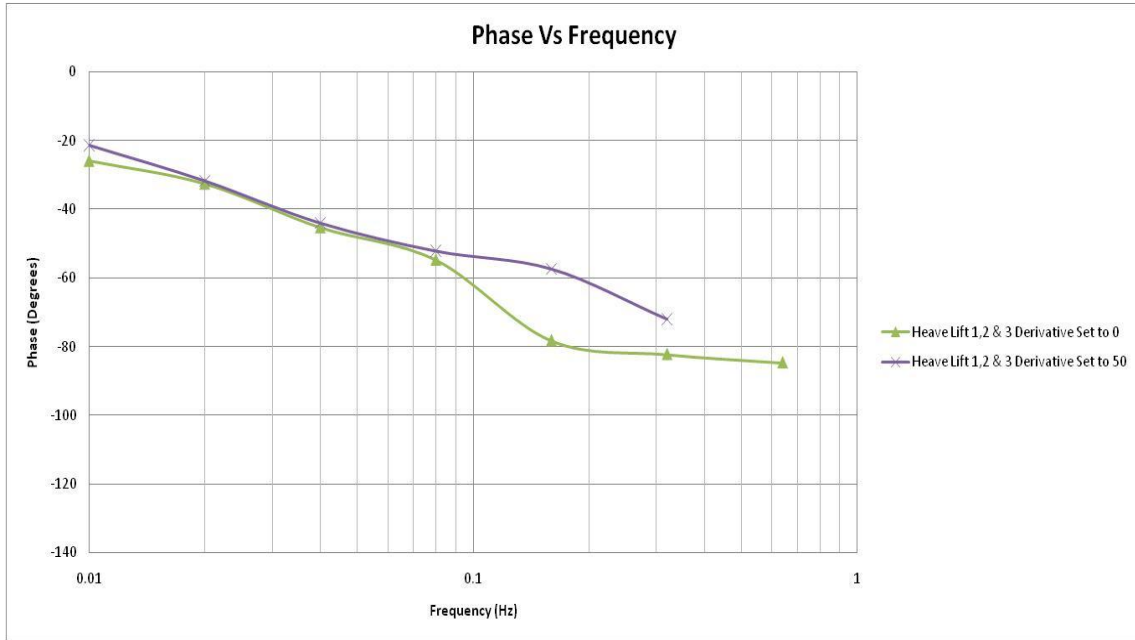


Figure 3.25: Initial Controller's Heave Phase Plot

Figure 3.25, indicates a similar result as that of the roll phase plot. The figure depicts the phase response of the heave testing. At approximately 0.16 Hz the output is running behind 40 to 60 degrees, depending on the resistance value. As previously mentioned, the heave testing was not run at the same high frequencies as that of roll and pitch. Therefore, the figure does not illustrate the sharp change in phase. If the test was run at a higher frequency the sharp increase in phase would approximately take place around 0.64 Hz.

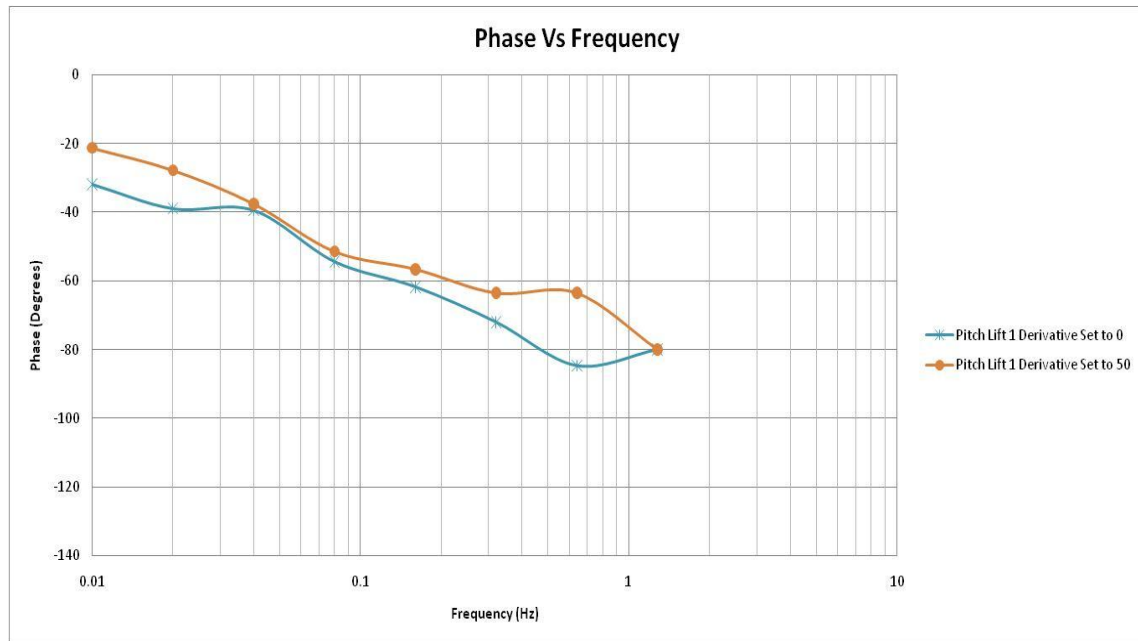


Figure 3.26: Initial Controller’s Pitch Phase Plot

As with the previous two figures, Figure 3.26 indicates phase shift of a particular DOF which in this case is pitch. At approximately 1.28 Hz the output lags behind 40 to 50 degrees. If extended to higher frequencies a sharp increase would be indicated past this point.

3.4.8 PD Bode Plot Comparison

Once data collection and calculations were completed a comparison was made against the previous controller design. As mentioned previously, the old controller included an internal PID controller that LabVIEW provided. The internal PID controller controlled the position of each lift by receiving a signal, in inches, from the string potentiometers as well as the desired position, also in inches. The output signal from the PID controller was then fed into an output code frame. The output of the PID controller was set within the limits of the output range, which were -10 V DC and 10 V DC. The proportional gain, integral time, and derivative time could be set individually for each lift.

Comparisons show that the external PD controller did give a better response than that of the built in PID controller provided by LabVIEW. However, consideration must be taken into account that the LabVIEW PID controller had to deal with operating system issues.

Figures 3.27, 3.28, and 3.29 show the comparison between roll, pitch, and heave separately.

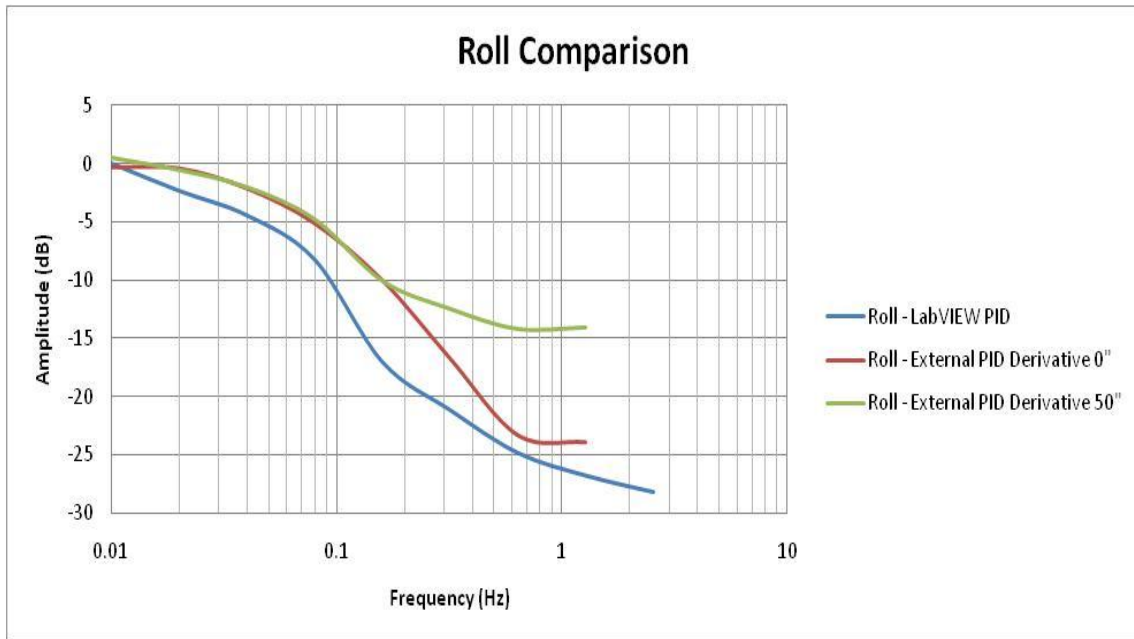


Figure 3.27: Roll Comparison

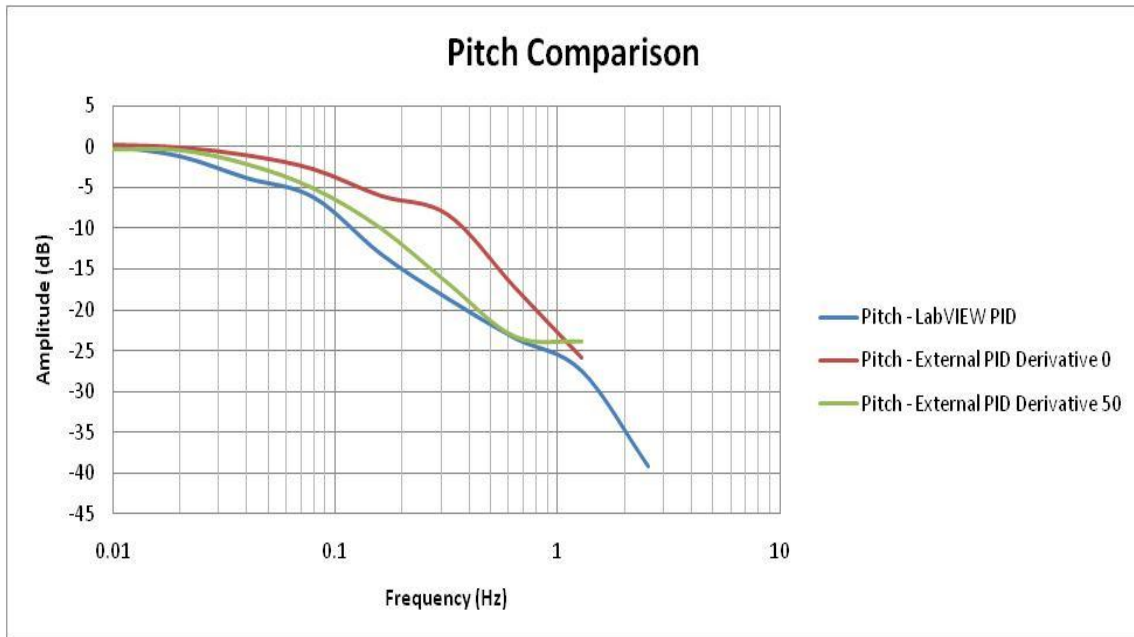


Figure 3.28: Pitch Comparison

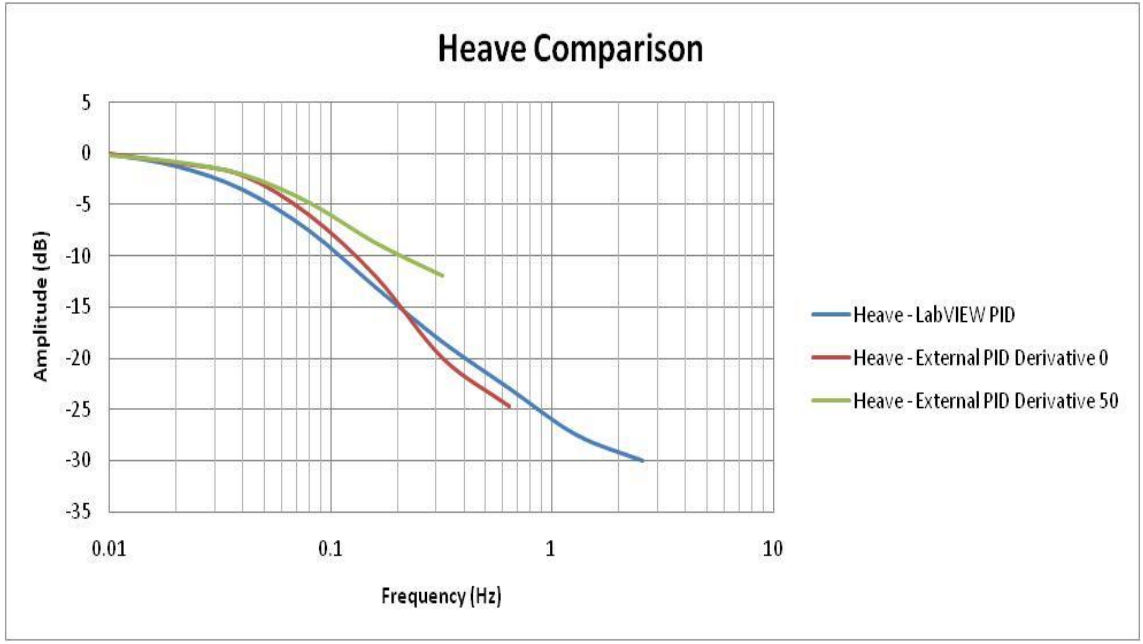


Figure 3.29: Heave Comparison

3.4.9 Initial PD Controller Conclusions

The initial PD controller performed to achieve the desires of a critically damped system. The controller also provided better control than the previous internal controller. However, issues became apparent with this system. First, the LabVIEW controller was cumbersome and provided the opportunity for operator error. Secondly, the proportional and derivative gain values were not known of the system. Additionally, the system was not able to duplicate the same results run to run. While trouble shooting this error memory leaks in the computer were noticed. Therefore, a decision was made to replace the controller and computer system. With this replacement we were hopefully that a system with better response could be designed and implemented.

Chapter 4: Current System Design

In this chapter, a discussion of the modifications of the hardware, electrical, and control systems will be discussed. The controller spoken about in Chapter 3 will be referred to as the initial controller, while the new controller is being referred to as the current controller. The testing methodology and results will be presented. Supporting appendices will be noted.

4.1 Hardware Modifications

The new system design, that replaced the initial system, contained many of the same components. The new system; however, no longer used an external PD controller. The external PD controller was removed and replaced with a LabVIEW PID controller, which was built directly into the LabVIEW program. The initial system used an older computer with a Windows XP operating system. With the implementation of the new controller system an upgrade in computer hardware was also implemented. A newer Dell model computer was used, which had a greater amount of processor speed, RAM, and hard drive space. Additionally, the operating system was upgraded to Windows 7 and the newest version of LabVIEW was installed. The hydraulic system for the platform was not altered during the upgrades to the system. Therefore, review Chapter 3 Section 3.2 for information on the hydraulic system.

4.2 Electrical Signal System Modifications

The electrical system can now be divided into three sections, instead of four as the previous system. These sections include:

- 1.) The feedback section which provides feedback of lift position to the PD controller and VI.
- 2.) The valve signal section which sends a signal to the proportional valves.
- 3.) The valve power and over-tilt safety system which provides power to the valves and shuts off power to the valves in emergency situations.

These sections are identical to the previous system except for the removal of the external PD controller. The potentiometers no longer receive the 5 V DC needed for operation from the project board power supply. Instead, the potentiometers were powered by an independent 5 V DC power supply. The terminal strip, labeled Terminal Strip 1 in Figure 4.1, allowed for connections with the break board as the previous system did. Terminal strips 2 and 3 allowed for connections between the DAQ cards and signals being sent from the proportional valves, valve meters, and potentiometers. The layout of the new electrical components can be found in Figure 4.1.

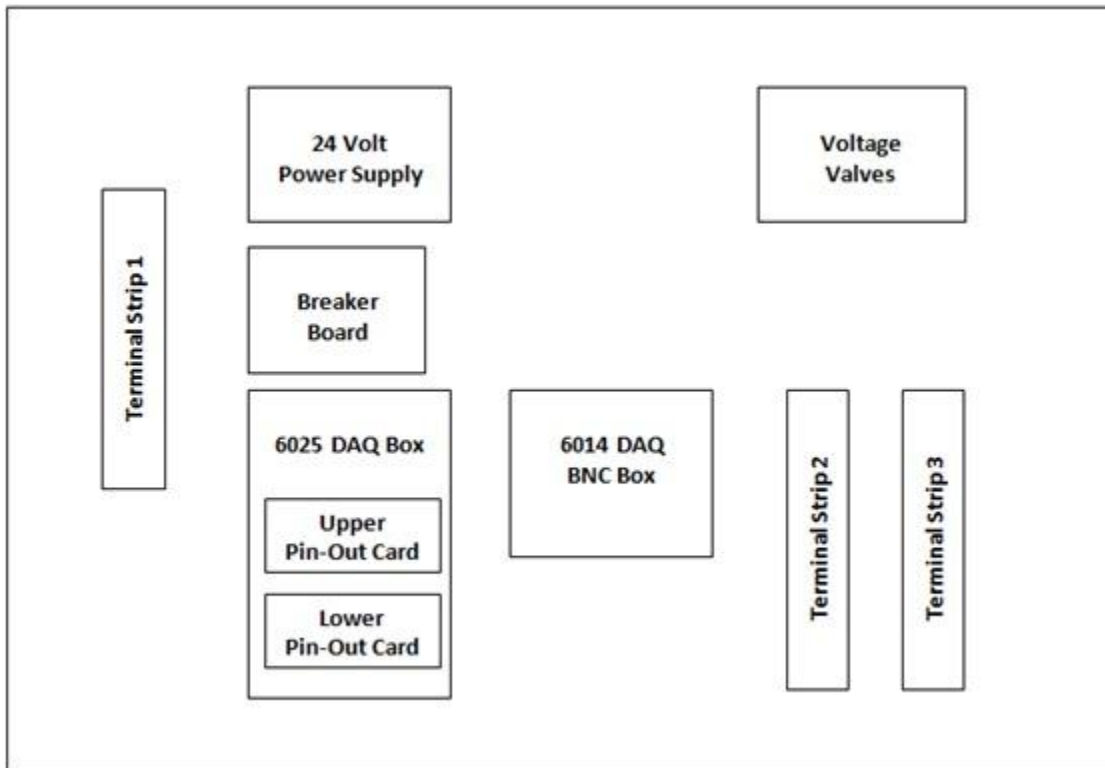


Figure 4.1: Modified Electrical Component Layout

The signals from the valves and potentiometers no longer feed through an external PD controller. The feedback signals from the potentiometers are now read by the DAQ cards, fed into the LabVIEW program, and the output from the program sent back out through the DAQ cards to the proportional valves. Figure 4.2 illustrates how the DAQ cards read in feedback from the string potentiometers as well as sending out signals to the proportional valves.

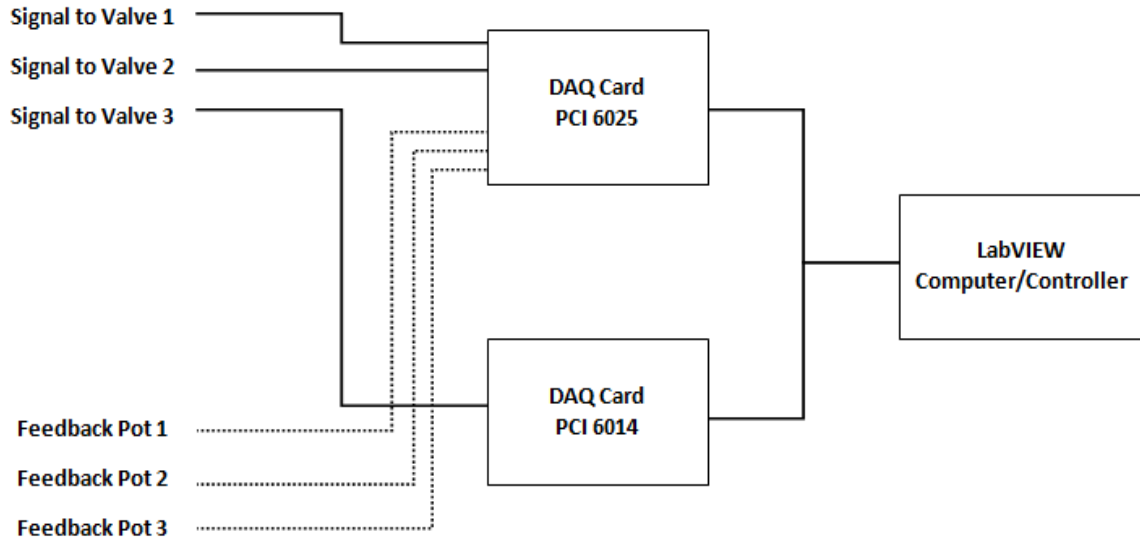


Figure 4.2: DAQ Card Signal and Feedback Schematic

The signals from the string potentiometers now run through the LabVIEW PD controller as well as the 6014 DAQ card. The DAQ cards send the desired position signal to the LabVIEW controller, which then sends the control signals to the proportional valves. Figure 4.3, illustrates the signal wire connections to terminal 2, which runs to the 6014 DAQ junction box.

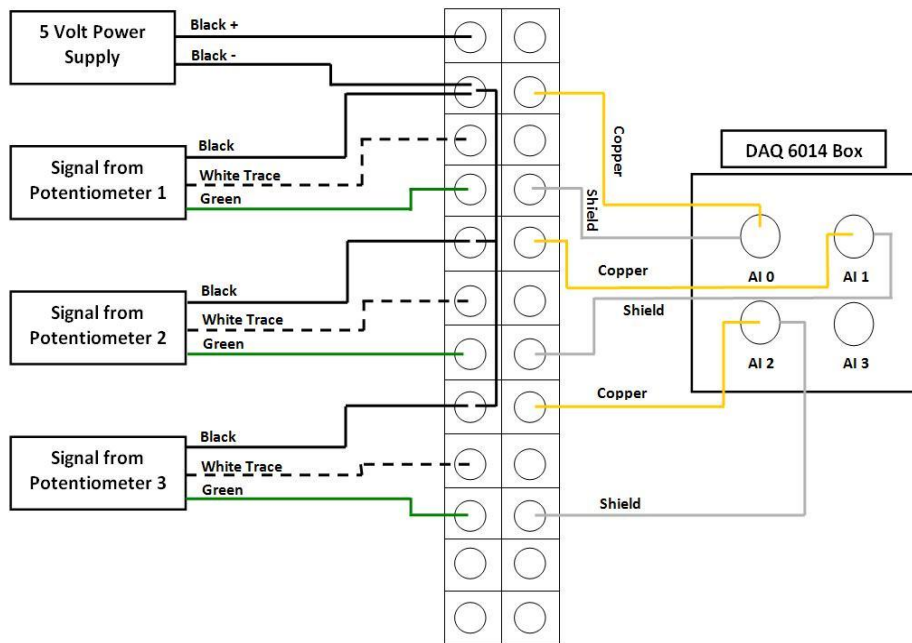


Figure 4.3: Modified Signal Wire Connections

The next modification included rewiring the signal cables to the valves. The signal for the valves is now generate solely by the LabVIEW controller. The signal from the valves still varies from -10 V DC to $+10\text{ V DC}$. The positioning signals were not changed, with the signals for valves 1 and 2 coming from the 6014 DAQ card and the signal for valve three coming from the 6025 DAQ card. Additionally, the valves still are powered by a 24 V DC power supply. The terminal connections, terminal 3, for these outputs is shown in detail in Figure 4.4.

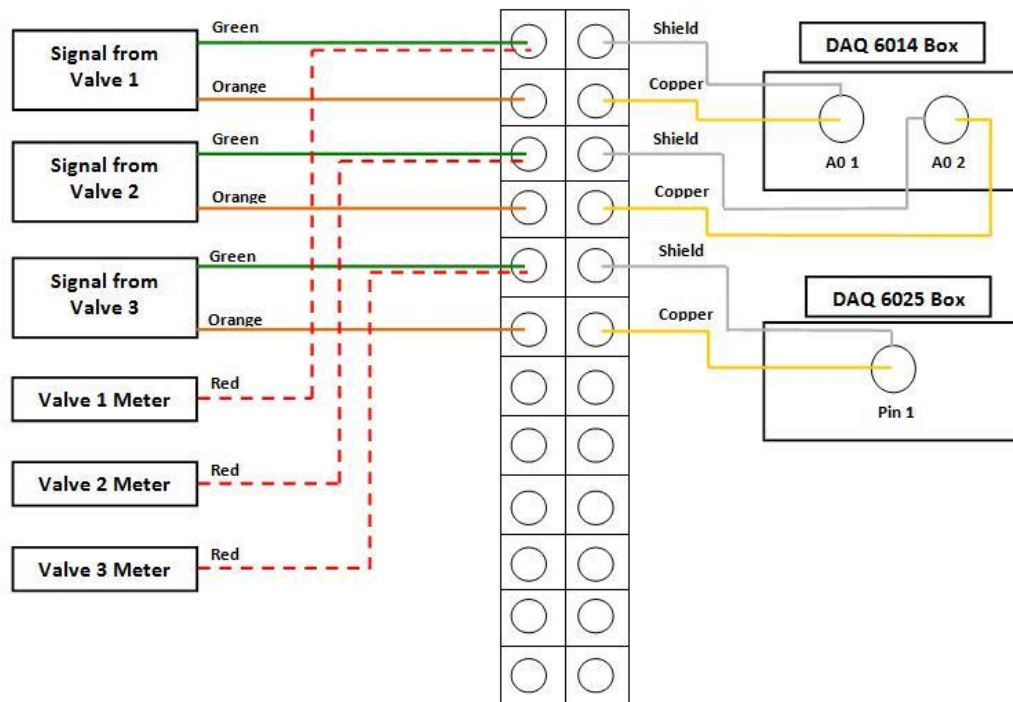


Figure 4.4: Modified Positioning and Meter Voltage Wire Diagram

The next modification to the electrical system involved the rewiring of the valve voltage meters. The voltage meters are now wired in terminal 3. Figure 4.4, illustrates how the meters are wired into the terminal. The meter is wired into the first pin valve signal pin, thus giving the ability to monitor the voltage of each proportional valve.

The final modification was to the emergency stop, also known as the e-stop, located on the operator desk. Previously, if the e-stop button was pressed the platform would stop, but the LabVIEW program would continue to run. This meant the possibility of operator error. If the operator was to disengage the e-stop without stopping the VI the platform would jump to the height indicated by the program at that time. Therefore, it

was determined that the e-stop needed to be wired into the control system. This was done by supplying a + 5 V DC power supply to the e-stop and connect the output to the DAQ 6025 card in pin A0-3. This would send a signal to the controller that the platform had been stopped and that the program needed to stop running. Figure 4.5, illustrates the wiring for the new e-stop.

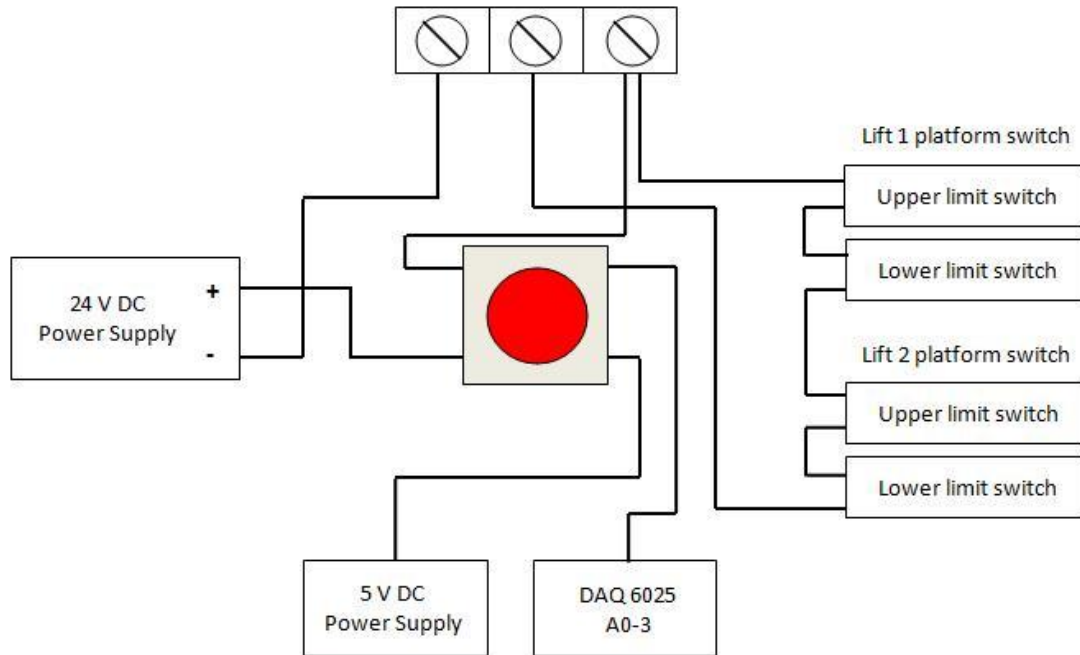


Figure 4.5: Emergency Stop Modified Wiring Diagram

Other than the the removal of the external PD controller and the rewiring that has been mentioned all other compoments mentioned in Chapter 3 were not changed.

4.3 Characterizing the Response of the System

In order to properly characterize the platform system values for m , b , and k had to be determined. The m value was determined by approximating the weight of the system. First, the steel plate thickness and dimensions were calculated. Once this was completed the weight value of 1/8 inch thick steel plate per square foot was researched. The values found ranged anywhere from 7.65 to 8.50 lbs/ft². Therefore, the weight was approximated to be 8 lbs/ft².

Next, the weight of the I-beams was calculated. The depth, flange width, and flange thickness of the I-beams were measured. These values were then compared to standard I-beam weight charts to determine the weight of each I-beam per foot. Additionally, the weight of the RMV mock-up, the weight of the material being lifted by each lift, and the painting material on the deck had to be approximated. The weight was approximated to be between 500-600 lbs. With all these factors taken into consideration the weight was approximated to be 2,000 lbs or 907 kg.

With m approximated the next step was to determine the value for k . First, the amount of pressure to move the platform 1% of volume change was determined. A height of 40 inches was determined to be the starting position. So, a 1% change of volume changed meant a position change of 0.4 inches. The value was determined to be 2,000 lbs/in². The area of the pistons was then calculated to be 1.5 inches. With this it was calculated the k value was approximately 7500 N/m. With m and k calculated, a determination on the natural frequency and the value of b could be made. The natural frequency was calculated to be approximately 2.88 Hz while the value of b was 5216 kg/s using equation 3.7 and 3.8 in Chapter 3.

4.4 LabVIEW Virtual Instrument Design

The new LabVIEW VI controller simplifies the use for the operator through various components and upgrades. The operator no longer has the multitude of dials and controls that the previous system offered. All the modifications to the data file that could be completed on the previous controller, such as perturbations, were moved to offline programming. Additional modifications included but were not limited to; the use of an internal LabVIEW PID, the removal of manual controls, and verification of program files. These modifications, in addition to the ones not mentioned, can be found in detail in the following sections.

4.4.1 Motion File Creation

A VI, named Motion File Generator, was created to generate a single input file when the platform was in operation. The theory behind this method was to reduce the possibility of an incorrect file being loaded. With this VI, the operator was able to browse the computer

and chose a file they desired to run. Once selected, the operator had to enable the file, which was simply completed by clicking the enable button on the front panel. When the enable button was clicked the program verified that the file did not exceed the parameters defined for height. These limits were set at a 70 inch maximum and a 5 inch minimum. If the file met these parameters an indicator light, located on the front panel, turned green. The VI could then be run, which then wrote a motion comma-separated value file run by the main platform VI controller. However, if the file failed the check the indicator turned red and the file was not written.

The operator during this process could also set the displacements. By default the x, y, and z coordinates were set to 0, which is considered to be the center of gravity for the ship. The operator could then also specify the frame rate and count if using a blank file.

Two other additional features were included on this VI. These functions were the ability to enable waves and perturbations. As previously mentioned, these functions are now completed in the offline programming of the input file. However, these functions were included on this sub VI for advanced use. If the operator desired more pitch or roll they could simply change the amplitude and reach their desired results. As for the perturbations, the operator was able to choose at what time, the duration, and the intensity they would like the perturbation to be. Once all these functions were determined and defined the operator pressed the run button and the file was verified and written to the main VI.

4.4.2 Platform Controller

As previously mentioned, the design and layout of the current platform controller was designed to be easier to read and comprehend than the initial controller. For simplicity, the controller has been broken down into sections in this document and will be discussed per section.

4.4.2.1 3-D Lift and Platform Representation

The first section of coding is for the 3D image of the lifts and platform. First, the base is created and dimensions are set. Next, each lift is individually created with its own set of

dimensions and their positions set in the 3D image. Finally, the platform dimensions are set. When the controller is initially started this is the very first section of coding that will be run, which builds the 3D image on the front panel. Figure 4.6, illustrates the 3D imaging code and layout.

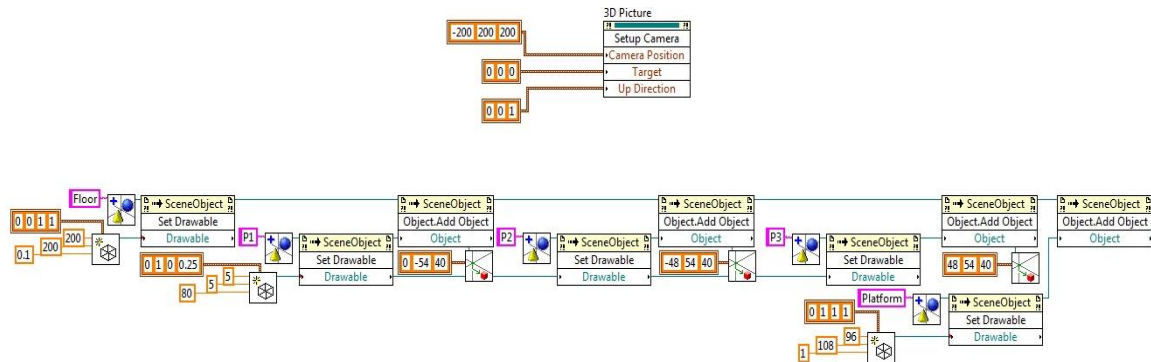


Figure 4.6: 3-D Imaging Code and Layout Diagram

Once the platform begins to run this 3D image must be updated. The coding for this is located within a while loop that continuously updates the image. First, the values from each lift are feed into the loop and computed from lift position to heave, pitch, and roll. Calculations are then performed to take the average distance between the lifts and the center point.

4.4.2.2 3-D Lift and Platform Representation Coding

To determine the roll the position of lifts 2 and 3, they are divided by their distance from one another, which is 96 inches. The value is then converted from radians to degrees by using the constant 0.01745. Heave is calculated by determining the center point between lifts 2 and 3 and adding them to the position value of lift 1. Once these values are summed they are then divided by two, which gives the average position of each lift. The calculation for determining pitch uses the center point between lifts 2 and 3 subtracted by the value of lift 1. This pitch value is then divided by 108 inches, which is the length of the platform. Finally, this value is converted from radians to degrees by using the same constant that roll was converted from.

The total magnitude for the pitch and roll values are then found and normalized to:

$$x = \frac{P}{T} \quad (4.1)$$

$$y = \frac{R}{T} \quad (4.2)$$

where P is pitch and R is roll.

These values are then checked to determine if the value is considered to be not a number (NAN). If they are determined to be NAN they are the set to 0. Since these calculations are feed into the function that will rotate the 3D image, heave is set to a constant of 0 also known as z = 0.

The value for heave is translated to the 3D image, separate from the rotate function. The values for pitch and roll are set at a constant of 0, while z is set to equal heave. These translations and rotations are cleared every frame, as to update the 3D image. Also located in the while loop is the coding for the lift position indicators. Each lift, also known as a mast, has a separate code, which updates every frame. This coding is illustrated by Figure 4.7.

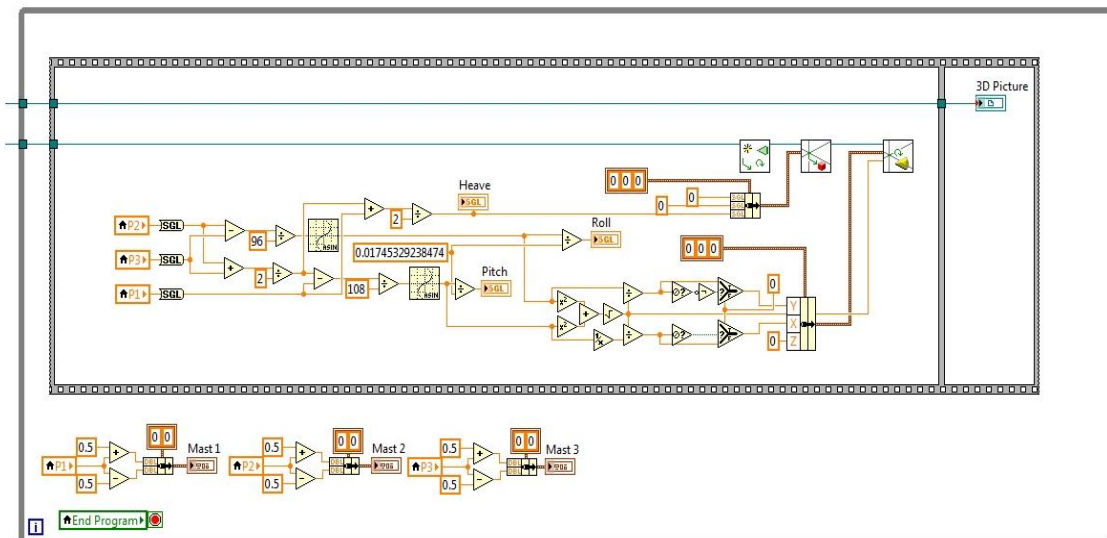


Figure 4.7: Lift Position Indicator Diagram

4.4.2.3 Platform Coding

The final while loop located on the back panel, controls the actual movements of the platform. Please view Appendix F and G for the breakdown of the back panel. This while loop is set to a period of 12 ms and the motion csv file is feed into this loop. The total length of the motion csv file is calculated. Then a calculation of frame number and percent complete is calculated. As previously mentioned, the operator may choose from six different operating states. These states are displayed and updated through the back panel.

Located within the while loop is a DAQ Assistant that reads the analog inputs. This input is then feed into each potentiometer. The potentiometers were calibrated by determining the voltage at ½ inch increments. These values were then plotted and a linear trend line added to determine the equation for each potentiometer. Initial testing of the new controller showed that the potentiometers read a start value ranging from 0.8 to 1 inch. Therefore, an offset function was added so each potentiometer could be adjusted to a height of 0 inches.

This value is then feed into the state select function. Additionally, the value of the maximum number of frames in the motion file, the current frame the program is on, and the file itself are feed into the state select function. Each state function performs a separate action:

- 1.) Stop state: runs the current position continuously
- 2.) Lower state: lowers the platform by a step function
- 3.) Ready state: either lifts or lowers the platform to the 40 inch mark through a step function
- 4.) Run state runs the motion csv file
- 5.) Loop state: runs the motion csv file continuously

The output of the selected state is then fed into the PID controller, where the gain values are determined and set. The values are then feed into each lift where the output of each

lift is then written into a feedback csv file. These state functions are controlled by the front panel, which can be found in Appendix H.

4.4.3 Determination of K_P and K_D Values

With the removal of the external PD controller values for the proportional and derivative gain had to be determined. To determine these values, simulations of an ideal second order system were run using MATLAB Simulink. The transfer function used in this simulation was:

$$T(s) = \frac{(K_P + K_D s)w_n^2}{(s^2 + 2\zeta w_n s + w_n^2) + (K_P + K_D s)w_n^2} \quad (4.3)$$

4.4.3.1 MATLAB Simulink

To determine the proper transfer function of the system values for K_P and K_D were initial set at 10 and 0.75 respectively. These values had no significant meaning except that these values were assumed to be appropriate through MATLAB simulation. A simple MATLAB program was written, which can be found in Appendix I, to determine this transfer function. The program used set values of 2.88 Hz for w_n and 1 for ζ . Additionally, the aforementioned K_P and K_D values were used. With these values the program gave a transfer function of:

$$\frac{245.7s + 3276}{s^2 + 281.9s + 3604} \quad (4.4)$$

In addition, a step response of the transfer function was plotted. The step response showed that the transfer function would have only a marginal overshoot of 0.435% with a rise time of 7.9 ms and settling time of 13.6 ms. With this a determination was made that these initial values were acceptable and progress could continue on the design of the Simulink simulation.

The Simulink program consisted of a signal generator, an error input, the PD controller, a saturation limit, and the plant itself. Figure 4.8, illustrates the program.

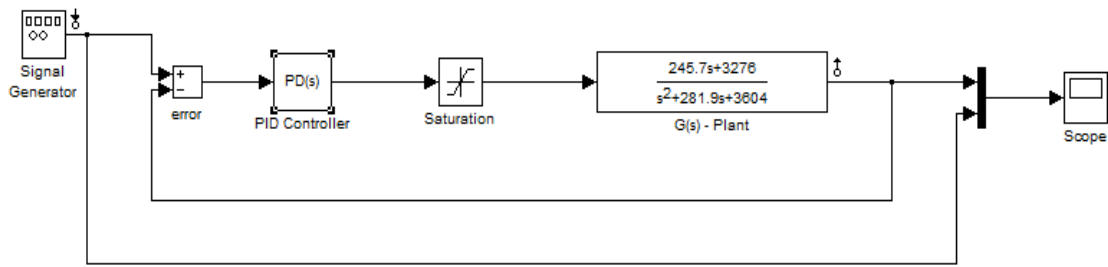


Figure 4.8: MATLAB Simulink Diagram

The PD tuner values were initial set to $K_P = 10$ and $K_D = 0.75$. The controller was set to an ideal system and the time domain as continuous. With the parameters set the PD controller could then be tuned.

The simulation returned a K_P value of 56.24 and a K_D value of 0. According to the simulation the rise time would be 0.156 ms with a settling time of 0.277 ms. The percent overshoot would be 0. With the platform weighing approximately a ton, a determination was made that the system would be unable to reach this rise and settling time safely. Therefore, the K_P value was scaled approximately $1/8^{\text{th}}$ for initial testing.

4.5 Response of the System

4.5.1 Square Wave Response Test

Initial testing of the new PD controller consisted of running a square wave test. The square wave had a maximum height of 50 inches and started at a base height of 40 inches. The square wave test lasted approximately 35 seconds with each step lasting 10 seconds each. The platform repeated this process twice before returning back to the ready position. During this test the data output from the potentiometers were fed into a feedback file. The graphical input and output file is illustrated in Figure 4.9.

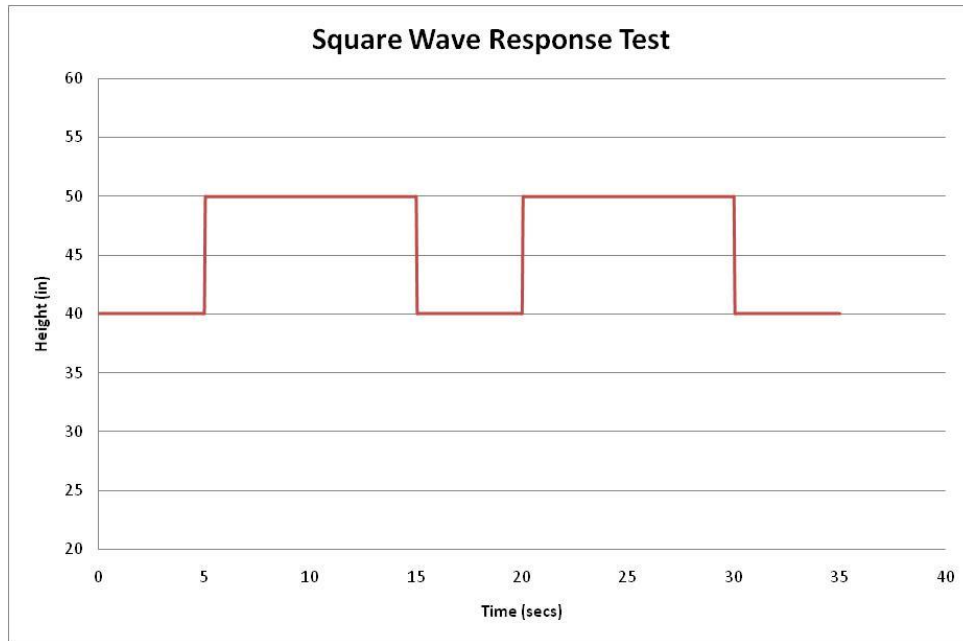


Figure 4.9: Square Wave Response Input

4.5.2 Square Wave Response Test Result

The square wave response test was run at a K_P value of 7 and a K_D value of 0. As previously mentioned the proportional gain value was scaled to increase the rise and settling times for safety reasons. The results, shown in Figure 4.10, show a response with no overshoot and a rise time of approximately one second. These results indicated that a critically damped system could be obtained with the new controller. Also, the results showed the system to be more responsive than the previous controller, since no general ramp up to the maximum height was apparent.

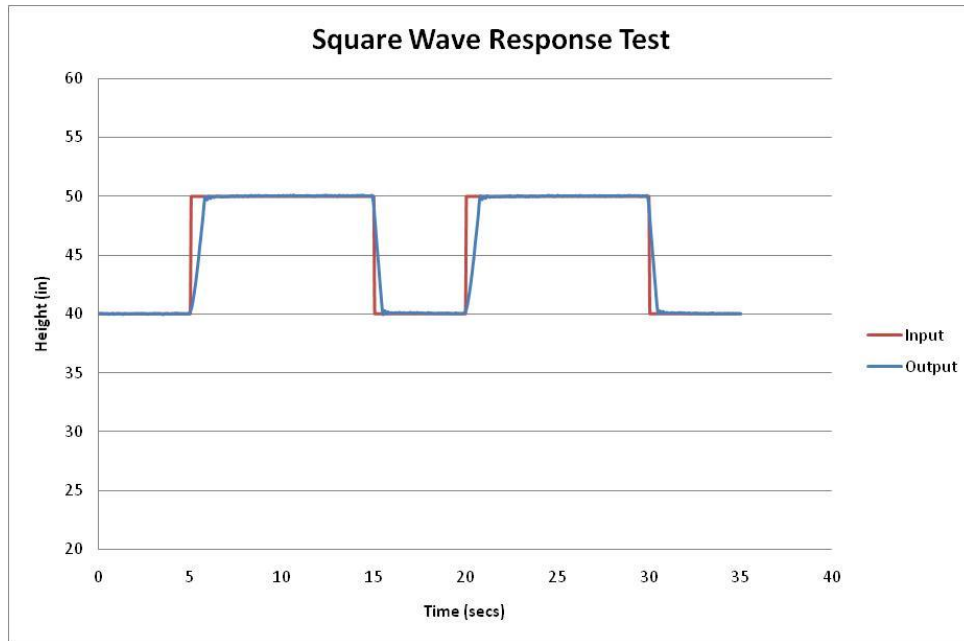


Figure 4.10: Square Wave Response Test

4.5.3 Sine Wave Response Test

As with the previous PD controller the sine wave tests were separated into heave, roll, and pitch. The input/output graphs can be found in Appendix J. Initial testing varied in frequency, normally taking steps from 0.01 Hz and up until 0.16 Hz was reached. Based on analyzation, it was determined that any frequencies above 0.16 Hz for heave could possibly damage the system. However, it was determined that higher frequencies could be achieved in roll and pitch. To determine these frequencies a base of 0.16 Hz was taken and doubled until the platform showed signs of instability. The final determination was made that pitch could not exceed 0.32 Hz and roll 0.64 Hz.

These tests were run at a period of 12.5 ms and approximately took 10 minutes for completion. A period of 12.5 ms was determined based on visualization. Previous test runs varied in period; however, higher periods caused the platform to shake due to a slower speed in reading the input file. Therefore, the period was adjusted until the shake in the platform could no longer be visualized.

4.5.4 PD Bode and Phase Plots

The recorded data was processed and converted exactly as the previous system, mentioned in Section 3.4.7. The equations and calculation can be found in Appendix D. A graphical representation of each bode plot and their respective DOF can be found in Figure 4.11, 4.12, and 4.13. View Figure 4.15 for a graphical representation of the comparison view of the phase changes for the 3 DOF.

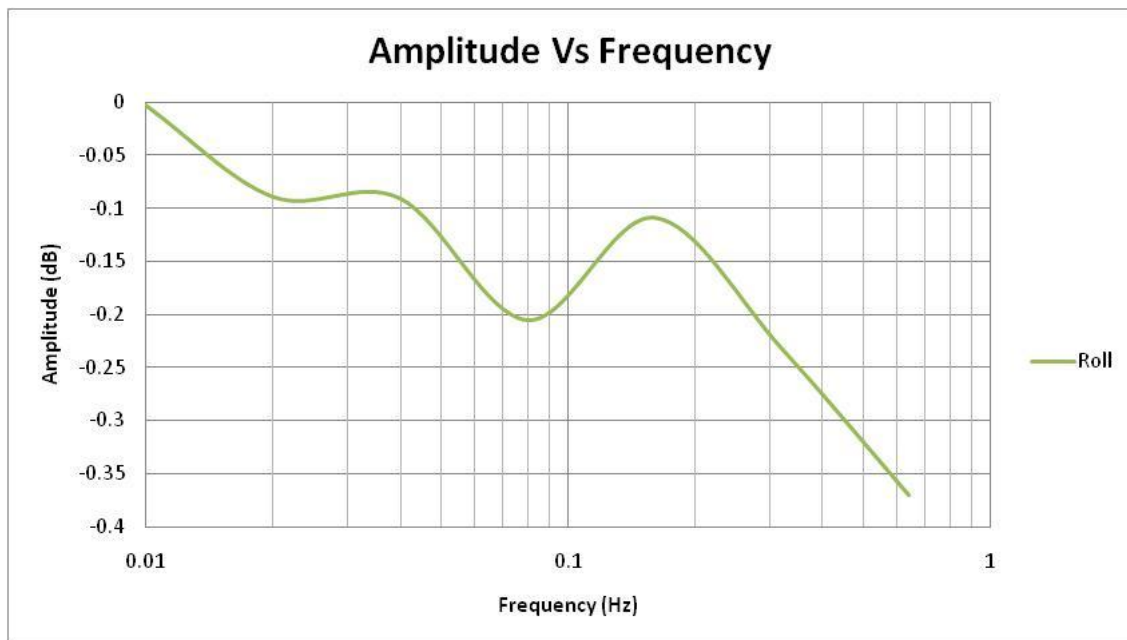


Figure 4.11: Roll Amplitude versus Frequency Current Controller Test

Figure 4.11, illustrate the roll bode plot of the current controller. Significant differences can be seen compared to that of the old controller. Previously, the system encountered amplitude drops ranging from 15 to 40 dB within a similar frequency range. This change from the previous to current controller indicates that the system is significantly more responsive. This means that unlike the previous controller the platform is capable of maintaining the proper input height with little change in displacement. Therefore, the change in amplitude is significantly smaller and the maximum safe frequencies for these tests are less.

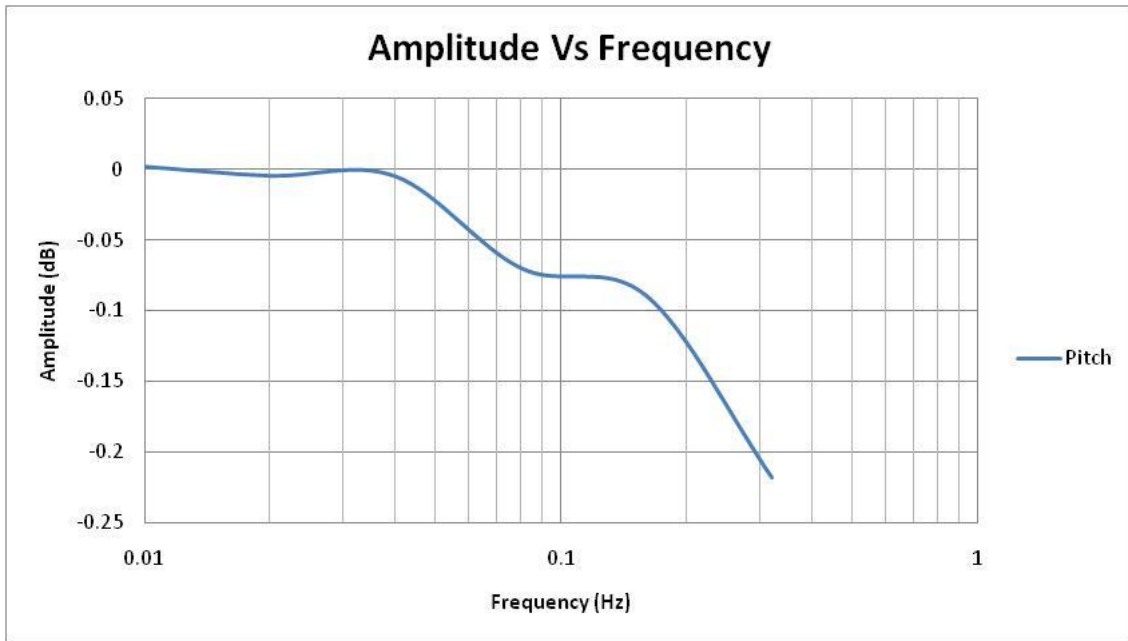


Figure 4.12: Pitch Amplitude versus Frequency Current Controller Test

Figure 4.12, illustrates the pitch bode plot. As with the previous graph the change in amplitude compared to the old controller is significantly less. In addition, it can be determined that at approximately 0.16 Hz to 0.32 Hz the system begins to encounter the point at which it no longer can keep up with the input file safely, possible causing some instability. Please skip to the next page for Figure 4.15.

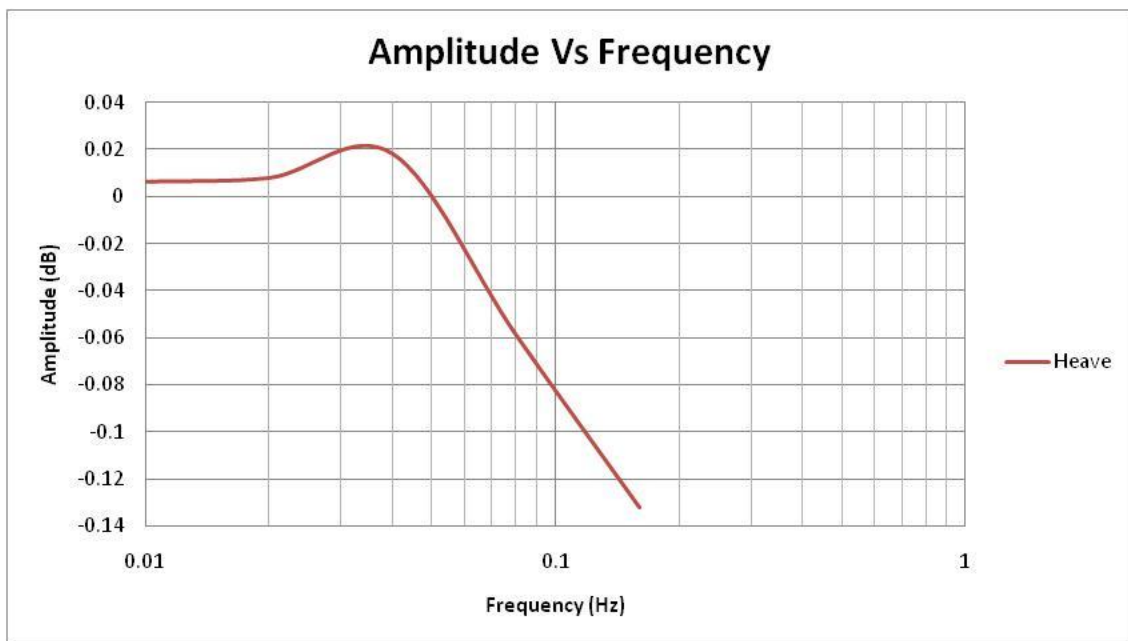


Figure 4.13: Pitch Amplitude versus Frequency New Controller Test

Figure 4.13, illustrates the heave bode plot. The results are similar to the previous two graphs as in it shows the same difference in amplitude. However, the range of frequencies the heave is able to complete successfully is less and at approximately 0.16 Hz the platform begins to show signs of instability.

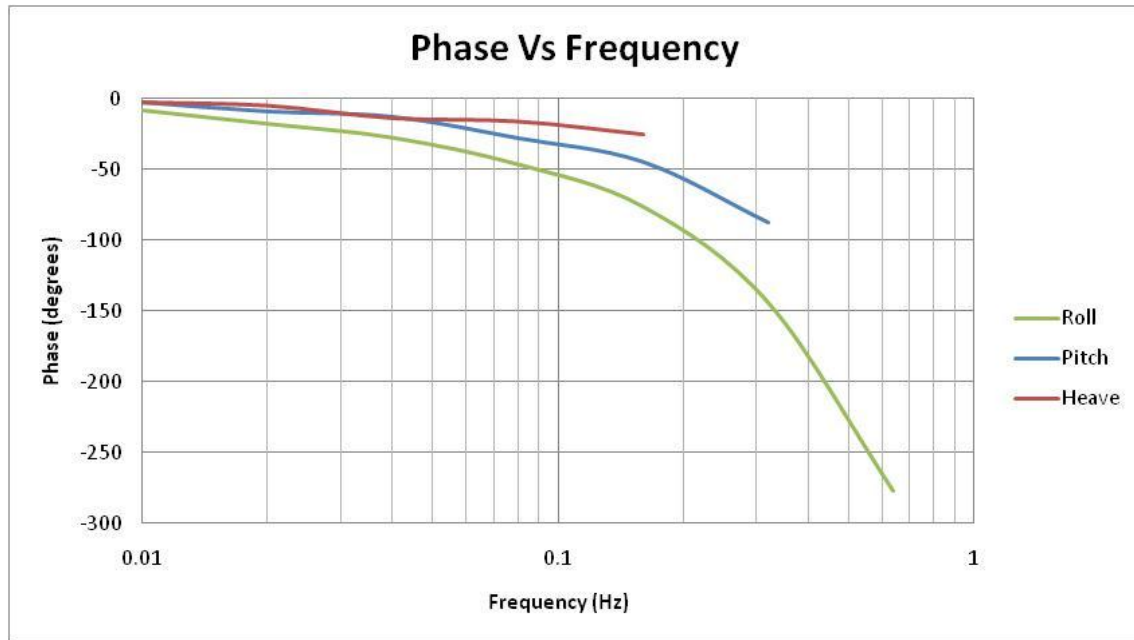


Figure 4.14: Current Controller's DOF Phase Change Comparison

Figure 4.14, illustrates the phase change for each DOF. At approximately 0.16 Hz each DOF begins to indicate a ramp in phase change. The roll clearly shows instability at approximately 0.64 Hz, as it exceeds the 180 degree phase change. Since the pitch and heave test frequencies were not as high they only show marginal changes in the phase. However, if the sine wave test was run at a higher frequency for these DOF similar results to that of roll would be seen.

4.6 Current PD Controller Conclusion

The current controller provided a range of improvements compared to the previous controller. The controller was more simplistic, provided built in safeties against improper control, and provided internal checks of input files. However, additional constraints to the input cvs file must be included in the offline programming. These constraints include the following:

- 1.) A maximum height of 70 inches to ensure lighting fixtures in the lab are not damaged.
- 2.) A minimum height of 5 inches to ensure the platform does not damage itself by hitting the floor.
- 3.) A maximum no greater than 10 degrees in pitch or roll to ensure the spherical joints do not bind and break.
- 4.) A frequency in heave no greater than 0.16 Hz to ensure the safety of participants, operators, and the platform.
- 5.) A frequency in pitch no greater than 0.32 Hz to ensure the safety of participants, operators, and the platform.
- 6.) A frequency in pitch no greater than 0.64 Hz to ensure the safety of participants, operators, and the platform.

In addition to the improvements of the PD controller, the results of the bode and phase plot illustrate that the new system controlling the platform is much more sensitive than the previous system. The new system had minute changes in the displacement amplitude, which meant that the platforms lag was significantly reduced. Previously, the platforms lag wouldn't allow the full range of motion, meaning if the input file told the platform to travel a distance of 20 inches at a frequency of 0.16 Hz it may actually only travel 10 inches, which was indicated on the phase plots in Section 3.4.7.

Chapter 5: Conclusions

With the use of simulation and control theory the characteristics of the system have been defined. The maximum frequencies that the platform can operate safely at have been defined as 0.64 Hz for roll, 0.32 Hz for pitch, and 0.16 Hz for heave. Based on the characteristics of our maximum sea-state, sea-state 3, the average frequency for roll was 0.137 Hz, 0.194 Hz for pitch, and 0.091 Hz for heave for any input file. Therefore, we can successfully operate in the ideal ranges of sea-states 0, 1, 2, and 3. Control theory has given us the ability to determine our optimal proportional and derivative values, which were scaled once the weight of platform was taken into consideration.

Greater speed and accelerations are possible within the nominal capabilities of the lifts and platform if higher capacity valves and hydraulic supply was provided. Additionally, sea-states beyond that of sea-state 3 would be possible with this system. Modifications to the lab and lifts would need to be made in order to reach the proper height of these sea-states. If the need for the other 3 DOF becomes apparent the platform could be retrofitted with an additional platform performing yaw, sway, and surge. Modifications could also provide the ability for the platform to test other scenarios besides that of sea-states. Scenarios such as vehicles in rough terrain and individuals working in unstable environments are just a few of the possibilities.

Bibliography

- [1] DiStefano, Joseph J., Allen R. Stubberud, and Ivan J. Williams. *Schaum's Outline of Theory and Problems of Feedback and Control Systems*. New York: McGraw-Hill, 1990. Print.
- [2] Dorf, Richard C., and Robert H. Bishop. *Modern Control Systems*. Upper Saddle River, NJ: Pearson Prentice Hall, 2005. Print.
- [3] Mituhiko, Araki. "PID Control." *Encyclopedia of Life Support Systems*. Web. 21 Oct. 2010
- [4] Carrico, Todd, Timothy C. Smith, Joel Park, and Mark Melendez. *LCS MODEL 5636 SEAKEEPING AND CAPSIZE*. Rep. no. NSWCCD-50-TR-2005/030. West Bethesda: Naval Surface Warfare Center, 2005. Print.
- [5] Belknap, William. *FREDYN Dynamic Stability Predictions for the Lockheed Martin LCS Hull Form*. Rep. no. NSWCCD-50-TR-2005/030. West Bethesda: Naval Surface Warfare Center, 2004. Print.

Appendices

Appendix A: Initial Controller LabVIEW Back Panel

Section 1: Light Orange

In this section of the back panel the data is prepared and fed into the system. First, the data was converted from meters to inches and fed into a feedback file, which was stored on the desktop. This data was represented in the first 3 columns in the csv file and shows what height the platform should reach. Next, the data is fed into a transform matrix. The input had to be transformed, since the tow tank data focused on the center of gravity of the ship and the area of interest is away from this area. The transformation matrix can be seen in Appendix E. Additionally, there are true false statements that controlled the manual slide bar, the reset button, and the pause button. The manual slider bar raised and lowered the platform. If the statement was false, i.e. the slider bar was not turned on; the signal from the slider was not summed into the final input. The reset button restarted the input file from the beginning while the pause button paused the input data being fed into the system. Lastly, is the amplitude time series dial. The dial could be adjusted from 0% to 100%, which will either take the input values for their maximum values or lower. This function allowed the ability to scale back sea-state 3 data into sea-state 2, or lower.

Section 2: Light Purple

Section 2 performed two primary functions, wave control and perturbation. First, the roll, pitch, and heave could be increased through the use of the wave control dial. In order to give more control in the roll, pitch, and heave multipliers, the frequencies and amplitude could be adjusted on each lift. If the wave control dial was turned off no values from this would be added into the input after it has completed the matrix transformation. Next, a perturbation could be added into the input. This caused either a small rise or drop while the platform was in motion. Each lift had an individual perturbation slider, so they each could be adjusted independently.

Section 3: Light Green

Section 3 contains the feedback file and the platform constraints. As previously mentioned, the input file was being stored in the feedback file. Additionally, the output values from the string potentiometers were stored in the feedback file. The platform constraints provided safety to the occupants and the platform itself. The constraints limit the platform to a height of 70 inches. The main concern of exceeding this height was the possibility of hitting the light fixtures in the lab. Therefore, whether controlling the platform through the manual slider or through simulation the system would not rise beyond this level. The constraints also slowed the platform once it lowered to the 5 inch mark. This constraint was put in place to prevent the platform from hitting the floor and damaging the system. Additionally, visual representations of where the lifts should have been were shown by using tank meters. This gave the ability to run the program offline and check for any possible issues with the input data, such as data points lying outside the constraints.

Section 4: Light Yellow

Section 4 contains a math script for conversion and three DAQ assistants representing each lift. Once the input data reached the math script, it was still in units of meters. Therefore, it had to be converted to inches before being fed into DAQs. Once converted the data was then sent to each lift causing the platform to roll, pitch, or heave depending on the input data.

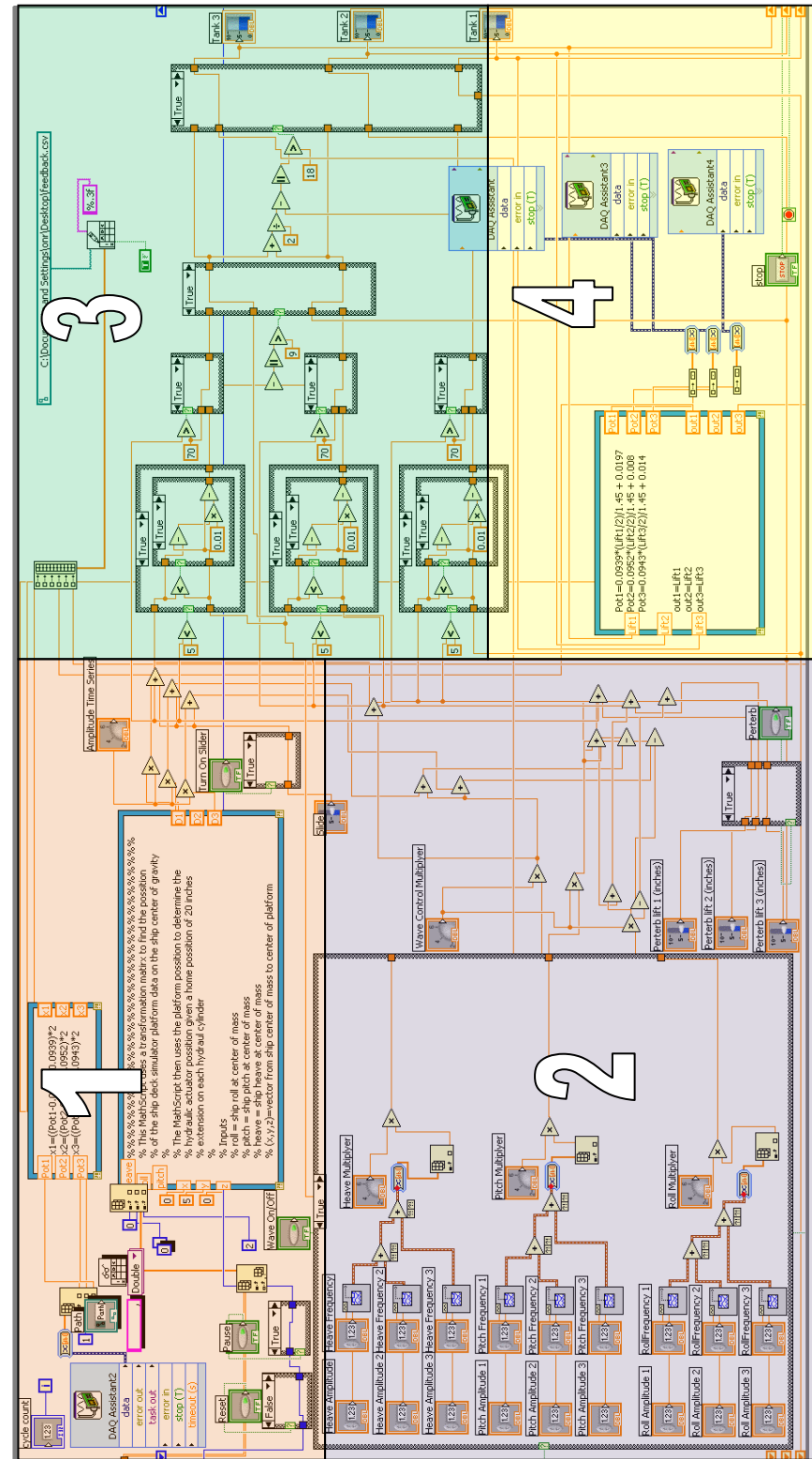


Figure A.1: Back Panel Display

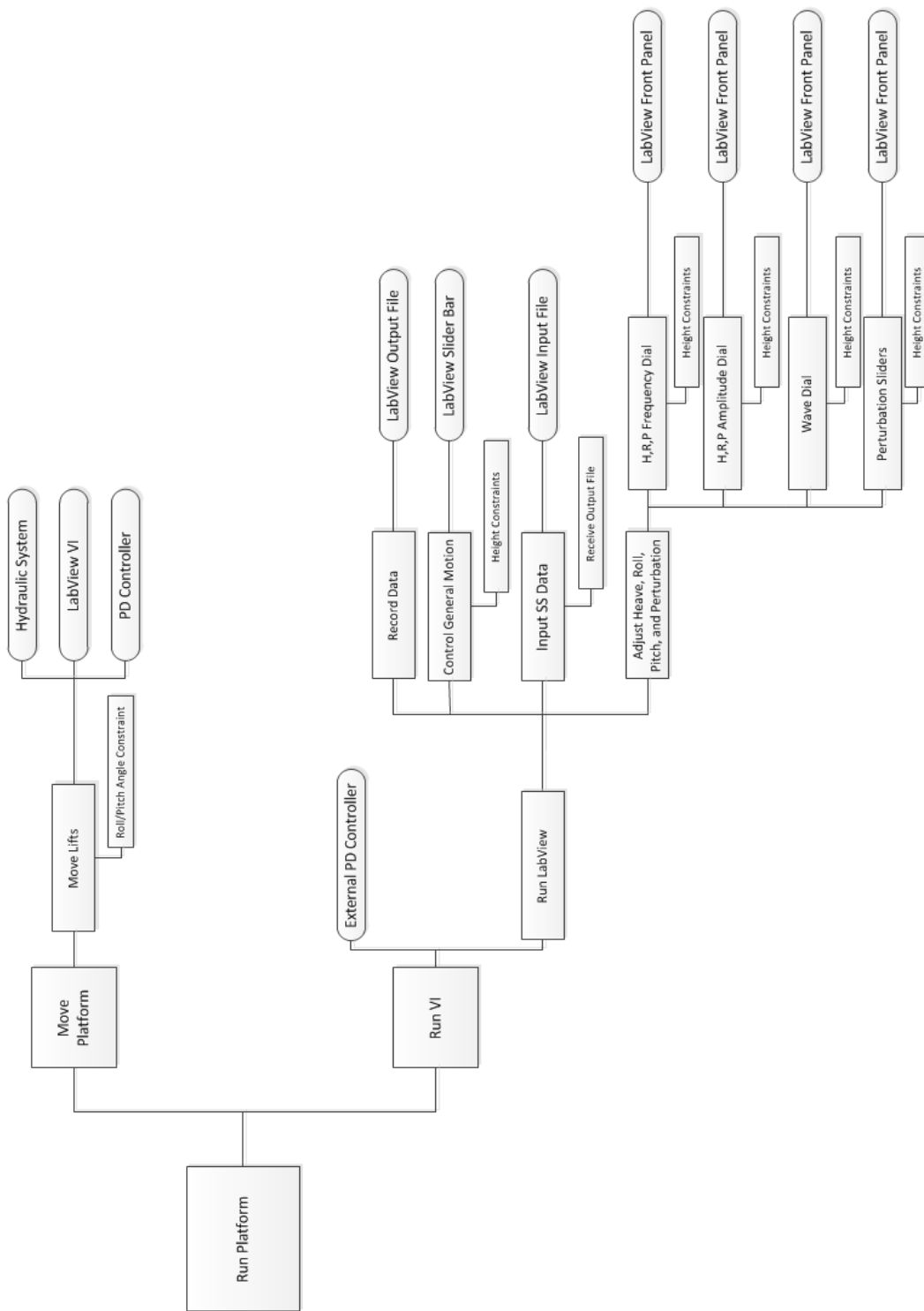


Figure A.2: Initial Controller Platform Function Block Diagram

Appendix B: Initial Controller Front Panel

Figure B.1, on page 65, shows the front panel to the LabVIEW VI. The front panel is broken down into two different sections, which are labeled and colored.

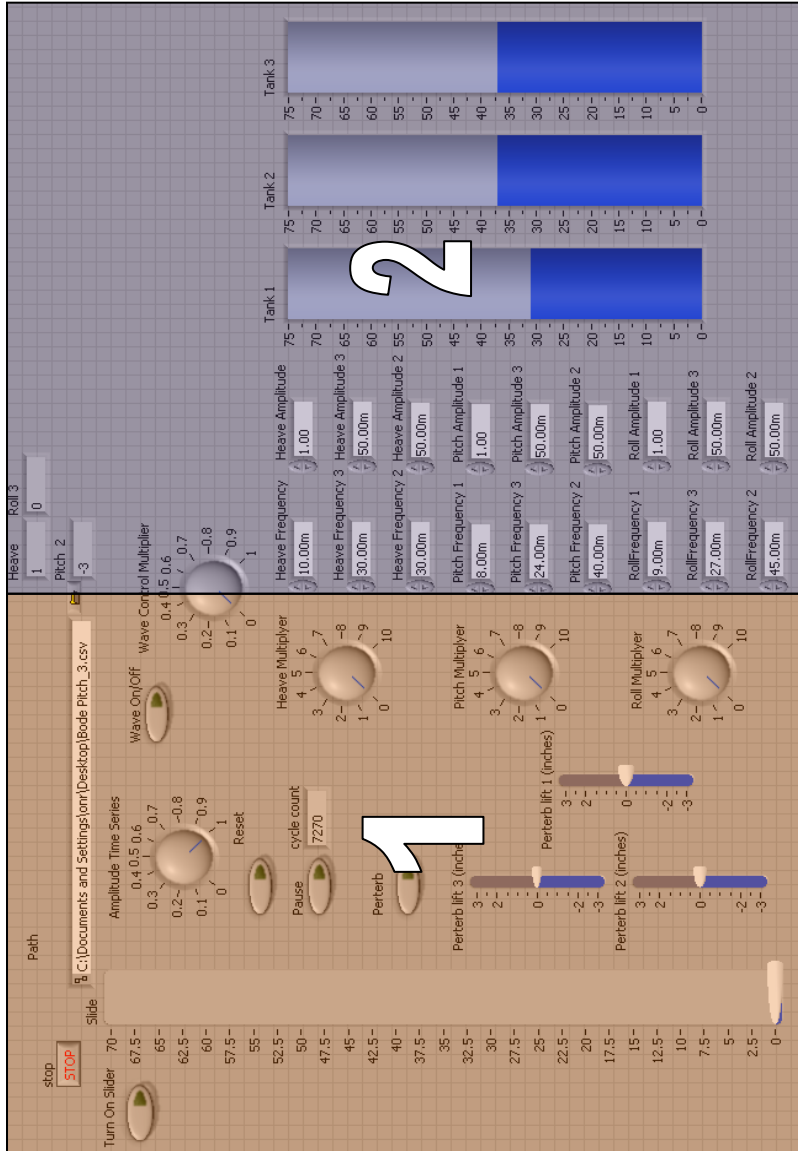
Section 1: Light Orange

Section 1 provides many of the controls for manually controlling the platform and adjustment of the input data while running the platform in simulation mode. First, is the manual slide bar which raised the platform from the ground level of 0 inches to the maximum height of 70 inches. The stop button located above the slide bar stopped the LabVIEW VI. Directly to the right of the stop button is the path file. The folder icon could be selected, which allowed the operator to browse and select which csv file they wanted to run. Underneath the path file is the amplitude time series dial. This allowed the operator the ability to determine what percentage of each data point they wanted to use. If set to 1, or 100%, the input data would be fed into the platform written. If set to, say, 40% the input data position would only be 40% of the written data in the csv file. Simply stated, if a height of 45 inches was being feed into the platform and the operator only wanted 40% of that height they could adjust the amplitude dial accordingly.

Underneath the amplitude time series dial is located the buttons for the pause and reset features, which involved pausing or resetting the input data. Next, are the perturb button and sliders. Each lift had an independent slider, which could be adjusted from +3 to -3 inches. Once adjusted the perturb button could be pressed and would cause a momentary jolt to the platform. Directly to the right of these functions are the wave control dials. The wave control dial had to be turned on manually and just like the amplitude dial was in percentages. If the operator wanted more roll, pitch, or heave all they had to do was adjust what percentage they would like summed into the original input data. Once completed the operator then determined how much they wanted to adjust the position of that DOF.

Section 2: Light Purple

In section 2, the visual display tanks, frequency dials, and amplitude dials are located. The display tanks gave a visual representation on what the input data would do once fed into the platform. The frequency and amplitude dials allowed independent variation for each lift.



Appendix C : Initial Controller Sine Wave Response Results

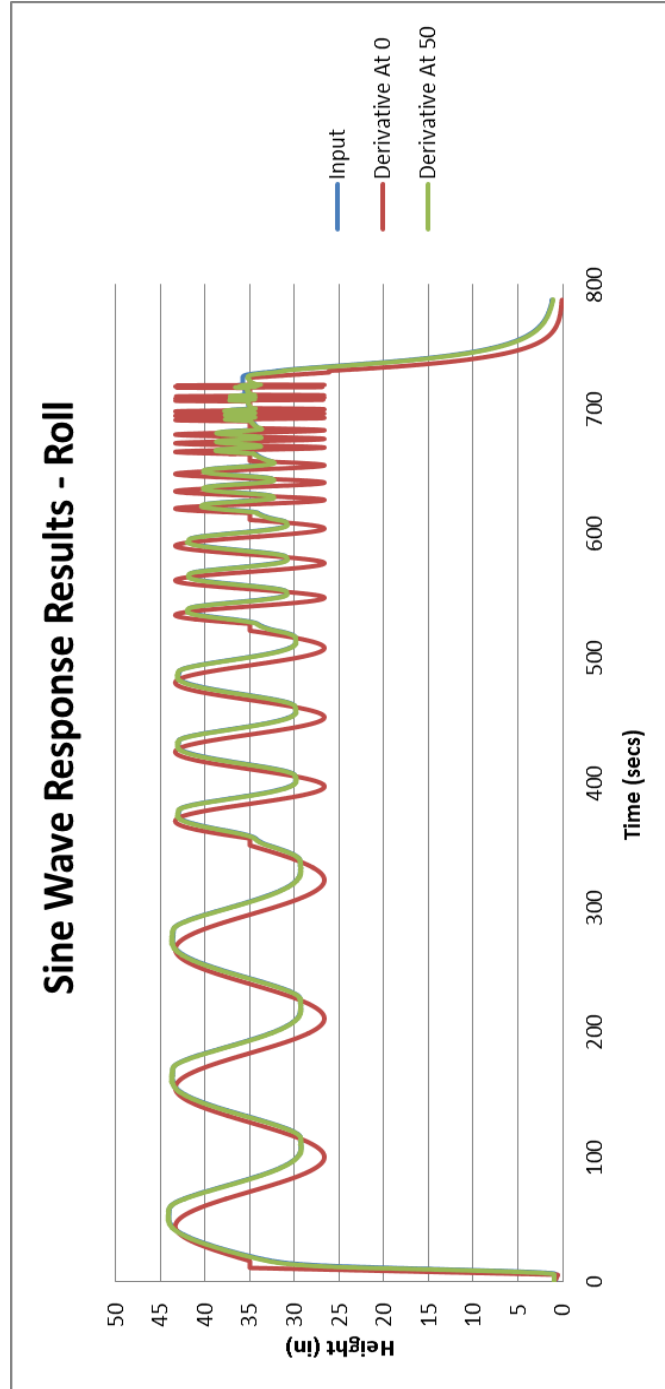


Figure C.1: Roll Sine Wave Response Results

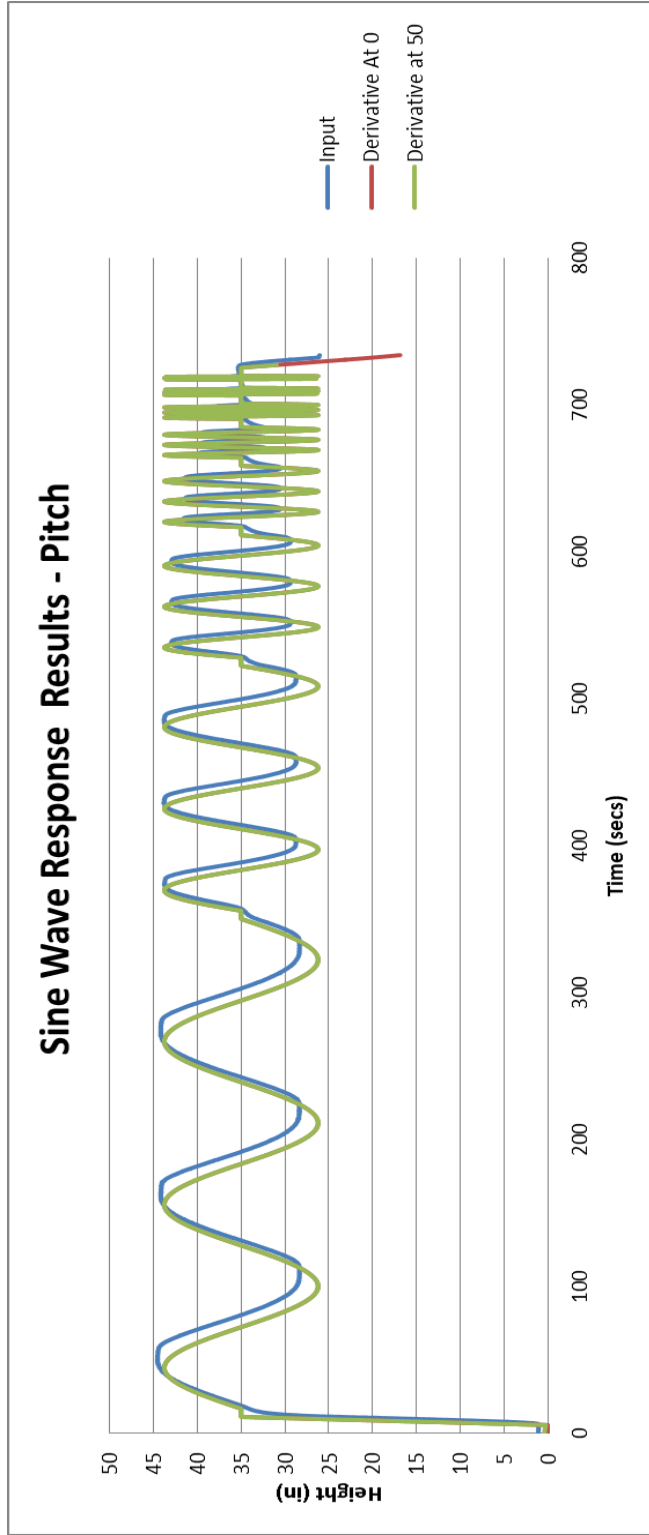


Figure C.2: Pitch Sine Wave Response Results

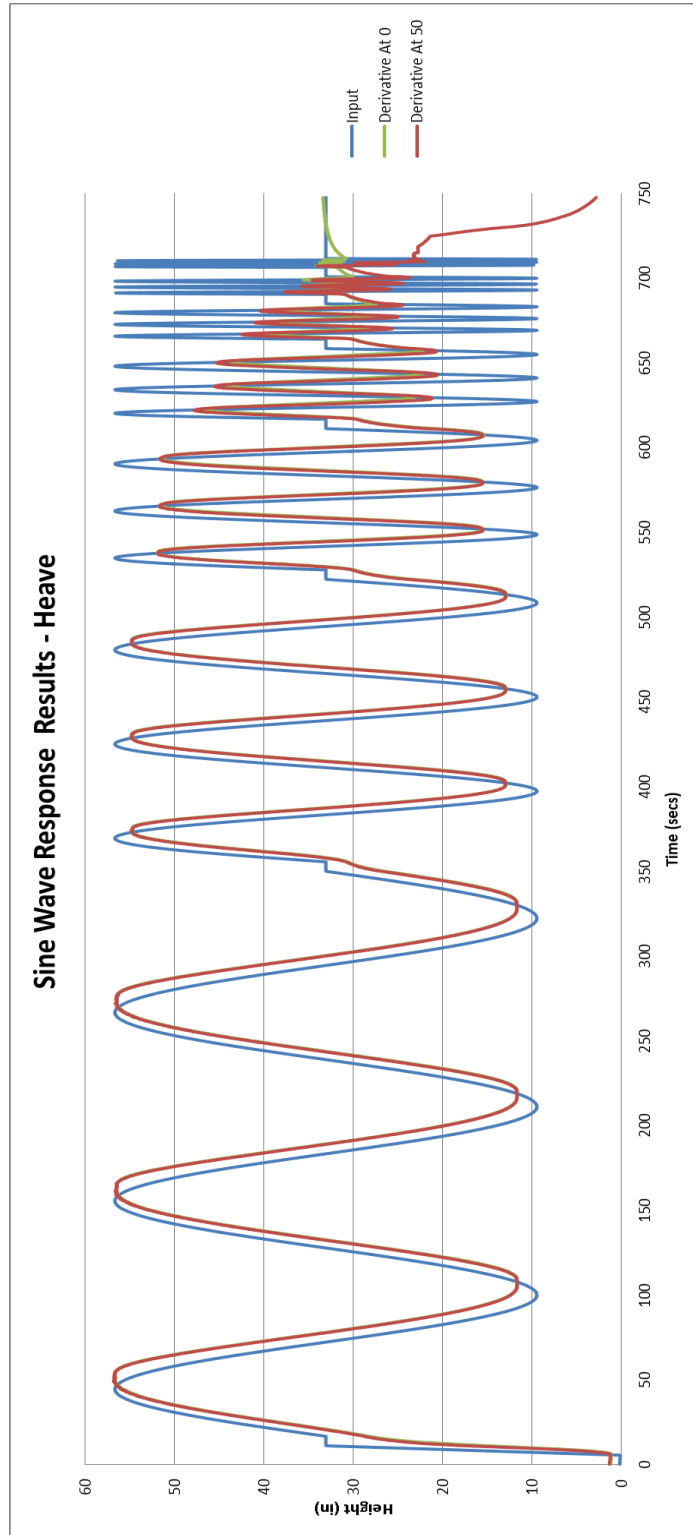


Figure C.3: Heave Sine Wave Response Results

Appendix D: Bode Plot Methodology and Results

The following Appendix includes the information calculated for creating the bode plot graphs, as seen in Chapter 4. First, Figure D.1 represents how the following were calculated.

- 1.) Run Start
- 2.) Run End
- 3.) Period Start
- 4.) Period End
- 5.) Displacement Max
- 6.) Displacement Min
- 7.) Displacement Offset

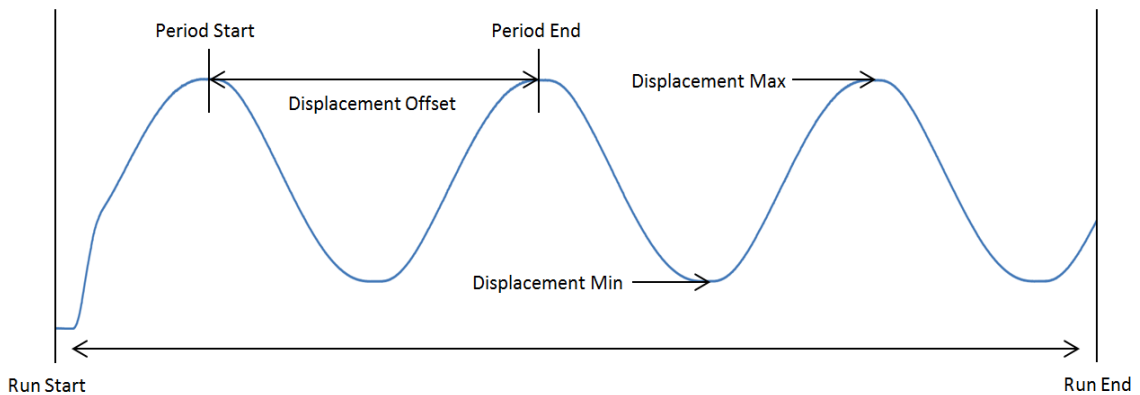


Figure D.1: Wave Bode Plot Calculation Diagram

This methodology was completed for each frequency. To determine the actual frequency, phase shift, displacement amplitude, and the dB value the following equations were used.

Actual Frequency

$$\frac{1}{(\text{Period End} - \text{Period Start})/10}$$

Phase Shift

$$\left(\frac{\text{Displacement Offset} - \text{Period Start}}{\text{Period End} - \text{Period Start}} \right) (360)$$

Displacement Amplitude

$$\frac{\text{Displacement Max} - \text{Displacement Min}}{2}$$

Amplitude (dB)

$$20\text{Log} \left(\left(\frac{\text{Displacement Amplitude}}{\text{Reference Amplitude}} \right)^{10} \right)$$

With this the following tables were created to determine the response of the original internal PID control and the external PD controller.

Table D.1: Original Internal PID Controller Roll Data

Frequency Hz	Run Start	Run End	Period Start	Period End	Frequency	Disp Offset
0.01	417	2546	322	1323	0.00999001	437
0.02	2875	3975	457	955	0.020080321	528
0.04	4121	4581	128	379	0.039840637	165
0.08	4620	4920	77	202	0.08	97
0.16	5000	5170	31	93	0.161290323	42
0.32	5250	5345	36	67	0.322580645	42
0.64	5480	5517	18	34	0.625	21
1.28	5656	5867	66	74	1.25	68
2.56	5656	5867	204	208	2.5	205

Phase Shift (deg.)	Disp Max	Disp Min	Disp Amp	Reference Amp	dB
-41.358	18.884	11.641	7.243	7	0.296409
-51.325	17.868	12.34	5.528	7	-2.0506
-53.067	17.673	13.332	4.341	7	-4.15017
-57.600	17.159	14.355	2.804	7	-7.9464
-63.870	15.33	14.31	1.02	7	-16.73
-69.677	15.582	14.947	0.635	7	-20.8465
-67.500	15.188	14.772	0.416	7	-24.5201
-90	15.214	14.881	0.333	7	-26.4531
-90	15.002	14.719	0.283	7	-27.8662

Table D.2: Original Internal PID Controller Pitch Data

Frequency Hz	Run Start	Run End	Period Start	Period End	Frequency	Disp Offset
0.01	440	2500	802	1810	0.009920635	873
0.02	2798	3917	226	727	0.01996008	290
0.04	4022	4600	268	518	0.04	305
0.08	4636	5078	88	214	0.079365079	108
0.16	5150	5353	23	86	0.158730159	35
0.32	5425	5538	22	53	0.322580645	29
0.64	5640	5700	4	20	0.625	7
1.28	5865	5890	6	14	1.25	8
2.56	6060	6095	5	9	2.5	6

Phase Shift (deg.)	Disp Max	Disp Min	Disp Amp	Reference Amp	dB
-25.357	21.882	8.46	13.422	11	1.728491
-45.988	21.073	9.41	11.663	11	0.508352
-53.280	19.298	10.712	8.586	11	-2.15204
-57.142	19.063	12.53	6.533	11	-4.5256
-68.571	16.435	13.485	2.95	11	-11.4314
-81.290	15.593	14.02	1.573	11	-16.8933
-67.5	15.054	14.15	0.904	11	-21.7045
-90	15.052	14.482	0.57	11	-25.7104
-90	14.552	14.404	0.148	11	-37.4226

Table D.3: Original Internal PID Controller Heave Data

Frequency Hz	Run Start	Run End	Period Start	Period End	Frequency	Disp Offset
0.01	500	2520	756	1759	0.00997009	831
0.02	2769	3789	131	629	0.020080321	184
0.04	4039	4559	65	314	0.040160643	97
0.08	4681	4939	33	158	0.08	57
0.16	5021	5215	15	78	0.158730159	28
0.32	5299	5429	7	38	0.322580645	13
0.64	5498	5598	3	19	0.625	7
1.28	5700	5773	9	17	1.25	12
2.56	5840	5890	3	7	2.5	4

Phase Shift (deg.)	Disp Max	Disp Min	Disp Amp	Reference Amp	dB
-26.919	2.106	0.895	1.211	0.5	7.683483
-38.313	2.022	0.966	1.056	0.5	6.493878
-46.265	1.896	1.087	0.809	0.5	4.17957
-69.120	1.744	1.235	0.509	0.5	0.154956
-74.285	1.601	1.333	0.268	0.5	-5.4167
-69.677	1.528	1.383	0.145	0.5	-10.752
-90	1.488	1.402	0.086	0.5	-15.2894
-135	1.456	1.405	0.051	0.5	-19.828
-90	1.459	1.421	0.038	0.5	-22.3837

Table D.4: External PD Controller Roll Data at Derivative 0

Frequency Hz	Run Start	Run End	Period Start	Period End	Frequency	Disp Offset
0.01	110	2700	420	1530	0.009	530
0.02	3480	5210	3683	4235	0.018	3755
0.04	5210	6105	5340	5620	0.036	5385
0.08	6105	6580	6198	6338	0.071	6225
0.16	5150	5353	6655	6725	0.143	6670
0.32	6885	6990	6910	6945	0.286	6920
0.64	7060	7105	7067	7084	0.588	7070
1.28	7170	7190	7171	7181	1.000	7174

Phase Shift (deg.)	Disp Max	Disp Min	Disp Amp	Reference Amp	dB
-35.676	41.213	27.712	6.751	7	-0.315
-46.957	42.125	28.789	6.668	7	-0.422
-57.857	41.829	30.885	5.472	7	-2.139
-69.429	40.168	32.420	3.874	7	-5.139
-77.143	38.428	34.017	2.206	7	-10.032
-102.857	37.069	35.036	1.017	7	-16.760
-63.529	36.383	35.430	0.477	7	-23.341
-108.000	36.536	35.648	0.444	7	-23.954

Table D.5: External PD Controller Roll Data at Derivative 50

Frequency	Run	Run	Period	Period	Frequency	Disp Offset
-----------	-----	-----	--------	--------	-----------	-------------

Hz	Start	End	Start	End		
0.01	110	3470	410	1515	0.009049774	515
0.02	3475	5205	3685	4235	0.018181818	3745
0.04	5205	6105	5340	5620	0.035714286	5380
0.08	6105	6580	6200	6337	0.072992701	6220
0.16	6630	6810	6655	6725	0.142857143	6670
0.32	6895	7000	6910	6945	0.285714286	6918
0.64	7060	7115	7067	7084	0.588235294	7070
1.28	7168	7196	7172	7181	1.111111111	7174

Phase Shift (deg.)	Disp Max	Disp Min	Disp Amp	Reference Amp	dB
-34.208	44.147	29.266	7.4405	7	0.530
-39.272	43.018	29.837	6.5905	7	-0.524
-51.428	41.954	30.821	5.5665	7	-1.990
-52.554	40.415	32.311	4.052	7	-4.749
-77.142	38.828	34.411	2.2085	7	-10.020
-82.285	37.777	34.427	1.675	7	-12.422
-63.529	37.219	34.472	1.3735	7	-14.145
-80	37.2	34.411	1.3945	7	-14.014

Table D.6: External PD Controller Pitch Data at Derivative 0

Frequency Hz	Run Start	Run End	Period Start	Period End	Frequency	Disp Offset
0.01	137	3485	408	1505	0.00911577	505
0.02	3485	5210	3675	4230	0.018018018	3735
0.04	5290	6100	5341	5615	0.03649635	5371
0.08	6100	6590	6197	6336	0.071942446	6218
0.16	6625	6850	6655	6725	0.142857143	6667
0.32	6900	7010	6911	6946	0.285714286	6918
0.64	7055	7120	7067	7084	0.588235294	7071
1.28	7165	7200	7172	7181	1.111111111	7174

Phase Shift (deg.)	Disp Max	Disp Min	Disp Amp	Reference Amp	dB
---------------------------	-----------------	-----------------	-----------------	----------------------	-----------

-31.832	44.509	28.99	7.7595	11	-0.001
-38.918	43.751	28.791	7.48	11	-0.320
-39.416	42.795	29.396	6.6995	11	-1.277
-54.388	41.567	30.582	5.4925	11	-3.002
-61.714	39.882	32.334	3.774	11	-6.262
-72	39.129	33.343	2.893	11	-8.571
-84.705	36.793	34.726	1.0335	11	-17.512
-80	36.793	36.029	0.382	11	-26.157

Table D.7: External PD Controller Pitch Data at Derivative 50

Frequency Hz	Run Start	Run End	Period Start	Period End	Frequency	Disp Offset
0.01	137	3485	411	1511	0.009090909	476
0.02	3485	5210	3680	4225	0.018348624	3722
0.04	5290	6100	5337	5615	0.035971223	5366
0.08	6100	6590	6195	6335	0.071428571	6215
0.16	6625	6850	6654	6724	0.142857143	6665
0.32	6900	7010	6911	6945	0.294117647	6917
0.64	7055	7120	7067	7084	0.588235294	7070
1.28	7165	7200	7172	7181	1.111111111	7174

Phase Shift (deg.)	Disp Max	Disp Min	Disp Amp	Reference Amp	dB
-21.272	44.544	28.304	8.12	11	-0.012
-27.743	43.693	28.73	7.4815	11	-0.723
-37.553	42.905	29.383	6.761	11	-1.603
-51.428	41.558	30.624	5.467	11	-3.448
-56.571	39.995	32.314	3.8405	11	-6.515
-63.529	38.418	33.64	2.389	11	-10.639
-63.529	37.502	33.596	1.953	11	-12.389
-80	36.874	35.148	0.863	11	-19.483

Table D.8: External PD Controller Heave Data at Derivative 0

Frequency Hz	Run Start	Run End	Period Start	Period End	Frequency	Disp Offset
0.01	110	3490	415	1525	0.009009009	495

0.02	3490	5220	3685	4237	0.018115942	3735
0.04	5220	6110	5342	5620	0.035971223	5377
0.08	6110	6585	6200	6338	0.072463768	6221
0.16	6630	6845	6656	6725	0.144927536	6671
0.32	6900	7010	6911	6946	0.285714286	6919
0.64	7055	7115	7067	7084	0.588235294	7071

Phase Shift (deg.)	Disp Max	Disp Min	Disp Amp	Reference Amp	dB
-25.945	56.67	10.47	23.1	0.5	0.001
-32.608	54.73	12.944	20.893	0.5	-0.871
-45.323	51.886	15.567	18.1595	0.5	-2.090
-54.782	46.475	23.296	11.5895	0.5	-5.991
-78.260	40.007	28.427	5.79	0.5	-12.019
-82.285	36.312	31.69	2.311	0.5	-19.996
-84.705	34.147	31.46	1.3435	0.5	-24.707

Table D.9: External PD Controller Heave Data at Derivative 50

Frequency Hz	Run Start	Run End	Period Start	Period End	Frequency	Disp Offset
0.01	110	3515	421	1534	0.008984726	487
0.02	3515	5290	3685	4241	0.017985612	3734
0.04	5290	5995	5343	5621	0.035971223	5377
0.08	6150	6600	6200	6338	0.072463768	6220
0.16	6630	6840	6656	6725	0.144927536	6667
0.32	6900	7010	6911	6946	0.285714286	6918

Phase Shift (deg.)	Disp Max	Disp Min	Disp Amp	Reference Amp	db
-21.34770889	56.644	11.657	22.4935	0.5	0.000
-31.72661871	54.772	12.99	20.891	0.5	-0.642
-44.02877698	51.85	15.531	18.1595	0.5	-1.859
-52.17391304	47.667	21.18	13.2435	0.5	-4.601
-57.39130435	42.445	25.616	8.4145	0.5	-8.541
-72	37.573	25.896	5.8385	0.5	-11.715

Table D.10: Current PD Controller Roll Data

Frequency Hz	Period Start	Period End	Period Start	Period End	Frequency	Disp Offset
0.01	0	16000	2000	10000	0.00125	2190
0.02	16001	24100	17060	21060	0.0025	17260

0.04	24101	28190	24675	26680	0.004988	24830
0.08	28191	30320	28540	29545	0.00995	28670
0.16	30321	31430	30530	31025	0.020202	30635
0.32	31430	32050	31570	31820	0.04	31670
0.64	32051	32400	32140	32270	0.076923	32240

Phase Shift (deg.)	Disp Max	Disp Min	Disp Amp	Reference Amp	db
-8.550	45.856	34.2	5.828	5.83	-0.00298
-18.000	45.782	34.241	5.7705	5.83	-0.0891
-27.830	45.77	34.231	5.7695	5.83	-0.09061
-46.567	45.643	34.255	5.694	5.83	-0.20502
-76.364	45.77	34.255	5.7575	5.83	-0.10869
-144.000	45.72	34.367	5.6765	5.83	-0.23176
-276.923	45.66	34.486	5.587	5.83	-0.3698

Table D.11: Current PD Controller Pitch Data

Frequency Hz	Period Start	Period End	Period Start	Period End	Frequency	Disp Offset
0.01	0	16000	2001	10011	0.001248	2059
0.02	16001	24050	17115	21110	0.002503	17215
0.04	24050	28180	24697	26671	0.005066	24767
0.08	28180	30310	28541	29536	0.01005	28618
0.16	30310	31420	30528	31028	0.02	30590
0.32	31420	32060	31569	31820	0.039841	31630

Phase Shift (deg.)	Disp Max	Disp Min	Disp Amp	Reference Amp	db
-2.607	48.761	31.297	8.732	8.73	0.00199
-9.011	48.761	31.31	8.7255	8.73	-0.00448
-12.766	48.76	31.31	8.725	8.73	-0.00498
-27.859	48.71	31.39	8.66	8.73	-0.06993
-44.640	48.69	31.409	8.6405	8.73	-0.08951
-87.490	48.6	31.573	8.5135	8.73	-0.21812

Table D.12: Current PD Controller Heave Data

Frequency	Run Start	Run End	Period Start	Period End	Frequency	Disp Offset
0.01	0	16200	2000	10000	0.00125	2052
0.02	16200	25000	17788	21748	0.002525253	17840

0.04	25000	29800	26071	28079	0.00498008	26147
0.08	29800	32450	30646	31635	0.010111223	30690
0.16	32450	35000	33326	33825	0.02004008	33361

Phase Shift (deg.)	Disp Max	Disp Min	Disp Amp	Reference Amp	dB
-2.340	67.46	12.62	27.42	27.4	0.006338
-4.727	67.475	12.625	27.425	27.4	0.007921
-13.625	67.545	12.63	27.4575	27.4	0.018209
-16.016	67.44	13.01	27.215	27.4	-0.05884
-25.251	67.124	13.152	26.986	27.4	-0.13224

Appendix E : Initial Controller's Matrix Transformation

The initial controller used a transformation matrix to find the position of the ship deck simulator platform data on the ship center of gravity. The math script used the platform position to determine the hydraulic actuator position given a home position of 20 inches extension on each hydraulic cylinder. The inputs of the math script were;

- roll = ship roll at center of mass
- pitch = ship pitch at center of mass
- heave = ship heave at center of mass
- (x,y,z)=vector from ship center of mass to center of platform

The (x,y,z) vector had to be in accordance with the ship coordinate system. The outputs of the system were;

- d1 = displacement of cylinders on mast 1
- d2 = displacement of cylinders on mast 2
- d3 = displacement of cylinders on mast 3

The ship coordinate system was centered at the center of mass with the x axis pointing to starboard, the y axis pointing to the stern, and the z axis pointing down. The pitch, roll, and yaw were all positive rotations about the x, y, and z axis respectively. The displacements of the joints are then set to:

$$dx = 0;$$

$$dy = 0;$$

$$dz = -\text{heave};$$

With the displacements set the location of spherical joints are calculated from meters to inches. The calculations are below:

$$x1=x;$$

$$x2=x+48*0.0254;$$

$$x3=x-48*0.0254;$$

$$y1=y-72*0.0254;$$

$$y2=y+36*0.0254;$$

$$y3=y+36*0.0254;$$

$$z1=z;$$

$$z2=z;$$

$$z3=z;$$

The next function was to convert the roll, pitch, and yaw from degrees to radians with the formulas:

$$\text{roll}=\text{roll}*\pi/180$$

$$\text{pitch}=\text{pitch}*\pi/180$$

$$\text{yaw}=0$$

With the conversion from degrees to radians the components of the transformation matrix were formed and simplified as follows:

$$r11 = \cos(\text{roll});$$

$$r12 = \sin(\text{roll})*\sin(\text{pitch});$$

$$r13 = (\text{roll})*\cos(\text{pitch});$$

$$r21 = 0;$$

$$r22 = \cos(\text{pitch});$$

$$r23 = \sin(\text{pitch});$$

$$r31 = \sin(\text{roll});$$

$$r32 = \cos(\text{roll}) * \sin(\text{pitch});$$

$$r33 = \cos(\text{roll}) * \cos(\text{pitch});$$

With the components complete the transformation matrix was assembled by:

$$R = [r11 \ r12 \ r13; r21 \ r22 \ r23; r31 \ r32 \ r33];$$

The position of each spherical bearing could then be found by multiplying the transformation matrix and the location of each spherical joint. Then these values were added to the displacements of each lift. These values used the formulas:

$$P1 = R * [x1; y1; z1] + [dx; dy; dz];$$

$$P2 = R * [x2; y2; z2] + [dx; dy; dz];$$

$$P3 = R * [x3; y3; z3] + [dx; dy; dz];$$

Finally, the z position of each spherical joint bearing had to be extracted. This value was multiplied by -0.5 to account for the axis orientation and the hydraulic mast doubling the effect. The value was converted from meters to inches and 20 inches was added to each value to achieve the correct neutral position. The formula for these calculations was as follows:

$$D1 = (P1(3,1) * -39.370079)$$

$$D2 = (P2(3,1) * -39.370079)$$

$$D3 = (P3(3,1) * -39.370079)$$

Appendix F : Current Controller Back Panel

Figures F.1, F.2, F.3, F.4, and F.5 portray the back panel of the current controller; multiple figures must be used do the length of the back panel and are shown in chronological order. The figures for the 3-D imaging, which is also located on the back panel, are not shown in this Appendix. Please view Section 4.4.2.1 and 4.4.2.2 for these Figures. Additionally, for a block diagram of the system please see Figure F.6.

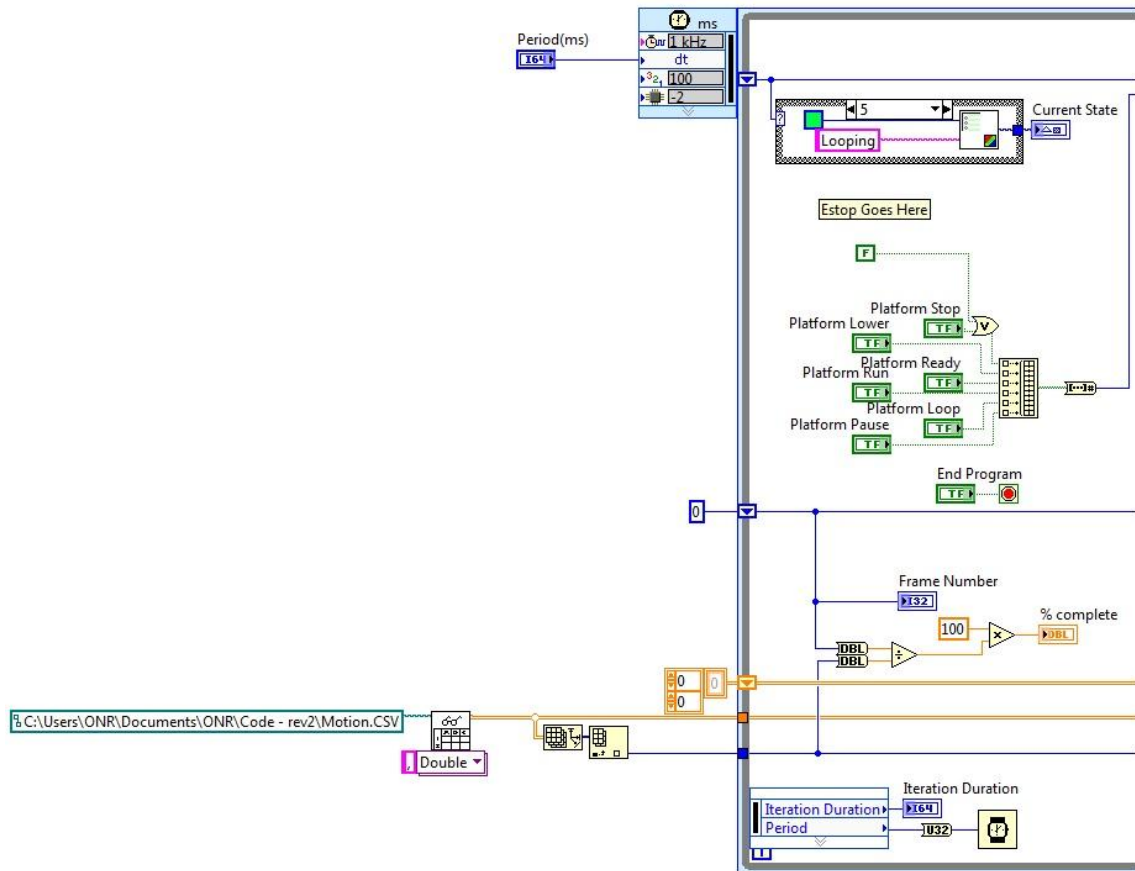


Figure F.1: Back Panel Input Section

Figure F-1, contains the functions for setting the period of the system and the control state. This section also reads in the input file, calculates the amount of frames in the file, sets the percentage complete on the input file, and creates control state buttons.

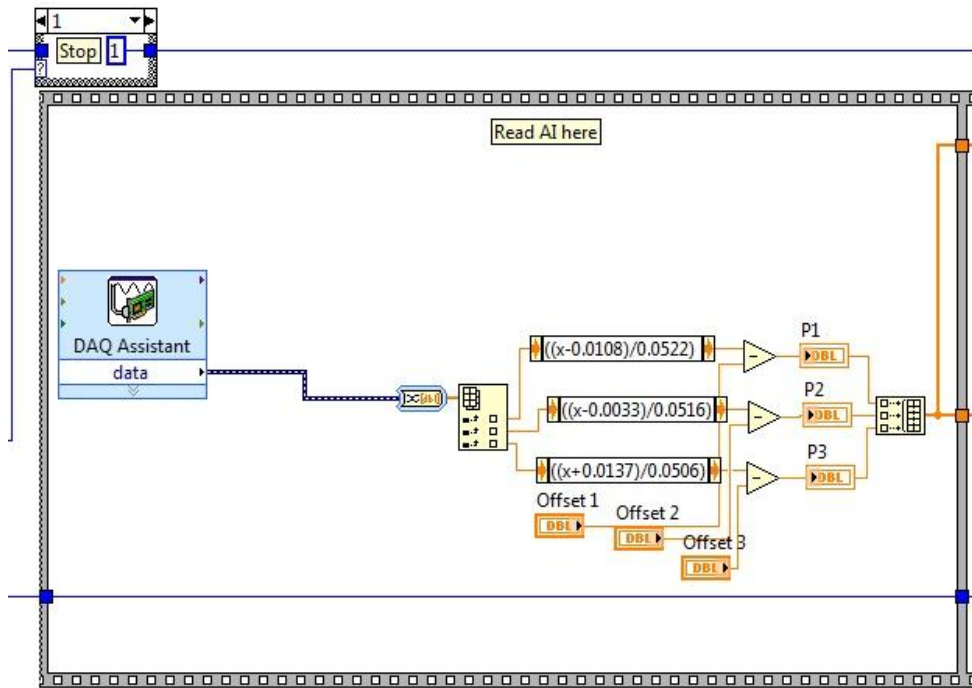


Figure F.2: Back Panel Potentiometer Conversion Section

Figure F.2, shows the analog input and the potentiometer conversions. Lift one is the top conversion, the second conversion the second lift, and the last conversion the third lift. The offset to position the lifts at the 0 inch mark are also set here.

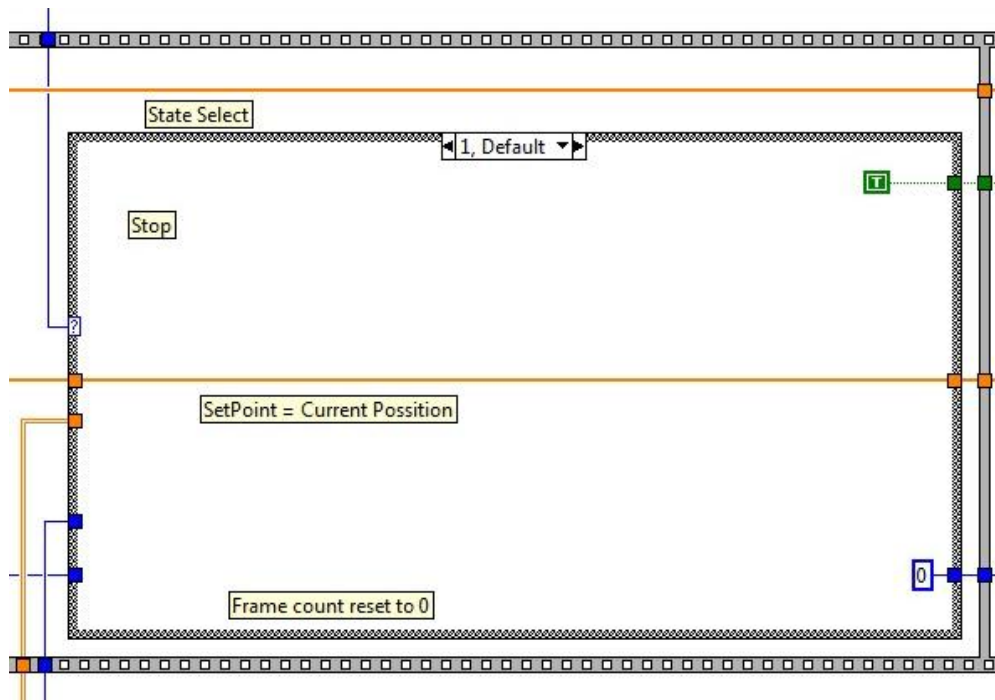


Figure F.3: Back Panel Control State Section

Figure F.3, is the control state of the platform. When the desired state, i.e. run, stop, pause, etc..., is chosen on the front panel the control state in the back panel changes to the selected state, thus changing the input to the platform. Please see Appendix G for the LabVIEW coding of each control state.

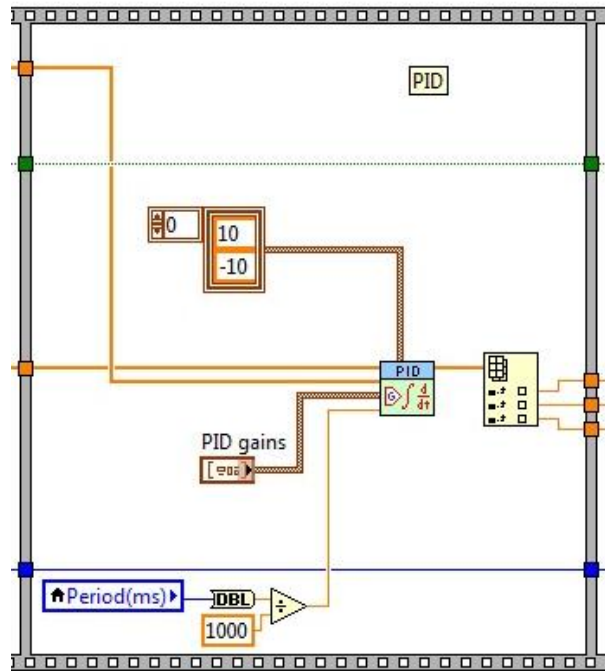


Figure F.4: Back Panel PD Controller

Figure F.4, is the PD Controller of the platform system. When the proportional and derivate gain values are set on the front panel the values are fed into this section. The maximum and minimum voltages of the system are also set in the section.

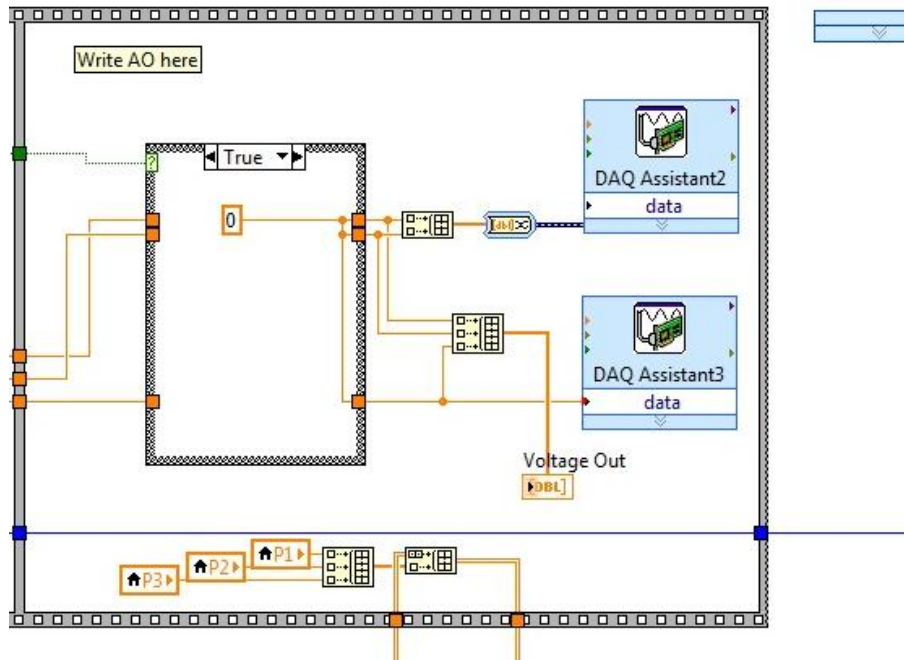


Figure F.5: Back Panel Output

Figure F.5, is the final section of the back panel and sends the output of the system to the DAQ cards which in return moves the platform. Also, in this section the position of the lifts and the voltage output are fed to the front panel.

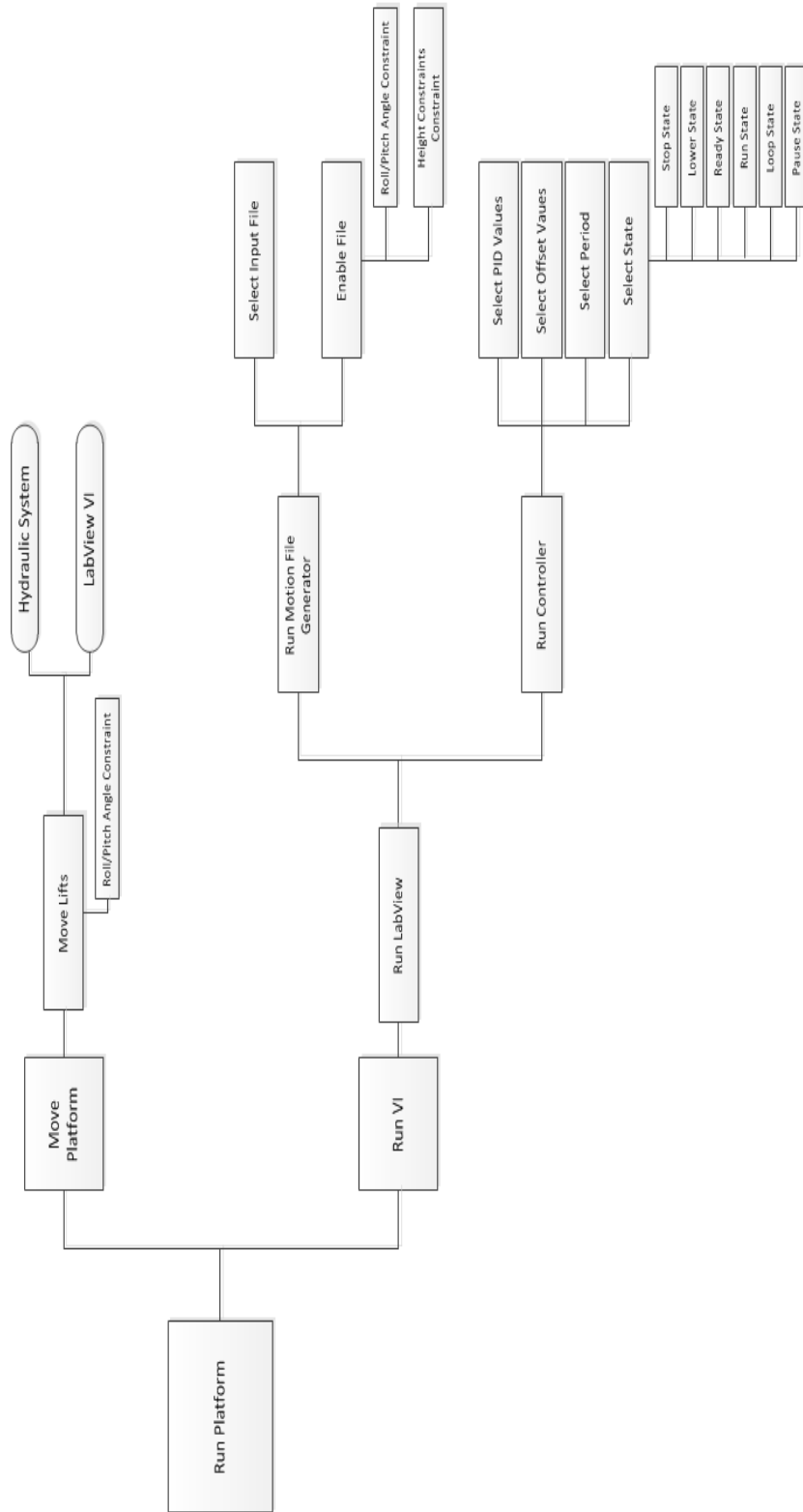


Figure F.6: Current Controller Function Block Diagram

Appendix G: Back Panel Control States

Figure G.1, G.2, G.3, G.4, G.5, and G.6 are the control states for the platform.

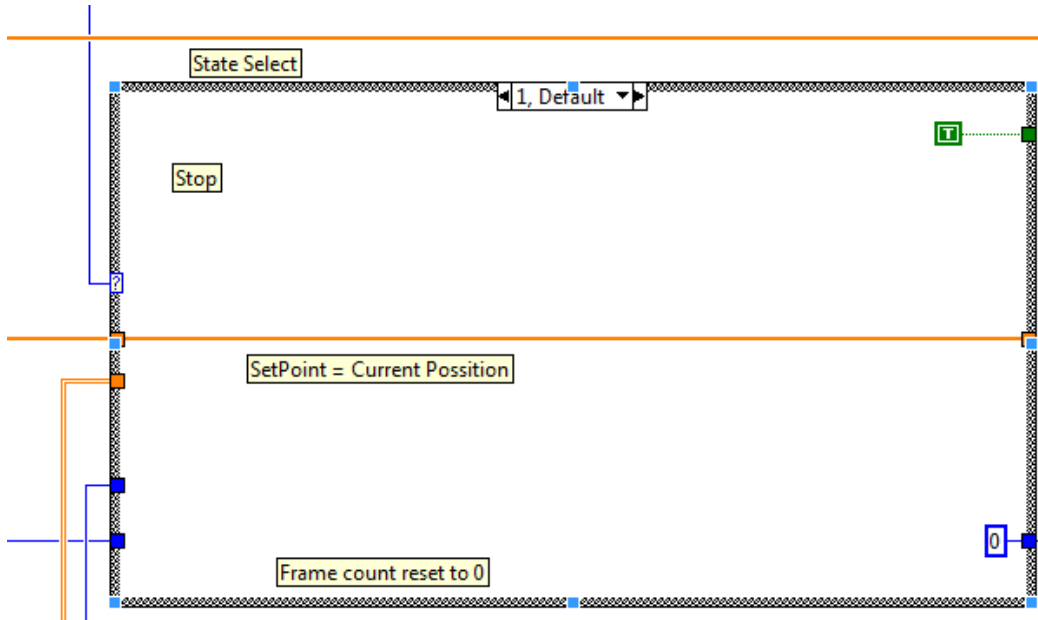


Figure G.1: Stop Control State

Figure G.1, is the stop control state. In this state a constant height is fed into the platform. This height is dependent on where the platform is at that current time, i.e. if the platform is at 30 inches a constant 30 inches will be fed into each lift.

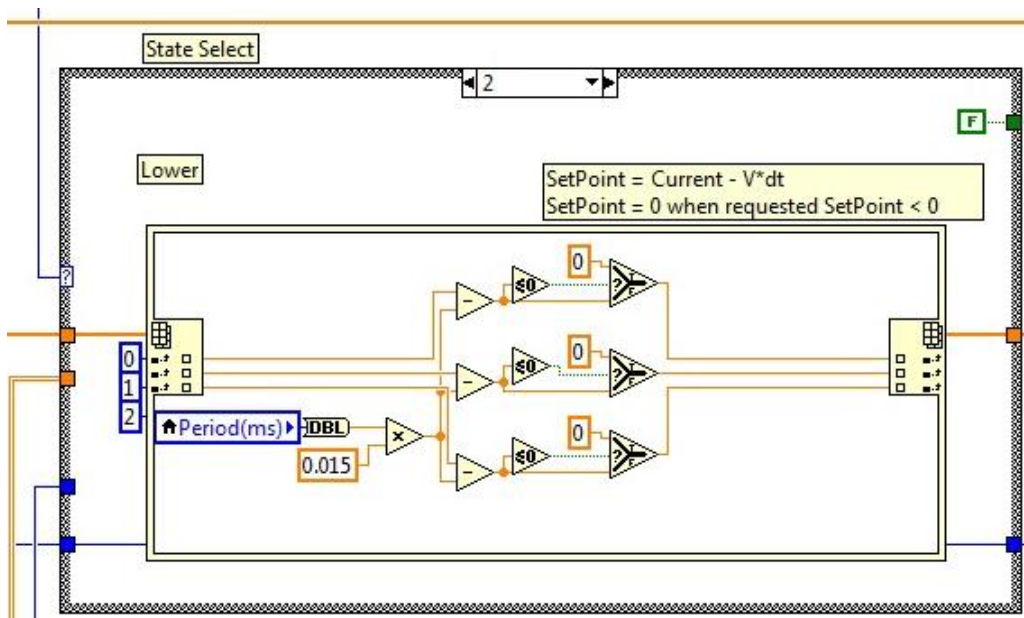


Figure G.2: Lower Control State

Figure G.2, is the lower control state. In this state a step function is fed into the platform to lower the unit back to the start state of 0 inches safely.

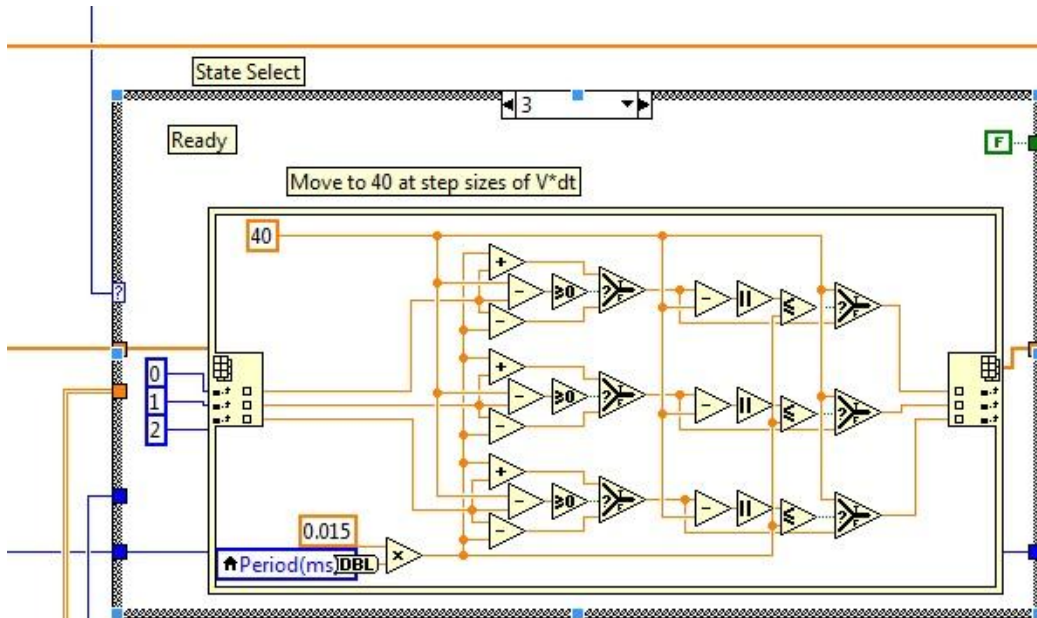


Figure G.3: Ready Control State

Figure G.3, is the ready control state. In this state a step function is fed into the platform until the platform reaches the 40 inch mark. This state can be used to raise or lower the platform back to the 40 inch mark.

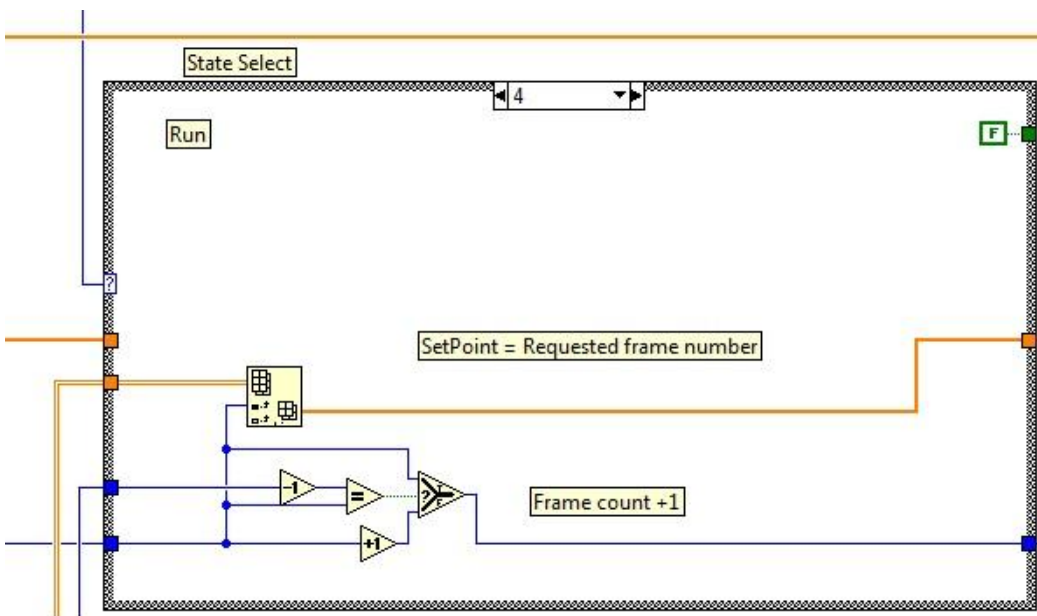


Figure G.4: Run Control State

Figure G.4, is the run control state. In this state the input file feeds into the controller which then relays the input to the lifts.

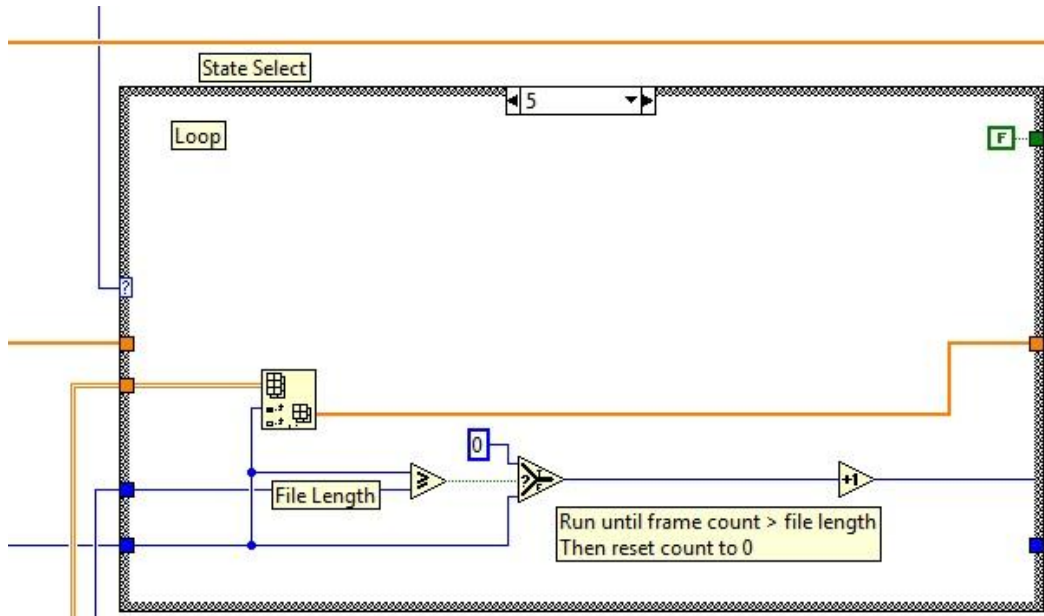


Figure G.5: Loop Control State

Figure G.5, is the loop control state. In this state the input file is looped continuously until stopped by the user. If this state is used the start and end of the file must match. Failure to match the file may cause possible damage the lifts.

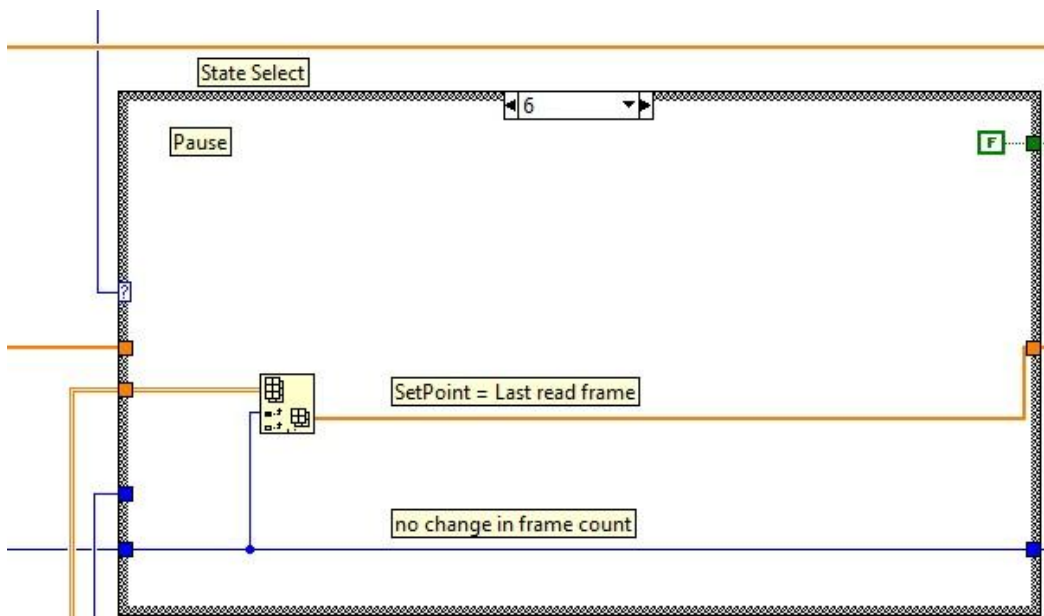


Figure G.6: Pause Control State

Figure G.6, is the pause control state. In this state the operator may pause the platform while the platform is in motion. When paused, a continuous feed of the last position paused will be fed into the appropriate lift. If paused, the operator can restart the motion by clicking the run button.

Appendix H : Current Controller Front Panel

Figure H.1, is a screen shot of the new controller's front panel. The front panel lists a number of options for controller of the platform. On the left hand side are the options for lowering, raising, running, pausing, and stopping the platform. An indicator that is located above the 3-D image changes text and color depending on which control option is selected, currently it is in the "Running Option". The front panel also indicates the frame number, percentage complete, voltage output, and the position of the lifts. Below the 3-D image of the platform is located the PD gain values, which can be changed manually. Additionally, the position offsets for the lifts are also located in this area.

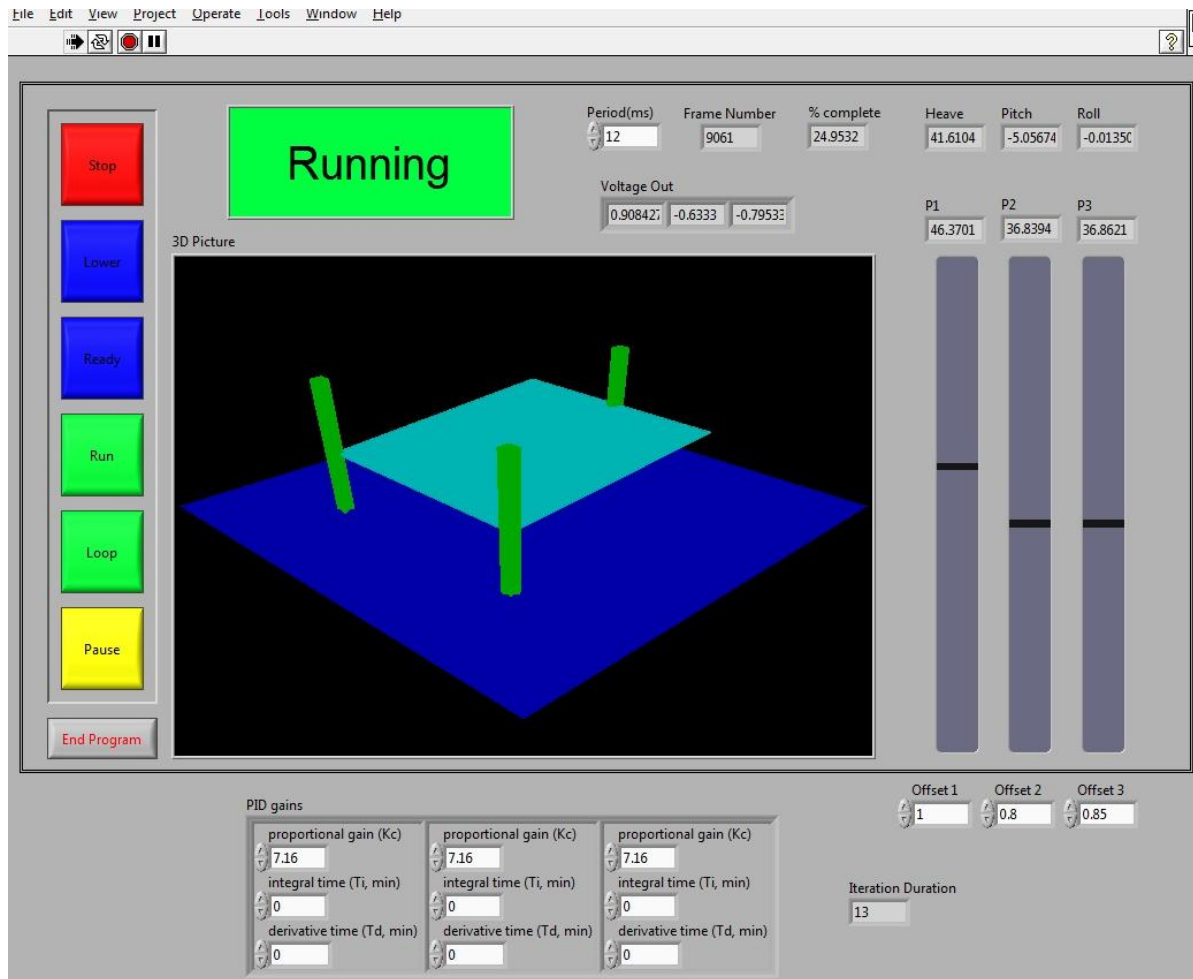


Figure H.1: Current Controller's Front Panel

Appendix I : MATLAB Gain Value Coding

Below is the coding to determine the initial testing values for the proportional and derivative gains.

```
z=1;
wn=18.1;
Kd=0.75;
Kp=10;
num1=[Kd Kp];
num2=[wn^2];
num=conv(num1,num2);
den1=[0 Kd Kp]*wn^2;
den2=[1 (2*z*wn) wn^2];
den= den1 + den2;
sys=tf(num,den);

subplot (2,2,1), step(sys);
subplot (2,2,2), rlocusplot(sys);
subplot (2,2,3), nyquist(sys);
subplot (2,2,4), pzplot(sys);
```

Appendix J: Current Controller Sine Wave Response

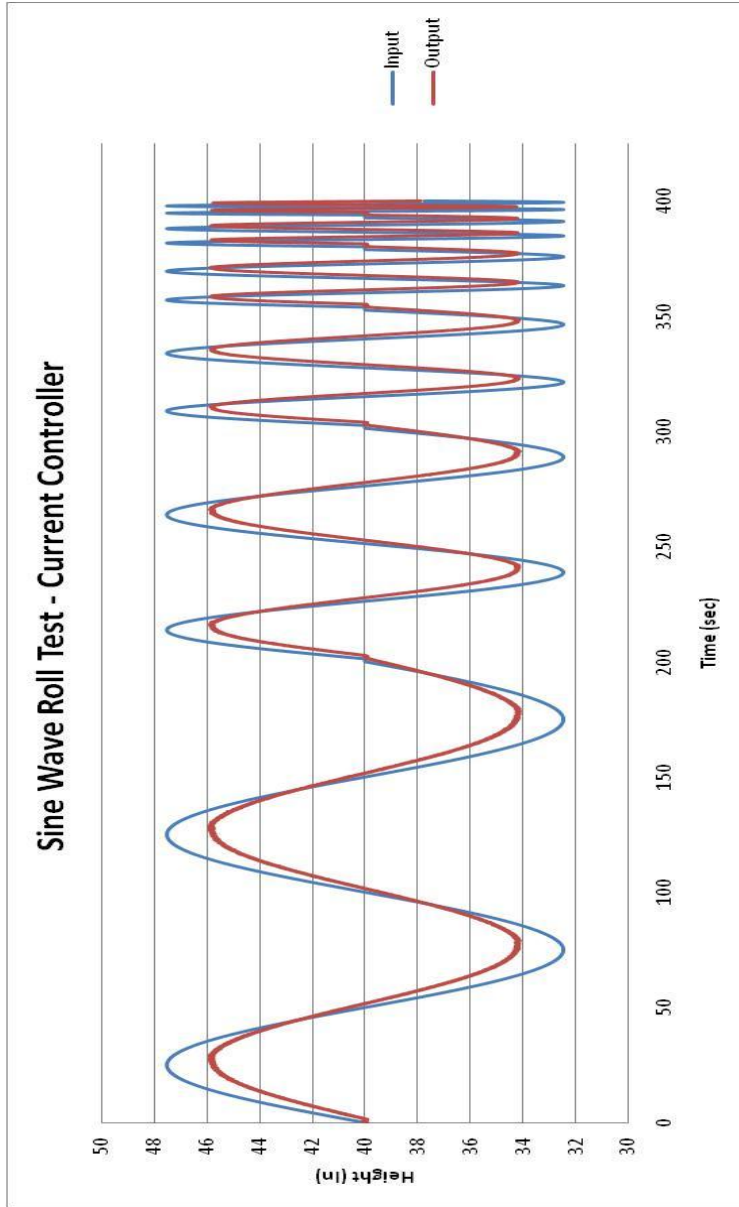


Figure J.1: Current Controller's Sine Wave Roll Test

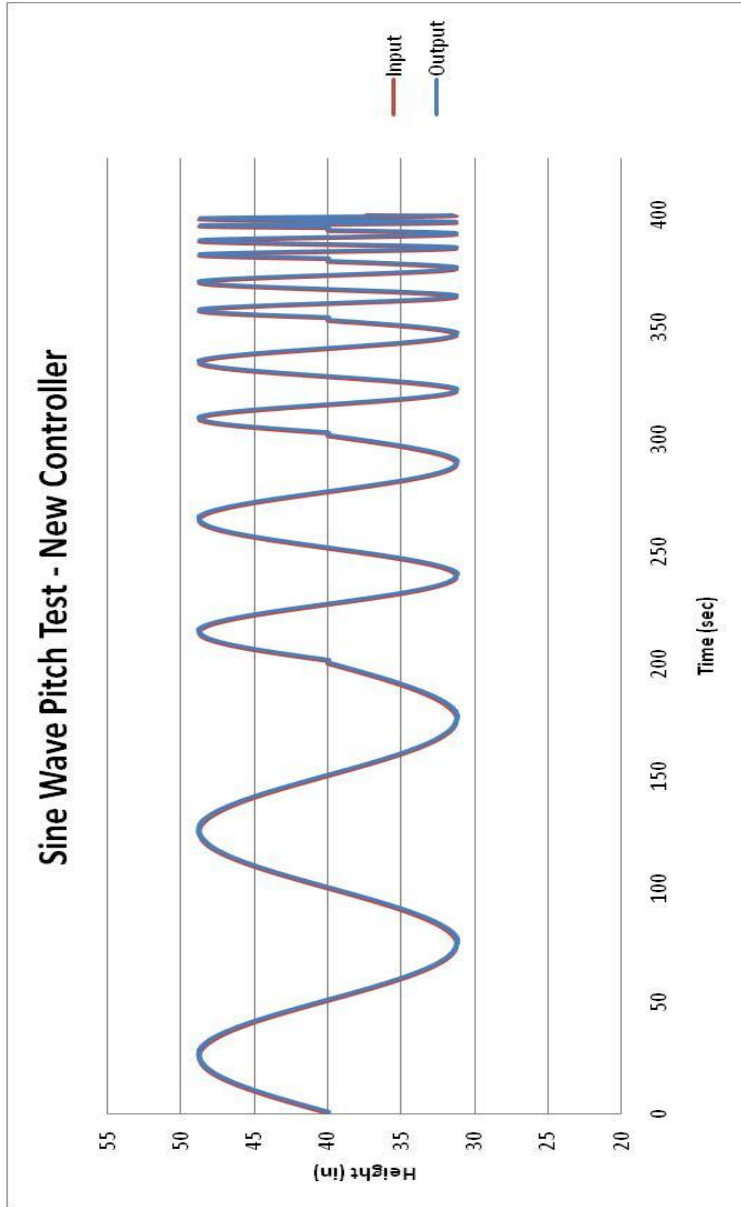


Figure J.2: Current Controller's Sine Wave Pitch Test

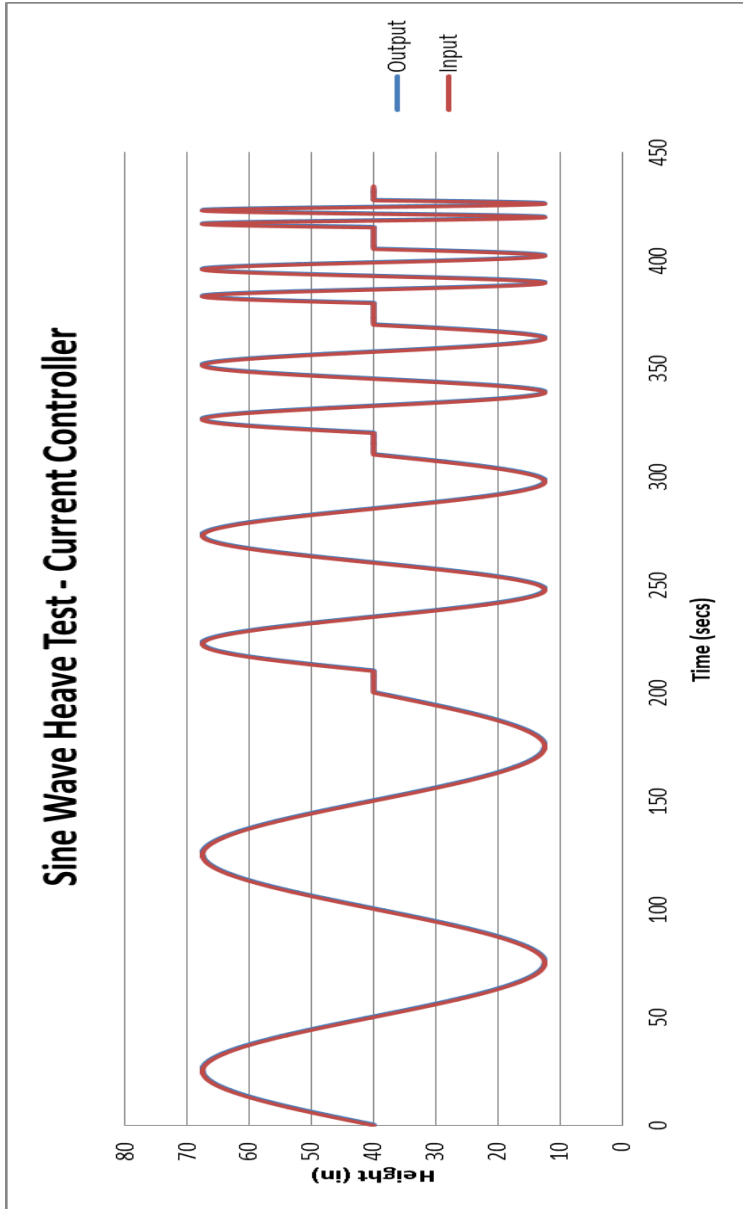


Figure J.3: Current Controller's Sine Wave Heave Test